STUDIES IN THE ASYMMETRIC REDUCTION OF (3*S*)-3-AMINO-1-CHLORO-4-PHENYL-2-BUTANONE DERIVATIVES

A Thesis
Presented to
The Academic Faculty

By

Kristen Kitagawa

In Partial Fulfillment
Of the Requirements for the Degree
Doctor of Philosophy in Chemistry

Georgia Institute of Technology

May 2010

STUDIES IN THE ASYMMETRIC REDUCTION OF (3*S*)-3-AMINO-1-CHLORO-4-PHENYL-2-BUTANONE DERIVATIVES

Approved by:

Dr. Charles Liotta, Co-Advisor
School of Chemistry and Biochemistry
Georgia Institute of Technology

Dr. Charles Eckert, Co-Advisor
School of Chemical and Biomolecular Engineering
Georgia Institute of Technology

Dr. Rigoberto Hernandez
School of Chemistry and Biochemistry
Georgia Institute of Technology

Dr. Amyn Teja
School of Chemical and Biomolecular Engineering
Georgia Institute of Technology

Dr. John Zhang
School of Chemistry and Biochemistry
Georgia Institute of Technology

Date Approved: December 9, 2009

ACKNOWLEDGEMENTS

I would like to thank my advisors, Professors Charles Liotta and Charles Eckert, for all of their support and guidance throughout this process. Dr. Liotta taught me that the results you never expected are often the most interesting. Dr. Eckert always emphasized the bottom line and encouraged us to think about the big picture. I would also like to thank the other members of my committee for their input and helpful suggestions.

Thank you to the past and present members of the Eckert-Liotta research group. I would not have made it this far without your support and friendship. There are a few group members whose contributions were especially helpful. Dr. Pamela Pollet was always willing to listen patiently to my questions and problems and helped tremendously in the revision of this document. Kyle Flack, Dr. Elizabeth Cope, Dr. Veronica Llopis-Mestre, and Dr. Rani Jha all contributed to the research presented in this thesis. Chris Sandhage helped with some of the MPV kinetics experiments. Ryan Hart collaborated with me on the OATS project and was a great travel buddy in Italy. Thank you to Dr. John Gohres for always keeping me entertained. Hillary Huttenhower went through this whole process with me and helped keep me on track through all of the important stepping stones.

Many people outside of graduate school helped to provide necessary distractions from the routine of work. Christine Fennessey has always been willing to go on exciting adventures and is a great climbing buddy. Glenn Fisher always came up with ways to get me off the couch and out into the real world. I would also like to thank Michelle Bahr and Ava Allen, Chen Chen, Alex Teodorescu, Ben Hamilton, and Anita Chow.

Finally, I would like to thank my family for encouraging and supporting me through graduate school.

TABLE OF CONTENTS

ACKNOWLEDGEMENTS iii

LIST OF TABLES ix

LIST OF FIGURES xi

LIST OF ABBREVIATIONS xvi

SUMMARY xviii

CHAPTER 1 INTRODUCTION 1

CHAPTER 2 BACKGROUND 5

Applications of (S,S)- and (R,S)-CMA 5
(S)-CMK Reduction 7
(S)-CMK Reduction Prior Art 9
Aluminohydride Reduction 9
Biotransformation 10
Borohydride Reduction 10
Catalytic Hydrogenation 11
Asymmetric Transfer Hydrogenation 12
Meerwein-Ponndorf-Verley Reduction 12

REFERENCES 13

CHAPTER 3 MEERWEIN-PONNDORF-VERLEY REDUCTIONS 14

INTRODUCTION 14

BACKGROUND 16

MPV Reduction Mechanism 16
Transition State Modeling Studies 18

RESULTS AND DISCUSSION 20

Investigation of Diastereoselectivity 20

Batch Scale Reactions 20
Reductions in Various Alcohol Solvents 20
Reduction with Synthesized Aluminum Isopropoxide 22
Reductions with Different Aluminum Alkoxides 22
Reductions in Various Organic Solvents 23
Reductions with Hydrogen Bonding Additives 24
Carousel Reactions 25
Reductions with Aluminum Alkoxides 26
Reductions in Various Organic Solvents 27
Investigation of Reaction Kinetics 28
Reduction of (S)-CMK 29
Reduction of Acetophenone 31
Reduction of Benzaldehyde 33
Aluminum Alkoxide States of Aggregation 35
CONCLUSIONS 37
EXPERIMENTAL METHODS 39
REFERENCES 51
CHAPTER 4 ASYMMETRIC TRANSFER HYDROGENATION REACTIONS 53
INTRODUCTION 53
BACKGROUND 55
Heterogeneous Catalytic Hydrogenation 55
Asymmetric Transfer Hydrogenation 56
RESULTS AND DISCUSSION 59
Heterogeneous Catalytic Hydrogenation 59
Asymmetric Transfer Hydrogenation 61
Original Reaction Apparatus 61
ATH in “Wet” Organic Solvents with the Achiral Catalyst (TsEN) 62
ATH in Pure Organic Solvents with the Achiral Catalyst (TsEN) 62
ATH in Water with the Achiral Catalyst (TsEN) 63
ATH in 1:1 Water/Organic Solvent Mixtures with the Achiral Catalyst (TsEN) 63

ATH in “Wet” Organic Solvents with the Chiral Catalyst [(1R,2R)-TsDPEN] 64
Reproducibility of ATH Reactions 65
New Reaction Apparatus 66
Optimization of Workup Procedures 67
Optimized Reaction Apparatus with Product Sampling 68
Test of Reproducibility 69
Reproducibility with Triethylammonium Formate 70
Effect of Different Reaction Conditions on ATH Reaction 71
ATH Reaction with Triethylammonium Formate in Various Organic Solvents 73
Effect of Temperature and Water on ATH Reaction with Triethylammonium Formate 75
Effect of Substrate-to-Catalyst Ratio 77
Effect of Formate-to-Substrate Ratio 77
Effect of Triethylamine-to-Formic Acid Ratio 78
Effect of Substrate Concentration 79
Effect of Time on ATH Reaction 80
Investigation of Various ATH Ligands 81
Effect of Various Metal Catalysts 82
CONCLUSIONS 85
EXPERIMENTAL METHODS 86
REFERENCES 101
CHAPTER 5 BORON REDUCING AGENTS 103
INTRODUCTION 103
BACKGROUND 106
Boron Triisopropoxide Reduction Mechanism 106
Oxazaborolidine Reduction Mechanism 107
RESULTS AND DISCUSSION 107
Reduction with Sodium Borohydride 107
Reduction with Boron Triisopropoxide 108
Reduction with Borane Catalyzed by Oxazaborolidines 109

Synthesis and Characterization of Oxazaborolidines 110
Reduction with Borane without Catalyst 111
Reduction with Borane Catalyzed by (R,S)-DPO or 1,3,2-Oxazaborolidine . 112
Reduction with Borane Catalyzed by (R)-(+)-CBS or (S)-(-)-CBS 113
Reproducibility of Oxazaborolidine-Catalyzed Reactions 115
CONCLUSIONS 115
EXPERIMENTAL METHODS 117
REFERENCES 122
CHAPTER 6 REDUCTION OF (S)-CMK WITH VARIOUS PROTECTING GROUPS .. 124
INTRODUCTION 124
BACKGROUND 125
RESULTS AND DISCUSSION 126
Synthesis of (S)-CMK with Different Amine Protecting Groups 126
Synthesis of (S)-CMK Ammonium Hydrochloride Salt 126
Synthesis of Phthalimide-Protected (S)-CMK 127
Synthesis of Trifluoroacetamide-Protected (S)-CMK 128
Reduction of (S)-CMK with Different Protecting Groups 128
Asymmetric Transfer Hydrogenation 128
Reduction with Boron Reducing Agents 129
Meerwein-Ponndorf-Verley Reduction 131
CONCLUSIONS 133
EXPERIMENTAL METHODS 134
REFERENCES 142
CHAPTER 7 RECOMMENDATIONS 143
REFERENCES 146
APPENDIX A MANGANESE(SALEN) CATALYST SYNTHESIS FOR APPLICATION IN ORGANIC AQUEOUS TUNABLE SOLVENT SYSTEMS 147
INTRODUCTION 147

BACKGROUND 148

Gas-Expanded Liquids 148

OATS System 150

Salen Catalysts 152

Epoxidation Reaction 153

RESULTS AND DISCUSSION 155

Synthesis of Mn(salen) Catalyst 155

Synthesis of 3-tert-Butyl-5-formyl-4-hydroxybenzenesulfonate 156

Synthesis of 5,5'-(1E,1'E)-(Cyclohexane-1,2-diylbis(azan-1-yl-1-ylidene))bis(methan-1-yl-1-ylidene)bis(3-tert-butyl-4-hydroxybenzenesulfonate) 157

Synthesis of Mn(salen) Catalyst Complex 158

Mn(salen) Catalyst Stability 158

CONCLUSIONS AND RECOMMENDATIONS 160

EXPERIMENTAL METHODS 162

REFERENCES 165

APPENDIX B PACLITAXEL SIDE CHAIN SYNTHESIS 167

INTRODUCTION 167

RESULTS AND DISCUSSION 169

Jacobi Synthesis 169

Protection of 2-phenylglycinol 170

Swern Oxidation 171

Dess-Martin Oxidation 172

Pyridinium Dichromate Oxidation 172

Manganese Dioxide Oxidation 173

Acylsilane Benzoin Condensation 174

Tungstophosphoric Acid Reaction 176

CONCLUSIONS AND RECOMMENDATIONS 177

EXPERIMENTAL METHODS 179

REFERENCES 183

LIST OF TABLES

Table 2.1: Reduction of (*S*)-CMK with aluminohydride reagents. 10

Table 2.2: Reduction of (*S*)-CMK using borohydride reducing agents.[5,6] 11

Table 3.1: MPV reductions in alcohol solvents. 22

Table 3.2: MPV reductions in various organic solvents. 24

Table 3.3: MPV reduction with aluminum alkoxides. 27

Table 3.4. MPV reduction of (*S*)-CMK in various organic solvents. 28

Table 3.5: HPLC solvent gradient. 41

Table 3.6: Reaction workup with aluminum alkoxides. 47

Table 3.7: Reaction workup for various organic solvent solutions. 48

Table 4.1: Catalytic hydrogenation of (*S*)-CMK with platinum oxide. 59

Table 4.2: ATH in "wet" organic solvents with achiral catalyst. 62

Table 4.3: ATH reaction in pure organic solvents with achiral catalyst. 63

Table 4.4: ATH reaction in 1:1 organic solvent/water mixture with achiral catalyst. 64

Table 4.5: ATH reaction in "wet" organic solvents and water with chiral catalyst. 64

Table 4.6: Repeated ATH reactions in "wet" organic solvents with achiral catalyst. 65

Table 4.7: Repeated ATH reactions in 1:1 water/organic solvent mixtures with achiral catalyst. 65

Table 4.8: Comparison of workup procedures in ATH reaction. 68

Table 4.9: Reproducibility of ATH reaction in pure and "wet" DMF. 69

Table 4.10: Reproducibility of ATH reactions with triethylammonium formate in ethyl acetate. 71

Table 4.11: Effect of different reaction conditions on ATH reaction. 72

Table 4.12: Effect of substrate-to-catalyst ratio on ATH reaction. 77

Table 4.13: Effect of formate-to-substrate ratio on ATH reaction. 78

Table 4.14: Effect of triethylamine-to-formic acid ratio on ATH reaction. 79

Table 4.15: Effect of varying (*S*)-CMK concentration on ATH reaction. 79

Table 4.16: Effect of ligand on ATH reaction. 82

Table 4.17: ATH reaction with Ru, Rh, and Ir catalyst precursors. 83

Table 5.1: Summary of boron reagents used in the reduction of (*S*)-CMK.[21,22] 105

Table 5.2: Reduction of (*S*)-CMK with borane. 112

Table 5.3: Reduction of (*S*)-CMK with (*R,S*)-DPO or 1,3,2-oxazaborolidine. 113

Table 5.4: Reduction of (*S*)-CMK with commercially available (*R*)-(+)-CBS and (*S*)-(-)-CBS. 114

Table 5.5: Comparison of (*R*)-(+)-CBS as a solution or as a solid. 115

Table 5.6: Reduction of (*S*)-CMK using stock solutions of oxazaborolidine catalysts. . 115

Table 6.1. MPV reduction of (*S*)-CMK, Phth-CMK, and TFA-CMK. 133

Table 6.2: Reagent loadings in MPV reduction of Phth-CMK and TFA-CMK. 139

LIST OF FIGURES

Figure 1.1: Structures of (*S,S*)- and (*R,S*)-CMA. 1

Figure 2.1: Illustration of HIV infection pathways with the effect of HIV protease inhibitors shown in orange (HIV-PI).[1] 5

Figure 2.2: Pharmaceutical products derived from (*S*)-CMK.[4] 6

Figure 2.3: Chemical structures of some HIV protease inhibitors. Portions of the molecules deriving from (*S,S*)-CMA or (*R,S*)-CMA are highlighted in red. 7

Figure 2.4: Synthetic route to (*S,S*)- and (*R,S*)-CMA from Boc-phenylalanine. 8

Figure 2.5: Structural characteristics of prochiral ketone (*S*)-CMK. 8

Figure 2.6: Possible dechlorination products from (*S*)-CMK reduction. 9

Figure 3.1: General MPV reduction scheme. 14

Figure 3.2: MPV reduction reaction mechanism. 17

Figure 3.3: Transition state complex between (*S*)-CMK and Al(O*i*Pr)$_3$ leading to the (*R,S*)-CMA product. 17

Figure 3.4: MPV reduction intermediate. A: Mono-chelation between aluminum and ketone. B: Hydrogen bonding and bi-chelation with ketone and nitrogen. 19

Figure 3.5: MPV reduction of (*S*)-CMK. 21

Figure 3.6: Brinkmann 12-reaction carousel apparatus. 26

Figure 3.7. Reaction conversion and yield as a function of time for the MPV reduction of (*S*)-CMK in isopropanol catalyzed by Al(O*t*Bu)$_3$ or Al(O*i*Pr)$_3$. 30

Figure 3.8. Reaction conversion and yield as a function of time for the MPV reduction of (*S*)-CMK in 9:1 toluene/isopropanol catalyzed by Al(O*t*Bu)$_3$ or Al(O*i*Pr)$_3$. 31

Figure 3.9. Reaction conversion and yield as a function of time for the MPV reduction of acetophenone in isopropanol catalyzed by Al(O*t*Bu)$_3$ and Al(O*i*Pr)$_3$. 32

Figure 3.10. Reaction conversion and yield as a function of time for the MPV reduction of acetophenone in 9:1 toluene/isopropanol catalyzed by Al(O*t*Bu)$_3$ and Al(O*i*Pr)$_3$. 33

Figure 3.11. Reaction conversion and yield as a function of time for the MPV reduction of benzaldehyde in isopropanol catalyzed by Al(O*t*Bu)$_3$ and Al(O*i*Pr)$_3$. 34

Figure 3.12. Reaction conversion and yield as a function of time for the MPV reduction of benzaldehyde in 9:1 toluene/isopropanol catalyzed by Al(O*t*Bu)$_3$ and Al(O*i*Pr)$_3$. 35

Figure 3.13. States of aggregation of Al(O*t*Bu)$_3$ and Al(O*i*Pr)$_3$. Nonbridging alkoxide groups are highlighted in red. 36

Figure 3.14: Comparison of ^{1}H NMR spectra for starting material and product diastereomers. 40

Figure 3.15: HPLC spectrum for sample mixture of (*S,S*)-CMA, (*R,S*)-CMA, and (*S*)-CMK. 41

Figure 3.16: HPLC calibration curve of (*S*)-CMK in methanol. 42

Figure 3.17: HPLC calibration curve for (*S,S*)-CMA in methanol. 43

Figure 3.18: HPLC calibration curve of (*R,S*)-CMA in methanol. 44

Figure 4.1: General ATH reaction scheme. 53

Figure 4.2: General heterogeneous catalytic hydrogenation reaction scheme. 55

Figure 4.3: ATH reaction on (*S*)-CMK. 56

Figure 4.4: ATH reaction ligands. A: (1*R*,2*R*)-*N*-(*p*-Toluenesulfonyl)-1,2-diphenylethylenediamine [(1*R*,2*R*)-TsDPEN].[28] B: *N*-Tolylsulfonylethylenediamine (TsEN).[29,30] 57

Figure 4.5: ATH catalyst formation mechanism. A: Pre-catalyst formation. B: *In situ* active catalyst formation. 58

Figure 4.6: ATH catalytic cycle. 58

Figure 4.7: Possible dehalogenation products. 60

Figure 4.8: Sample HPLC spectrum of hydrogenation of (*S*)-CMK showing starting material, desired products, and dechlorinated side products. 60

Figure 4.9: ATH results in new apparatus. 67

Figure 4.10: ATH with triethylammonium formate in various organic solvents using a S/C of 1000:1. 74

Figure 4.11: ATH with triethylammonium formate in various organic solvents using a S/C of 100:1. 74

Figure 4.12: ATH with triethylammonium formate in various organic solvents at 40°C. . 76

Figure 4.13: ATH reaction with triethylammonium formate in various solvents with 10% water at 40°C. 76

Figure 4.14: Effect of time on ATH reaction. 81

Figure 4.15: ATH reaction with Rh catalyst in various organic solvents. 84

Figure 4.16: ATH reaction with Rh catalyst in pure organic solvents and in organic solvents with 10% water. 85

Figure 4.17: (*S*)-CMK calibration curve in DMSO. 87

Figure 4.18: (*S,S*)-CMA calibration curve in DMSO. 88

Figure 4.19: (*R,S*)-CMA calibration curve in DMSO. 88

Figure 4.20: (*S*)-CMK calibration curve in methanol. 89

Figure 4.21: (*S,S*)-CMA calibration curve in methanol. 90

Figure 4.22: (*R,S*)-CMA calibration curve in methanol. 90

Figure 4.23: Shaker type hydrogenation apparatus. 91

Figure 5.1: Reduction of benzaldehyde with triethylborane.[2] 104

Figure 5.2: Mechanism of the boron triisopropoxide reduction of ketones. 106

Figure 5.3: Mechanism of the reduction of ketones by 2-methyl-CBS-oxazaborolidine.[23] 107

Figure 5.4: Structures of oxazaborolidine catalysts. A: (4*R*,5*S*)-4,5-Diphenyl-1,3,2-oxazaborolidine [(*R,S*)-DPO]. B: 1,3,2-Oxazaborolidine. C: (*R*)-(+)-CBS or (*S*)-(-)-CBS. 110

Figure 5.5: Synthesis of (*R,S*)-DPO. 111

Figure 5.6: Synthesis of 1,3,2-oxazaborolidine. 111

Figure 5.7: Reduction of (*S*)-CMK with borane without catalyst. 112

Figure 6.1: Structures of phthalimide-protected (*S*)-CMK (A) and trifluoroacetamide-protected (*S*)-CMK (B). 125

Figure 6.2: Formation of (*S*)-4- chloro-3-oxo-1-phenylbutan-2-aminium chloride through deprotection of (*S*)-CMK. 126

Figure 6.3: Synthesis of *N*-phthaloyl-(3*S*)-3-amino-1-chloro-4-phenyl-2-butanone (Phth-CMK). 127

Figure 6.4: Synthesis of *N*-trifluoroacetyl-(3*S*)-3-amino-1-chloro-4-phenyl-2-butanone (TFA-CMK). 128

Figure 6.5: ATH reduction of Phth-CMK. 129

Figure 6.6: Reduction of ammonium salt.[9] 130

Figure 6.7: Boc protection of (*S*)-CMK ammonium hydrochloride salt. 130

Figure 6.8: Reduction of phthalimide carbonyl and subsequent removal of phthalimide protecting group. 131

Figure 6.9: MPV reduction of (*S*)-CMK ammonium hydrochloride salt. 131

Figure 6.10: MPV reduction of Phth-CMK. 132

Figure 6.11: MPV reduction of TFA-CMK. 132

Figure 6.12: X-ray crystal structure of (*R,S*)-Phth-CMA. 140

Figure 6.13: X-ray crystal structure of (*S,S*)-TFA-CMA. 141

Figure 7.1: (*S*)-CMK with different protecting groups on the tertiary amine. 144

Figure 7.2: *N*-Alkyl-*N′*-tosyl-1,2-ethanediamine ligand. 145

Figure A.1: Relative properties of GXLs compared to other solvent classes. 150

Figure A.2: OATS process schematic. 151

Figure A.3: Summary of OATS benefits. 152

Figure A.4: Synthesis of generic salen ligand. 153

Figure A.5: Preparation of Crixivan® from indene. 154

Figure A.6: Water-soluble Mn(salen) catalyst. 155

Figure A.7: Synthesis of Mn(salen) catalyst. 156

Figure A.8: Synthesis of 3-*tert*-butyl-5-formyl-4-hydroxybenzenesulfonate. 157

Figure A.9: Synthesis of 5,5'-(1*E*,1'*E*)-(cyclohexane-1,2-diylbis(azan-1-yl-1-ylidene))bis(methan-1-yl-1-ylidene)bis(3-*tert*-butyl-4-hydroxybenzenesulfonate). 158

Figure A.10: Synthesis of Mn(salen) catalyst. 158

Figure A.11: UV-Vis spectra of Mn(salen) catalyst in water or H_2O_2. 159

Figure A.12: Reduction and methylation of Mn(salen) catalyst. 161

Figure B.1: Structure of paclitaxel with side chain highlighted. 168

Figure B.2: Proposed synthetic pathway to paclitaxel side chain using Jacobi method.[5] 169

Figure B.3: Benzoyl protection and subsequent oxidation of 2-phenylglycinol. 170

Figure B.4: Benzoyl protection of 2-phenylglycinol amino group. 171

Figure B.5: Attempted Swern oxidation of *N*-benzoyl-2-phenylglycinol. 171

Figure B.6: Attempted Dess-Martin oxidation of *N*-benzoyl-2-phenylglycinol. 172

Figure B.7: Attempted pyridinium dichromate oxidation of *N*-benzoyl-2-phenylglycinol. 173

Figure B.8: Oxidation of *N*-benzoyl-2-phenylglycinol with manganese dioxide. 173

Figure B.9: Acylsilane benzoin condensation general reaction scheme. 174

Figure B.10: Capperucci (trimethylsilyl)cuprate reaction scheme. 175

Figure B.11: Katritzky benzotriazole reaction scheme. 176

Figure B.12: Tungstophosphoric acid catalyzed oxidation of *trans*-cinnamic acid. 177

LIST OF ABBREVIATIONS

AIDS	Acquired Immunodeficiency Syndrome
ATH	Asymmetric Transfer Hydrogenation
BINOL	1,1'-Bi-2-naphthol
Boc	*tert*-Butyloxycarbonyl
(*R*)-(+)-CBS	(*R*)-(+)-2-Methyl-CBS-oxazaborolidine
(*S*)-(-)-CBS	(*S*)-(-)-2-Methyl-CBS-oxazaborolidine
(*R,S*)-CMA	*N*-(*tert*-Butyloxycarbonyl)-(3*S*)-3-amino-1-chloro-4-phenyl-(2*R*)-butan-2-ol
(*S,S*)-CMA	*N*-(*tert*-Butyloxycarbonyl)-(3*S*)-3-amino-1-chloro-4-phenyl-(2*S*)-butan-2-ol
(*S*)-CMK	*N*-(*tert*-Butyloxycarbonyl)-(3*S*)-3-amino-1-chloro-4-phenyl-2-butanone
DCM	Dichloromethane
DIBAL-H	Diisobutylaluminum hydride
DMF	Dimethylformamide
DMSO	Dimethylsulfoxide
DR	Diastereomeric Ratio [(*R,S*)-CMA:(*S,S*)-CMA]
ESI-MS	Electron Spray Ionization Mass Spectrometry
GXL	Gas-Expanded Liquid
HIV	Human Immunodeficiency Virus
HPLC	High Performance Liquid Chromatography
IBCF	Isobutylchloroformate
IR	Infrared
LAH	Lithium aluminum hydride
MS	Mass Spectrometry

MPV	Meerwein-Ponndorf-Verley
NMR	Nuclear Magnetic Resonance
OATS	Organic Aqueous Tunable Solvent
Phth-CMK	*N*-Phthaloyl-(3*S*)-3-amino-1-chloro-4-phenyl-2-butanone
S/C	Substrate-to-Catalyst ratio
SCF	Supercritical Fluid
TBAF	Tetrabutylammonium fluoride
TFA-CMK	*N*-Trifluoroacetyl-(3*S*)-3-amino-1-chloro-4-phenyl-2-butanone
THF	Tetrahydrofuran
(1*R*,2*R*)-TsDPEN	(1*R*,2*R*)-*N*-(*p*-toluenesulfonyl)-1,2-diphenylethylenediamine
(1*S*,2*S*)-TsDPEN	(1*S*,2*S*)-*N*-(*p*-toluenesulfonyl)-1,2-diphenylethylenediamine
TsEN	*N*-Tolylsulfonylethylenediamine
UV-Vis	Ultraviolet-visible

SUMMARY

This thesis focuses on the asymmetric reduction of *N*-protected derivatives of (3*S*)-3-amino-1-chloro-4-phenyl-2-butanone to their corresponding diastereomeric alcohol products, which are key intermediates in the synthesis of HIV protease inhibitors. Although the stereoselective synthesis of the (*S,S*) alcohol product is easily achieved, preparing the (*R,S*) diastereomer is much more challenging. I investigated three diastereoselective reduction processes: 1) Meerwein-Ponndorf-Verley (MPV) reduction, 2) asymmetric transfer hydrogenation, and 3) boron reducing agents. The diastereoselectivity of the MPV reduction still favored the (*S,S*) product; however, I discovered a significant rate enhancement when the standard catalyst (aluminum isopropoxide) was replaced with aluminum *tert*-butoxide. Many reaction variables were investigated in the asymmetric transfer hydrogenation reaction and the diastereoselectivity was improved to give a ratio of the desired (*R,S*) diastereomer to the undesired (*S,S*) alcohol of 9.5:1. Using chiral oxazaborolidine catalysts, an unprecedented (*R,S*) to (*S,S*) ratio of 9.5:1 was achieved. Finally, I investigated the effect of the *N*-protecting group on the stereoselectivity of the reduction. When the original boc-protecting group was replaced with a phthalimide group, the diastereoselectivity of the MPV reduction was reversed to favor the desired (*R,S*) product.

CHAPTER 1 INTRODUCTION

Protease inhibitors are a class of pharmaceutically active compounds that have been developed to treat infections caused by viruses. One type of protease inhibitor targets the Human Immunodeficiency Virus (HIV), the cause of Acquired Immunodeficiency Syndrome (AIDS). Researchers have identified and synthesized a few HIV protease inhibitors for commercial production, including Amprenavir®, Saquinavir®, and Atazanavir®. Because the structures of these protease inhibitors are rather complex, often with multiple chiral centers, their synthesis is difficult and expensive. The optically active *N*-(*tert*-butyloxycarbonyl)-(3*S*)-3-amino-1-chloro-4-phenyl-(2*R*)-butan-2-ol [abbreviated (*R,S*)-CMA] and *N*-(*tert*-butyloxycarbonyl)-(3*S*)-3-amino-1-chloro-4-phenyl-(2*S*)-butan-2-ol [abbreviated (*S,S*)-CMA] are important intermediates in the synthesis of HIV protease inhibitors (Figure 1.1).

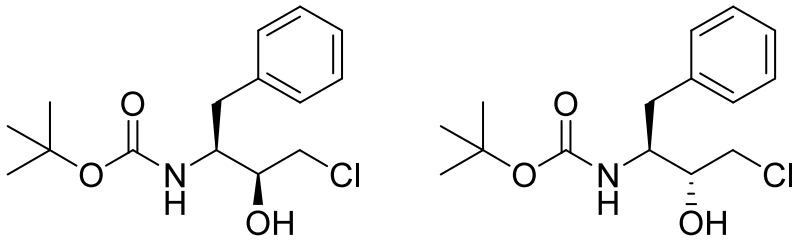

(*S,S*)-CMA **(*R,S*)-CMA**

Figure 1.1: Structures of (*S,S*)- and (*R,S*)-CMA.

Researchers in both academia and industry have investigated the means to selectively prepare the diastereomers (*S,S*)-CMA and (*R,S*)-CMA from the corresponding prochiral ketone, *N*-(*tert*-butyloxycarbonyl)-(3*S*)-3-amino-1-chloro-4-phenyl-2-butanone [abbreviated (*S*)-CMK]. It should be highlighted that the carbon

adjacent to the carbonyl group is chiral (*S* configuration) and thus can contribute to the stereoselectivity of the carbonyl reduction process. For instance, previous studies showed that the Meerwein-Ponndorf-Verley (MPV) reduction of (*S*)-CMK using aluminum isopropoxide in isopropanol proceeded cleanly and stereoselectively to (*S,S*)-CMA primarily. However, establishing an economically competitive method to stereoselectively prepare (*R,S*)-CMA is still a major challenge.

In this thesis, three cost-effective and diastereoselective processes to prepare (*R,S*)-CMA from (*S*)-CMK were successfully developed. The synthetic strategies that were investigated are: 1) MPV reduction, 2) asymmetric transfer hydrogenation (ATH), and 3) reduction with boron reducing reagents.

Chapter 2 (Background) overviews the prior research that scientists have conducted using a large number of reducing agents to stereoselectively prepare (*R,S*)-CMA with varying levels of success. Although a few techniques producing high yields and stereoselective production of (*R,S*)-CMA have been identified, the transfer of these methodologies to an industrial scale is often too intensive and/or costly.

In Chapter 3 (Meerwein-Ponndorf-Verley Reductions), the reduction of (*S*)-CMK through the MPV reduction is presented. The classic MPV reduction (aluminum isopropoxide in isopropanol) favors the formation of the (*S,S*) diastereomer. The diastereoselectivity – induced by the α-chiral carbon of (*S*) configuration – and the reaction rates were shown to be dependent on the aluminum alkoxide reagent's capabilities to hydrogen bond with the substrate as well as its state of aggregation. In addition, I discovered a significant rate enhancement when the common MPV catalyst, aluminum isopropoxide, was replaced with aluminum *tert*-butoxide. Not only was this rate enhancement observed in the reduction of (*S*)-CMK but it was also applied to the reduction of acetophenone and benzaldehyde. This is new intellectual property that can significantly impact the efficiency of MPV processes.

ATH reactions often utilize sodium formate or alkylammonium formates as a hydrogen source combined with a homogeneous chiral catalyst (e.g., ruthenium, rhodium, or iridium). Chapter 4 (Asymmetric Transfer Hydrogenation Reactions) discusses the results of the ATH reactions run on (*S*)-CMK. I first focused on achieving reproducible results by changing the apparatus and the reaction procedure. Once I established a reliable procedure, I optimized the reaction by varying reaction conditions such as solvent, hydrogen source, reagent concentrations, ligand, and metal catalyst center. I achieved significant improvement in diastereoselectivity with the use of a rhodium catalyst and chiral ligand, increasing the ratio of (*R,S*)-CMA to (*S,S*)-CMA to 9.5:1.

The results of the reductions with boron reducing agents are presented in Chapter 5 (Boron Reducing Agents). Oxazaborolidines are useful reducing agents that are commercially available or can be synthesized *in situ* from chiral amino alcohols and boranes. Using chiral oxazaborolidines (*R*)-(+)-2-methyl-CBS-oxazaborolidine or (*S*)-(-)-2-methyl-CBS-oxazaborolidine [abbreviated (*R*)-(+)-CBS and (*S*)-(-)-CBS, respectively], the ratio of (*R,S*)-CMA to (*S,S*)-CMA was improved to 9.5:1. The reduction of (*S*)-CMK with high diastereoselectivity using (*R*)-(+)-CBS is new intellectual property. Furthermore, oxazaborolidines can be chemically bonded onto solid supports, allowing for recycling or continuous processes.

Chapter 6 [Reduction of (*S*)-CMK with Various Protecting Groups] summarizes the alteration of the amine protecting group from the original *tert*-butyloxycarbonyl (Boc) group. The diastereoselectivity – induced by the α-chiral carbon of *S* configuration – is dependent on the aluminum alkoxide reagent's capabilities to hydrogen bond with the NH of the Boc-protected (*S*)-CMK. By varying the protecting group on the amine, the diastereoselectivity could be altered. First, (*S*)-CMK was synthesized with the chosen different *N*-protecting groups (phthalimide or trifluoroacetamide). Then each newly

protected (*S*)-CMK was reduced under classic MPV reduction, ATH reaction, or boron reagents conditions. With the phthalimide group, the protected amine cannot hydrogen bond with the aluminum isopropoxide and the diastereoselectivity towards (*R,S*)-CMA was improved from a (*R,S*)-CMA to (*S,S*)-CMA ratio of 0.06:1 to 1.10:1. The phthalimide- and trifluoroacetamide-protected alcohols and their preparation are new intellectual property.

Finally, Chapter 7 (Recommendations) provides some ideas for future work in the stereoselective reduction of (*S*)-CMK. Furthermore, a provisional patent has been filed and two publications have been written and will be submitted to *Journal of Organic Chemistry* and *Angewandte Chemie*.

CHAPTER 2 BACKGROUND

Applications of (*S,S*)- and (*R,S*)-CMA

(*S,S*)- and (*R,S*)-CMA are pharmaceutically relevant intermediates in the synthesis of HIV protease inhibitors. The virus requires HIV proteases for replication within an infected cell and also for release of mature viruses to infect other cells.[1] Figure 2.1 depicts the infection pathways of a cell by HIV and where protease inhibitors can alter these pathways and prevent further infection.

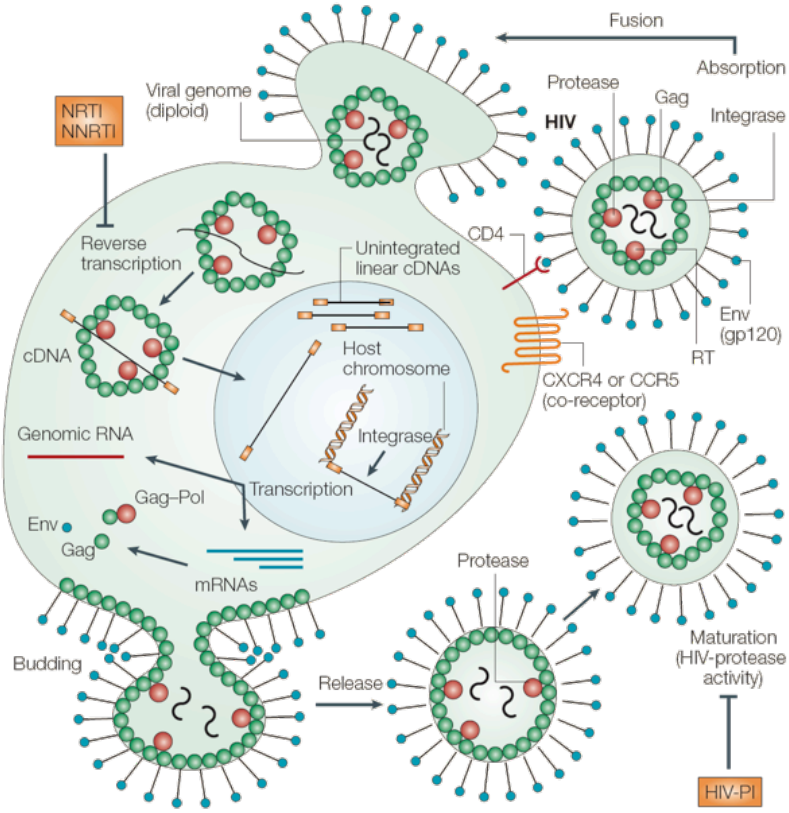

Figure 2.1: Illustration of HIV infection pathways with the effect of HIV protease inhibitors shown in orange (HIV-PI).[1]

A synthetic route to HIV protease inhibitors is well known and Figure 2.2 shows the retrosynthetic scheme to derive a few HIV protease inhibitors from (*S*)-CMK and its reduction products, (*S,S*)- and (*R,S*)-CMA. Specifically, Saquinavir®, the first HIV protease inhibitor approved by the Food and Drug Administration, and Amprenavir® derive from (*R,S*)-CMA. Likewise, (*S,S*)-CMA is a precursor to Atazanavir®. Figure 2.3 depicts the structures of these protease inhibitors. Not only do these drugs prevent the spread of HIV, but they also hold much potential for cancer treatments.[2,3]

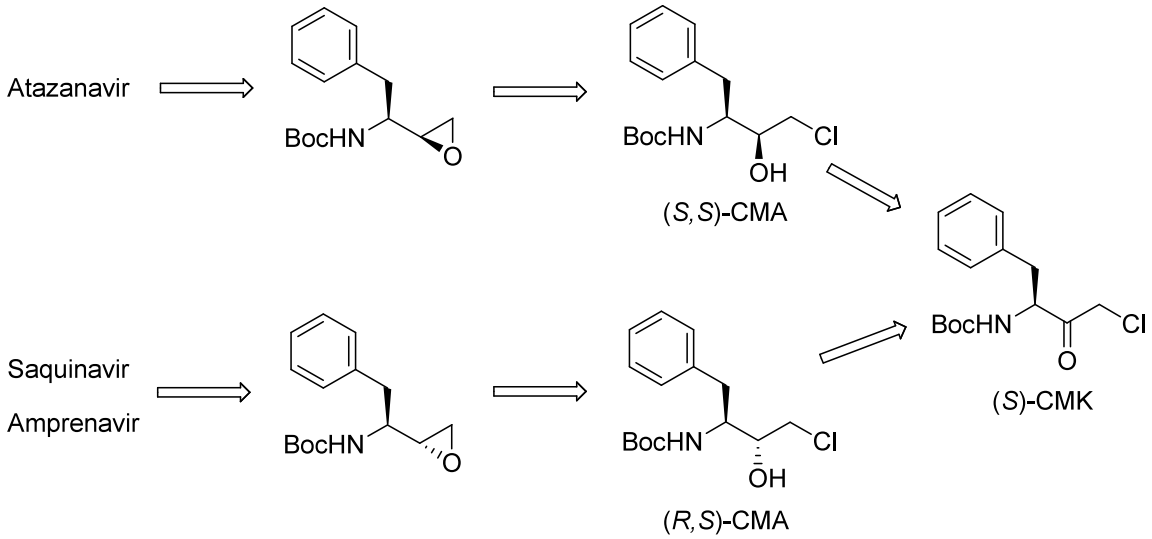

Figure 2.2: Pharmaceutical products derived from (*S*)-CMK.[4]

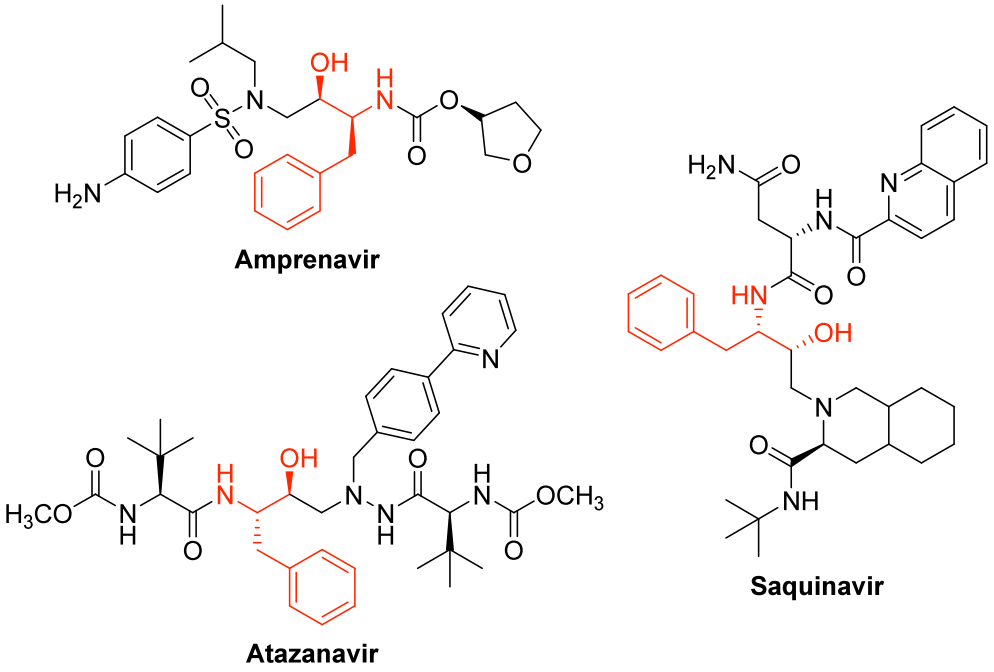

Figure 2.3: Chemical structures of some HIV protease inhibitors. Portions of the molecules deriving from (*S,S*)-CMA or (*R,S*)-CMA are highlighted in red.

(*S*)-CMK Reduction

Researchers have investigated the asymmetric synthesis of (*S,S*)- and (*R,S*)-CMA from the corresponding prochiral ketone (*S*)-CMK. Specifically, a reaction pathway starting from Boc-phenylalanine has been proposed (Figure 2.4). Boc-phenylalanine first reacts with isobutyl chloroformate (IBCF) to form a mixed anhydride. *In situ* addition of diazomethane produces a diazoketone intermediate. The diazoketone is quenched with hydrochloric acid to give (*S*)-CMK, which is finally reduced to form (*S,S*)- and (*R,S*)-CMA.

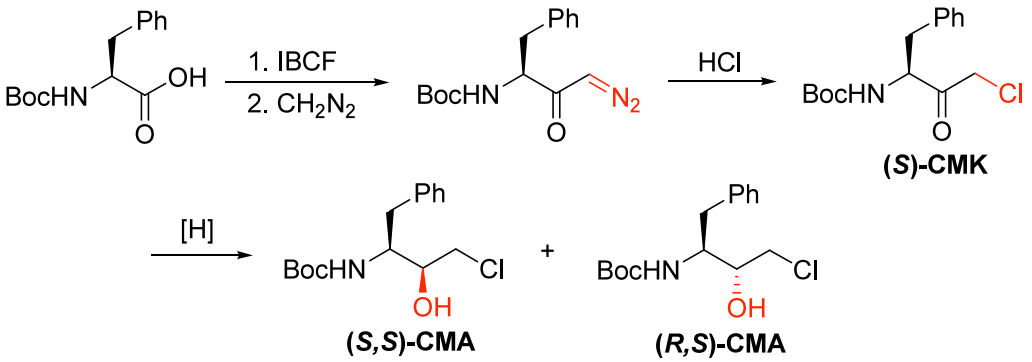

Figure 2.4: Synthetic route to (*S,S*)- and (*R,S*)-CMA from Boc-phenylalanine.

(*S*)-CMK (Figure 2.5) is a prochiral ketone with structural characteristics that must be carefully considered: (1) the carbonyl group is adjacent to a chiral center (of *S* configuration), (2) the amine is protected with a Boc group, and (3) the chloro group is in the α-position relative to the ketone. The first characteristic, the adjacent chiral center, is critical as it can be taken advantage of to induce stereoselective induction through specific interactions (steric effects or hydrogen bonding). Such interactions can participate in directing the approach of the reagent. The Boc group, although identified as the protecting group in the original synthesis of (*S*)-CMK, can be changed if necessary. In addition, as an α-chloroketone, (*S*)-CMK is highly susceptible to dehalogenation and the reaction conditions will have to be chemoselective toward the reduction of the carbonyl (Figure 2.6).

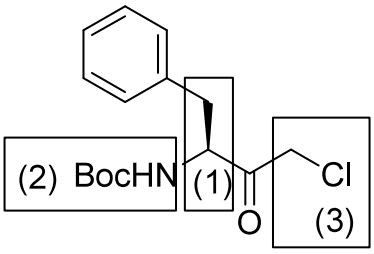

Figure 2.5: Structural characteristics of prochiral ketone (*S*)-CMK.

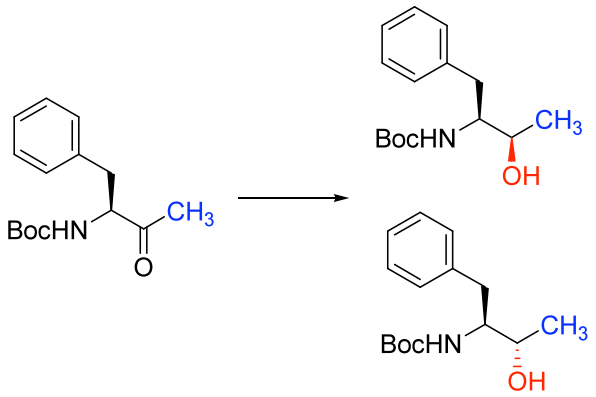

Figure 2.6: Possible dechlorination products from (*S*)-CMK reduction.

The stereoselective synthesis of the (*S,S*)- and (*R,S*)-CMA diastereomers from the corresponding prochiral ketone (*S*)-CMK was extensively investigated by academia and industry alike. The MPV reduction of (*S*)-CMK using aluminum isopropoxide in isopropanol proceeds cleanly to yield (*S,S*)-CMA in 97% yield and 94% diastereomeric excess.[5,6] The stereoselective synthesis of (*R,S*)-CMA is much more challenging. The research presented in this thesis focuses on the diastereoselective reduction of (*S*)-CMK to (*R,S*)-CMA.

(*S*)-CMK Reduction Prior Art

Aluminohydride Reduction

Aluminohydride reducing reagents, such as lithium aluminum hydride (LAH), are well known for the reduction of carbonyl groups. Researchers have investigated these reagents for the reduction of (*S*)-CMK to the corresponding alcohols. Table 2.1 summarizes these results. The highest ratio of (*R,S*)-CMA to (*S,S*)-CMA published was 8:1 with lithium tri-(*tert*-butoxy) aluminum hydride as the reagent.[5,6] Reagents like LAH or DIBAL-H (diisobutylaluminum hydride) gave much lower diastereomeric ratios of 0.5:1 or less.[7] Although lithium tri-(*tert*-butoxy) aluminum hydride has produced a good

product distribution, aluminohydride reducing reagents are expensive for large-scale industrial considerations and are sensitive to atmospheric moisture, making them difficult to handle.

Table 2.1: Reduction of (*S*)-CMK with aluminohydride reagents.

Reagent	(*R,S*):(*S,S*)	Reference
$Li(OtBu)_3AlH$	8:1	5,6
LAH	0.5:1	5,6
DIBAL-H	0.08:1	7

Biotransformation

Microorganisms like enzymes make excellent chiral catalysts and have been widely studied in the literature for asymmetric transformations. Bristol-Myers Squibb Pharmaceuticals reported extensive studies on microorganism-catalyzed reduction of (*S*)-CMK. They originally screened 120 microorganisms and obtained yields as high as 98% with 99% diastereomeric excess of the (*R,S*) product in their best system.[8] The researchers also analyzed the microorganisms for the optimal synthesis of (*S,S*)-CMA.[9,10] From a practical standpoint, however, microorganisms are expensive and their handling requires specific conditions (temperature, solvents, pH, etc.) that may limit their application to large-scale synthesis.

Borohydride Reduction

Borohydride reagents alone or with modifiers represent a powerful group of reducing reagents that often offer greater chemoselectivity than their aluminohydride analogs. Borohydride reagents are also much cheaper and not overly sensitive to air or moisture. Borohydride reagents, such as selectrides (K, L, N, KS, LS)[5,6] and sodium

borohydride,[5-7,11] were investigated for the stereoselective reduction of (*S*)-CMK. K-Selectride provided the best stereoselectivity of all the reagents investigated, yielding a diastereomeric ratio [(*R,S*)-CMA:(*S,S*)-CMA] of 2:1. Table 2.2 summarizes the results of the borohydride reductions.

Table 2.2: Reduction of (*S*)-CMK using borohydride reducing agents.[5,6]

Reagent	(*R,S*):(*S,S*)
K-Selectride	2:1
KS-Selectride	2:1
L-Selectride	0.9:1
N-Selectride	0.7:1
$NaCNBH_3$	0.7:1
$NaBH_4$	0.6:1
LS-Selectride	0.5:1

Catalytic Hydrogenation

The stereoselective reduction of (*S*)-CMK can be induced by the adjacent chiral center. However, Pennington and Hodgson[12] utilized chiral homogeneous ruthenium, rhodium, and iridium catalysts to achieve high diastereoselectivity. The metal center was coordinated to a chiral phosphine and amine group, which have been previously shown to increase the catalyst's activity and stereoselectivity. The researchers reported good conversions and ratios of (*R,S*)-CMA to (*S,S*)-CMA as high as 19:1 with moderate pressures of hydrogen in various alcohol solvents like methanol and ethanol. However, the use of expensive chiral catalysts somewhat mitigate the potential industrial interest in this strategy.

Asymmetric Transfer Hydrogenation

ATH reactions often utilize sodium formate or alkylammonium formate as a hydrogen source combined with a homogeneous chiral catalyst.[13-15] Metals that have been used to catalyze ATH reactions include rhodium, iridium, and ruthenium. ATH reactions have been investigated with (*S*)-CMK as the starting material in a variety of solvents with similar results: ~90% selectivity for either diastereomer (depending on the chirality of the catalyst).[4] Although these reactions give very high selectivity, the chiral ligands are expensive and usually must be synthesized.

Meerwein-Ponndorf-Verley Reduction

MPV reductions use aluminum isopropoxide (or another metal alkoxide) with an alcohol to perform the hydrogen transfer.[16,17] The MPV reduction of (*S*)-CMK generally favors (*S,S*)-CMA, even when run in various solvents. Researchers reported diastereomeric ratios of (*R,S*)-CMA to (*S,S*)-CMA of 0.05:1.[5,6]

REFERENCES

(1) Monini, P.; Sgadari, C.; Toschi, E.; Barillari, G.; Ensoli, B. *Nature Reviews Cancer* **2004**, *4*, 861-875.

(2) Pyrko, P.; Kardosh, A.; Wang, W.; Xiong, W.; Schonthal, A.; Chen, T. *Cancer Research* **2007**, *67*, 10920-10928.

(3) Gills, J.; Lo Piccolo, J.; Tsurutani, J.; Shoemaker, R.; Best, C.; Abu-Asab, M.; Borojerdi, J.; Warfel, N.; Gardner, E.; Danish, M.; Hollander, M.; Kawabata, S.; Tsokos, M.; Figga, W.; Steeg, P.; Dennis, P. *Clinical Cancer Research* **2007**, *13*, 5183-5194.

(4) Hamada, T.; Torii, T.; Onishi, T.; Izawa, K.; Ikariya, T. *Journal of Organic Chemistry* **2004**, *69*, 7391-7394.

(5) Malik, A. A.; Clement, T. E.; Palandoken, H.; Robinson III, J.; Stringer, J. A. US Patent, 2003.

(6) Malik, A. A.; Clement, T. E.; Palandoken, H.; Robinson III, J.; Stringer, J. A. US Patent, 2005.

(7) Yin, J. J.; Huffman, M. A.; Conrad, K. M.; Armstrong, J. D. *Journal of Organic Chemistry* **2006**, *71*, 840-843.

(8) Patel, R. N.; Chu, L.; Mueller, R. *Tetrahedron-Asymmetry* **2003**, *14*, 3105-3109.

(9) Patel, R. N. *Journal of the American Oil Chemists Society* **1999**, *76*, 1275-1281.

(10) Patel, R. N.; Banerjee, A.; McNamee, C. G.; Brzozowski, D. B.; Szarka, L. J. *Tetrahedron-Asymmetry* **1997**, *8*, 2547-2552.

(11) Wang, D. J.; Schwinden, M. D.; Radesca, L.; Patel, B.; Kronenthal, D.; Huang, M. H.; Nugent, W. A. *Journal of Organic Chemistry* **2004**, *69*, 1629-1633.

(12) Pennington, M.; Hodgson, A. In *WO 2006/016116* 2006.

(13) Alonso, D. A.; Brandt, P.; Nordin, S. J. M.; Andersson, P. G. *Journal of the American Chemical Society* **1999**, *121*, 9580-9588.

(14) Yamakawa, M.; Ito, H.; Noyori, R. *Journal of the American Chemical Society* **2000**, *122*, 1466-1478.

(15) Noyori, R.; Yamakawa, M.; Hashiguchi, S. *Journal of Organic Chemistry* **2001**, *66*, 7931-7944.

(16) de Graauw, C.; Peters, J.; van Bekkum, H.; Huskens, J. *Synthesis* **1994**, 1007-1017.

(17) Wilds, A. *Organic Reactions* **1944**, *2*, 178-223.

CHAPTER 3 MEERWEIN-PONNDORF-VERLEY REDUCTIONS

INTRODUCTION

The Meerwein-Ponndorf-Verley (MPV) reduction[1-3] of a carbonyl-containing substrate to its corresponding alcohol has been used extensively in organic chemistry because of its simple and inexpensive reaction procedure.[4-6] The MPV reduction is straightforward, utilizes mild reagents (aluminum alkoxides), and is chemoselective. However, more than catalytic amounts of the metal catalyst may be required to achieve high yields in a reasonable amount of time. Generally, the MPV reduction is catalyzed by metal alkoxides and utilizes a secondary alcohol as a hydride source. Most often, this reaction is carried out using aluminum isopropoxide in isopropanol (Figure 3.1), but other metal reagents, such as lanthanide metals, have also been reported.[7-9]

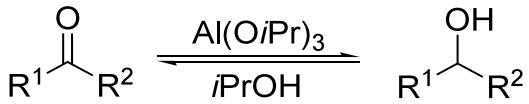

Figure 3.1: General MPV reduction scheme.

Stereoselective MPV reductions have been performed by varying the reaction conditions. One approach capitalized on using optically active alcohols as the solvent. Although enantioselectivity was successfully observed in a few cases, the enantiomeric excess usually remains moderate and mostly unpractical.[10] For example, when methylcyclohexylketone was reduced in the presence of (*S*)-3-methyl-2-butanol, the product (*S*)-1-cyclohexylethanol was produced in 22% enantiomeric excess.[11] Another

approach focused on utilizing chiral and/or bulky groups, such as 1,1'-bi-2-naphthol (BINOL), on the aluminum.[12-14] When BINOL was added to the reduction of 2-chloroacetophenone, the product, (*R*)-chloromethylbenzyl alcohol, was produced in 80% enantiomeric excess.[15] In addition to the moderate enantiomeric induction, the cost of these approaches can be prohibitive to large scale applications. Therefore, achieving sustainable (efficient and cost-effective) stereoselective induction via MPV mediated processes remains a major challenge.

As discussed in Chapter 2, many scientists have investigated the means to selectively prepare (*S,S*)- and (*R,S*)-CMA from the corresponding prochiral ketone (*S*)-CMK. The MPV reduction of (*S*)-CMK using aluminum isopropoxide in isopropanol proceeds cleanly to yield (*S,S*)-CMA in 97% yield and 94% diastereomeric excess.[16,17] The stereoselective synthesis of (*R,S*)-CMA, however, remains an ongoing challenge. Although a wide variety of reagents for the production of (*R,S*)-CMA were investigated, the techniques that produce (*R,S*)-CMA with high yields and stereoselectivity remain expensive or inefficient.

This work aims to develop a cost-effective and diastereoselective MPV reduction process to produce (*R,S*)-CMA. The transition state complex between aluminum isopropoxide and (*S*)-CMK was studied using Spartan® modeling calculations. Based on these models, potential approaches to favor (*R,S*)-CMA selectively were identified, experimentally tested, and analyzed. Additionally, experiments showed that the states of aggregation of the aluminum alkoxides are critical to the rates of the reactions. A comparison between aluminum isopropoxide (a tetramer) and aluminum *tert*-butoxide (a dimer) is presented.

BACKGROUND

MPV Reduction Mechanism

Figure 3.2 shows the mechanism of the MPV reduction of a ketone.[18] The reaction is equilibrium limited; in fact, the opposite reaction is known as the Oppenauer oxidation,[19] which oxidizes an alcohol to a ketone. In order for the MPV reduction to proceed, at least one of the alkoxide groups attached to the metal center must have an α-hydrogen. The α-hydrogen from the alkoxide on the catalyst is transferred to the ketone via a six-member ring concerted mechanism. The chair conformation of this six-member ring is shown in Figure 3.3. The alcohol product is released upon substitution by another alcohol moiety or quenching with water or acid.

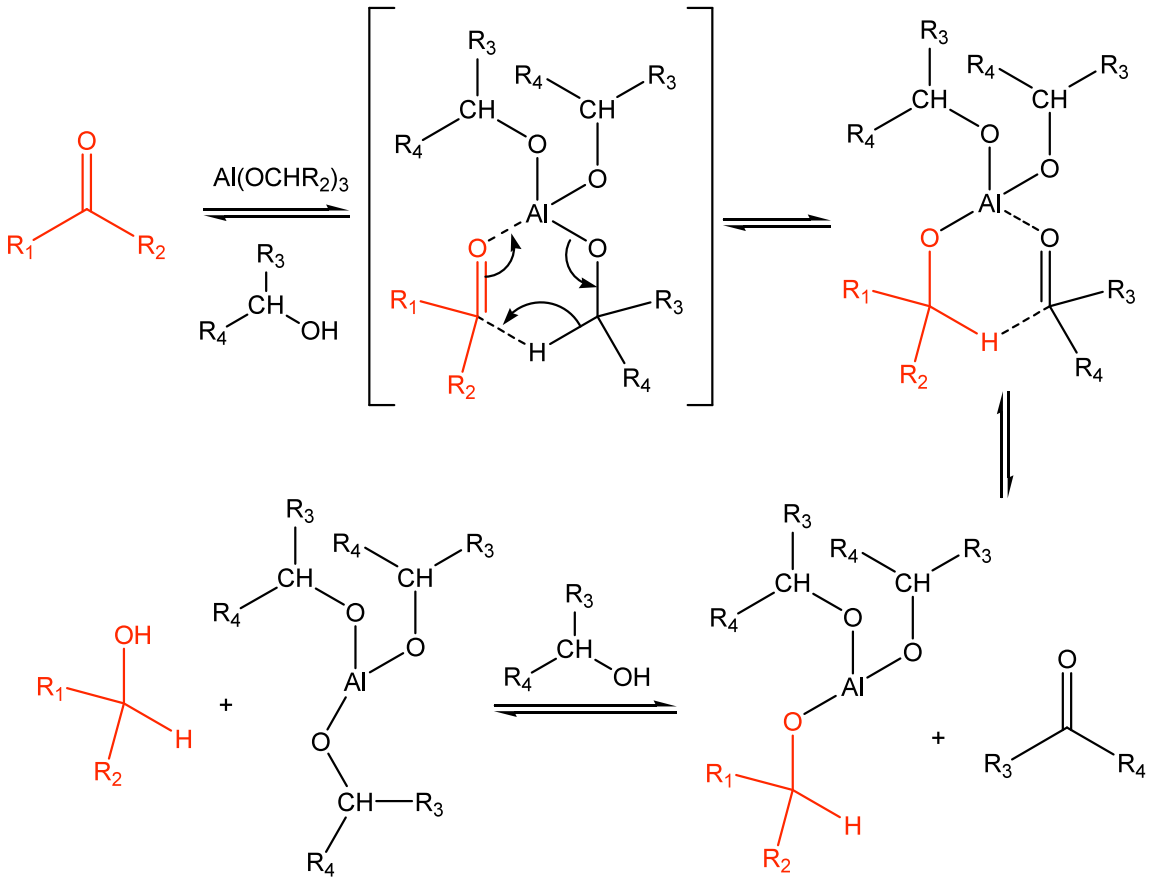

Figure 3.2: MPV reduction reaction mechanism.

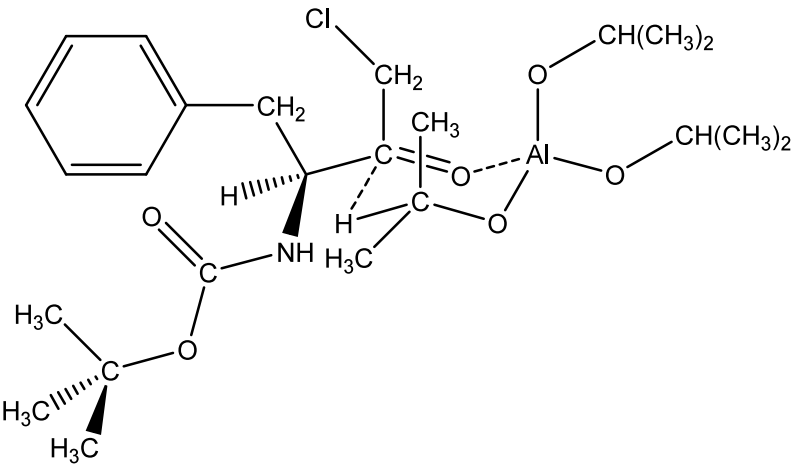

Figure 3.3: Transition state complex between (*S*)-CMK and Al(O*i*Pr)$_3$ leading to the (*R,S*)-CMA product.

Transition State Modeling Studies

The chiral center adjacent to the ketone of (*S*)-CMK is crucial as it can be taken advantage of to induce stereoselective induction through specific interactions (steric effects and hydrogen bonding).[20] For instance, the Boc-protected amine group leaves a relatively acidic hydrogen free to engage in hydrogen bonding. Such interactions can participate in directing the approach of the reagent. Ideally, these effects would favor the desired product without the use of chiral catalysts and ligands. Spartan® modeling studies (Hartree Fock level with a basis set of 6-31G*) indicate that the chelation between the aluminum species and the Boc-protected amine on (*S*)-CMK is central to the final stereochemistry of the product. If the aluminum chelates with only the ketone, hydrogen transfer on the least hindered face results in the (*R,S*) diastereomer (Figure 3.4 A). On the other hand, if the aluminum isopropoxide coordinates with both the ketone and amide groups, hydrogen transfer to the least hindered face results in the (*S,S*) diastereomer (Figure 3.4 B). Most importantly, the oxygen from the alkoxide and the hydrogen on the amide can engage in hydrogen bonding. Because of these interactions, the hydrogen transfer preferentially favors the formation of the (*S,S*)-CMA product, as observed by the experimental results.

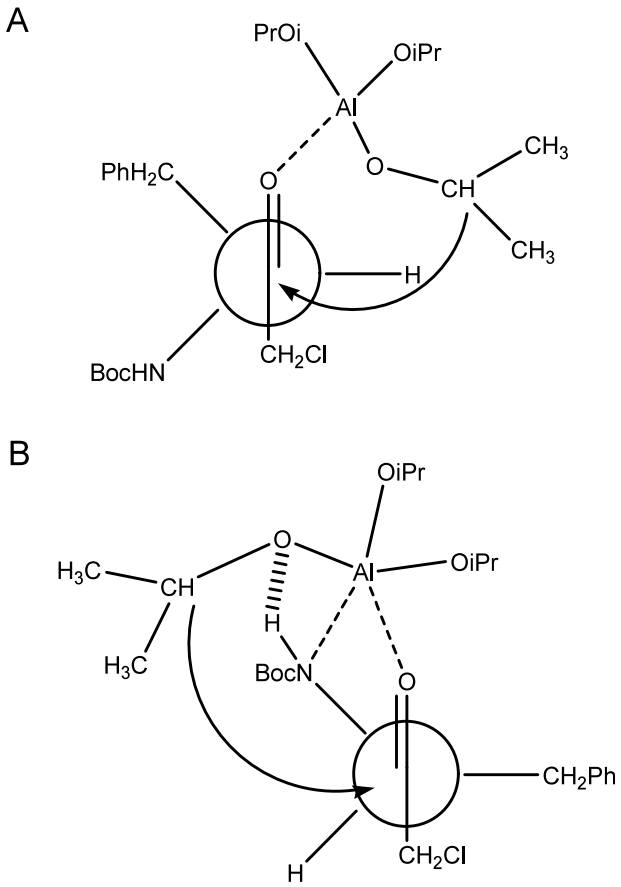

Figure 3.4: MPV reduction intermediate. A: Mono-chelation between aluminum and ketone. B: Hydrogen bonding and bi-chelation with ketone and nitrogen.

In light of these studies, approaches to disrupt the hydrogen bonding and alter the diastereoselectivity were investigated as a function of (1) steric bulkiness of the aluminum reagent, (2) solvents, and (3) amine protecting groups on (*S*)-CMK. The results of the first two effects are discussed below and the effect of the protecting group will be discussed in Chapter 6.

RESULTS AND DISCUSSION

Investigation of Diastereoselectivity

I started my investigation of the MPV reduction by looking into the effect of a few reaction conditions on the diastereoselectivity of the reaction. The reactions were first run on a batch scale and then repeated in a 12-reaction carousel apparatus to improve reproducibility.

Batch Scale Reactions

I initially performed the MPV reductions on a 20 mL batch scale in round bottom flasks. The reaction products were isolated and analyzed by proton nuclear magnetic resonance (^{1}H NMR) and/or high performance liquid chromatography (HPLC). Each reaction was run once.

Reductions in Various Alcohol Solvents

I first ran the MPV reduction in anhydrous isopropanol using aluminum isopropoxide as described in the literature for the preparation of the (*S,S*) diastereomer (Figure 3.5).[16,17] This reaction allowed me to validate my analytical methods and provided a reference point. The starting material, (*S*)-CMK, was dissolved in anhydrous isopropanol at 50°C followed by the addition of aluminum isopropoxide. The reaction went to near completion after two hours, at which point the product precipitated out of solution. The organic product was collected by filtration and characterized by ^{1}H NMR and HPLC. The HPLC analysis resulted in a diastereomeric ratio of (*R,S*):(*S,S*) (abbreviated DR) of 0.06:1, comparable to literature results of 0.05:1.[16] (*R,S*)-CMA was not detected by ^{1}H NMR.

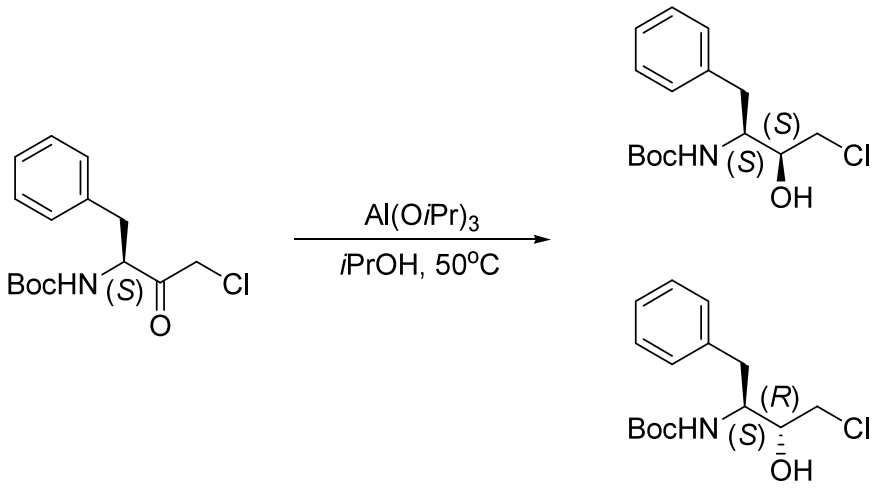

Figure 3.5: MPV reduction of (*S*)-CMK.

The MPV reduction was run in other anhydrous alcohol solvents including 2-butanol, *tert*-butanol, and a 1:1 mixture of isopropanol and *tert*-butanol. I hypothesized that increasing the steric bulk around the aluminum center would improve the diastereoselectivity of the reaction. The results are summarized in Table 3.1. Complete conversion was observed after one hour when 2-butanol was the solvent, but the reaction in *tert*-butanol was much slower. After four hours, there was still 90% of the starting material remaining. The mixed isopropanol/*tert*-butanol solvent showed about 10% starting material left after four hours. The *tert*-butanol partially displaces the isopropoxy groups on the aluminum, replacing them with *tert*-butoxy groups, which do not have an available α-hydrogen. As a consequence, the reaction was expected to be slower. Most interestingly, the increased steric hindrance of the *tert*-butoxy groups had little effect, if any, on the diastereoselectivity. Although the rate of the reactions changed, the distribution of products remained consistently in favor of (*S,S*)-CMA. Table 3.1 clearly shows that the effect was negligible on the DR and detrimental on the reaction rate.

Table 3.1: MPV reductions in alcohol solvents.

Al Catalyst	Alcohol	Time (h)	Conversion	DR (HPLC)	DR (NMR)
$Al(O\text{-}i\text{-}Pr)_3$	*i*-PrOH	2	95%	0.06:1	[a]
$Al(O\text{-}i\text{-}Pr)_3$	2-BuOH	1	95%	0.06:1	0.03:1
$Al(O\text{-}i\text{-}Pr)_3$	*i*-PrOH/*t*-BuOH (1:1)	4	88%	0.06:1	0.08:1
$Al(O\text{-}i\text{-}Pr)_3$	*t*-BuOH	4	10%	[b]	[a]

[a]Quantity of (*R,S*)-CMA too small to see by ^{1}H NMR.
[b]Quantity of (*R,S*)-CMA too small to see by HPLC.

Reduction with Synthesized Aluminum Isopropoxide

I synthesized aluminum isopropoxide to compare to the results obtained using the commercially available aluminum isopropoxide. Aluminum isopropoxide was synthesized according to a reported literature procedure.[21] The reaction between aluminum foil and anhydrous isopropanol was catalyzed by carbon tetrachloride. The reaction was run at reflux until all of the foil had been consumed. Although the reaction mixture had black suspended flakes, I used the aluminum isopropoxide solution directly in an MPV reduction, assuming complete conversion of the foil to calculate the concentration of aluminum isopropoxide.

The reaction was run in isopropanol and the product crashed out of solution after two hours. Although the reaction mixture was slightly grey, the product became white after washing. The product was analyzed by HPLC and ^{1}H NMR to give DRs of 0.1:1 and 0.07:1, respectively. These results are comparable to the commercial aluminum alkoxide DR of 0.06:1.

Reductions with Different Aluminum Alkoxides

Aluminum-tri-*sec*-butoxide and aluminum *tert*-butoxide, were investigated as potential catalysts to evaluate the relationship between the structure of the alkoxide on the catalyst and the diastereoselective induction. Aluminum-tri-*sec*-butoxide and

aluminum *tert*-butoxide are both available for purchase from Aldrich. Following the classic MPV procedure described previously, reactions with aluminum-tri-*sec*-butoxide and aluminum *tert*-butoxide were carried out in anhydrous 2-butanol. No visible product crashed out after a few hours therefore the reactions were continued at 50°C overnight. After running overnight, the product crashed out and analyses showed the complete conversion of the starting material to the two product diastereomers. HPLC analysis showed no significant change from the reaction with aluminum isopropoxide, giving DRs of 0.04:1 and 0.06:1, respectively. Since there did not seem to be any improvement in diastereoselectivity with the change in aluminum alkoxide catalyst, this strategy was not investigated further.

Reductions in Various Organic Solvents

In an attempt to alter the potential hydrogen bonding between the oxygen of the aluminum alkoxide and the hydrogen of the amine group of (*S*)-CMK, the reaction was run in various solvents with a wide range of polarity and hydrogen bond donor/acceptor abilities. I tested acetonitrile, tetrahydrofuran (THF), ethyl acetate, diethylether, benzene, and dimethyl sulfoxide (DMSO). Although the concentrations of the starting material and the aluminum isopropoxide were kept constant, the volume of isopropanol was decreased from 20 mL to 0.5 mL and the additional organic solvent (19.5 mL) was added. It should be iterated that isopropanol is the hydrogen source and is actively involved in the reaction mechanism. Because these reactions were slower, all of them were run at 50°C overnight. The products were analyzed by HPLC and the results of these reactions are given in Table 3.2.

Table 3.2: MPV reductions in various organic solvents.

Solvent	Conversion	DR
MeCN	62%	0.35:1
THF	56%	0.19:1
EtOAc	21%	0.17:1
Et_2O	56%	0.11:1
Benzene	63%	0.09:1
DMSO	7%	[a]

[a]Quantity of (*R,S*)-CMA too small to see by HPLC.

Although some of the solvents showed improved diastereoselectivity, the overall conversion was much lower than in the alcohol solvents, which gave >95% conversion. Most notably, acetonitrile, with the strongest hydrogen bond donating and accepting properties, gave the highest DR of 0.35:1.

Reductions with Hydrogen Bonding Additives

The addition of compounds with hydrogen bonding properties was investigated as a means to alter the diastereoselectivity of the MPV reduction. First, lithium fluoride was investigated. It was added to the reaction in a 1:1 molar ratio to (*S*)-CMK. The reaction was run overnight. The HPLC results showed no improvement in the DR (0.04:1) with respect to the reaction performed without lithium fluoride.

Tetrabutylammonium fluoride (TBAF) also contains a fluoride anion that can engage in hydrogen bonding. In addition, it is more soluble in organic media than the inorganic salt lithium fluoride due to the lipophilic tetraalkylammonium cation. TBAF is commercially available as a solution in THF with about 5 weight% water. The presence of water is a limitation because the aluminum isopropoxide reagent is water sensitive. Therefore, the TBAF solution was dried for 24 hours over molecular sieves. After the removal of the molecular sieves, the reagents were added as described previously. I

initially used a 0.1:1 molar ratio of TBAF to (*S*)-CMK. HPLC analysis showed a slight improvement in the production of (*R,S*)-CMA, giving a DR of 0.14:1. Because of this slight improvement, I increased the molar ratio of TBAF to (*S*)-CMK up to 1:1. The DR was identical at 0.14:1.

Carousel Reactions

In order to ensure the reproducibility of our results, a 12-reaction carousel from Brinkmann was purchased (Figure 3.6). The apparatus allows for twelve reactions to be carried out simultaneously with a controlled temperature, controlled stirring, and options of being under inert atmosphere as well as operating under reflux conditions. The workup procedure was also modified. Rather than isolating the products, the post-reaction mixtures were diluted with ethyl acetate or methanol, quenched with hydrochloric acid, and injected directly in the HPLC for analysis. The reactions were run on a 5 mL scale and, unless otherwise noted, these reactions were all run in triplicate.

Figure 3.6: Brinkmann 12-reaction carousel apparatus.

Reductions with Aluminum Alkoxides

One method originally proposed to increase the diastereoselectivity of the MPV reduction was to vary the alkoxide group on the aluminum catalyst. As stated previously, we hypothesized that increasing the steric bulk around the aluminum metal center would improve the diastereoselectivity. In addition to using the aluminum isopropoxide catalyst, we also tested aluminum *tert*-butoxide and aluminum ethoxide. We heated a solution of (*S*)-CMK and the aluminum catalyst in anhydrous isopropanol to the reaction temperature of 50°C. At 50°C the solutions were all homogeneous. Interestingly, the aluminum *tert*-butoxide reactions precipitated after about five minutes, the aluminum ethoxide reactions precipitated after about an hour, and the aluminum isopropoxide reactions precipitated after one and a half hours. Since the product is less soluble in isopropanol than the starting ketone, the rate of precipitation is indicative of the rate of the reaction. An increase in reaction rate was unexpected and this effect was

investigated separately. The results of these kinetic studies are presented below. Although the reactions qualitatively appear complete, they were carried out regardless for two hours and then quenched with 2 M hydrochloric acid. The products were extracted into ethyl acetate. The results of the HPLC analysis are given in Table 3.3. Despite slight differences in conversion and yield among the aluminum alkoxides, there was no significant improvement in diastereoselectivity.

Table 3.3: MPV reduction with aluminum alkoxides.

	DR	% Conversion	% Yield
$Al(O\textit{t}Bu)_3$	0.05 ± 0.01	99 ± 0.2	86 ± 1.3
$Al(OEt)_3$	0.06 ± 0.00	90 ± 2.1	76 ± 0.7
$Al(O\textit{i}Pr)_3$	0.06 ± 0.00	89 ± 5.4	71 ± 5.2

Reductions in Various Organic Solvents

The Spartan® molecular modeling discussed previously suggests that hydrogen bonding could occur between the oxygen atoms of aluminum isopropoxide and the NH group of (*S*)-CMK. As a consequence, preventing this hydrogen bonding from occurring might alter the diastereoselectivity. To validate this hypothesis, MPV reductions were run in various organic solvents, some of which might disrupt the hydrogen bonding between the aluminum isopropoxide and (*S*)-CMK. Isopropanol (10 vol%) was added to each solvent for the reaction to proceed in a reasonable time. The solvents chosen for these experiments were ethyl acetate, THF, isopropyl acetate, *tert*-butanol, 2-butanol, dichloromethane (DCM), and toluene. After loading the reaction tubes with (*S*)-CMK, aluminum isopropoxide, and the anhydrous solvent mixtures, the reactions were run overnight at 50°C. Then each post-reaction mixture was put in an ice bath, diluted with methanol, and quenched with 2 M hydrochloric acid before being analyzed by HPLC. Table 3.4 shows the results of these reactions.

Table 3.4. MPV reduction of (*S*)-CMK in various organic solvents.

Solvent	(*R,S*)/(*S,S*)	% Conversion	% Yield
EtOAc	0.24 ± 0.01	73 ± 1.1	58 ± 1.0
THF	0.13 ± 0.01	92 ± 5.2	85 ± 5.2
iPrOAc	0.09 ± 0.00	100 ± 0.0	91 ± 0.6
t-BuOH	0.08 ± 0.00	98 ± 0.6	85 ± 1.3
2-BuOH	0.05 ± 0.00	98 ± 0.2	91 ± 0.6
DCM	0.05 ± 0.00	100 ± 0.0	95 ± 1.5
Toluene	0.05 ± 0.01	100 ± 0.0	90 ± 1.4

The DR increased when the reaction was run in aprotic polar solvents like ethyl acetate and THF. However, these solvents also generally produce lower yields and conversions. The hydrogen bonding between (*S*)-CMK and aluminum isopropoxide most likely contributes to increasing the rate of reaction by keeping (*S*)-CMK coordinated with the aluminum center, bringing to close proximity the two reactive centers. I hypothesized that the MPV reduction in ethyl acetate may lead to more byproducts because the solvent and isopropanol can undergo trans-esterification, decreasing the amount of isopropanol that is available for proton transfer. This was confirmed by running the MPV reduction in isopropyl acetate. The product yield dramatically increased from 58% in ethyl acetate to 91% in isopropyl acetate. Unfortunately, the DR decreased from 0.24:1 in ethyl acetate to 0.09:1 in isopropyl acetate.

Investigation of Reaction Kinetics

It was observed that the rate of the reaction was drastically increased by switching the catalyst from aluminum isopropoxide to aluminum *tert*-butoxide. This is a critical observation because utilizing aluminum *tert*-butoxide instead of aluminum isopropoxide for MPV reductions could save both time and money in industrial processes. The MPV reductions of (*S*)-CMK, acetophenone, and benzaldehyde were investigated with aluminum isopropoxide and aluminum *tert*-butoxide.

Reduction of (*S*)-CMK

The MPV reduction of (*S*)-CMK was initially performed in isopropanol at 50°C using aluminum isopropoxide. A set of twelve identical reactions were run simultaneously and quenched at ten-minute intervals over the course of two hours. The same experiment was run using aluminum *tert*-butoxide as the catalyst with the reactions quenched every five minutes for one hour. These kinetic experiments were run in triplicate and the results are shown in Figure 3.7. The reactions with aluminum *tert*-butoxide achieve 90% yield in fifteen minutes, while the aluminum isopropoxide reactions reach less than 10% yield in the same time period. These reactions were repeated in a 9:1 toluene/isopropanol solvent mixture (Figure 3.8). Again, aluminum *tert*-butoxide showed higher activity than aluminum isopropoxide. Because of a dilution effect, the MPV reduction in toluene required about twice as long to achieve the same product yield as the reaction in pure isopropanol.

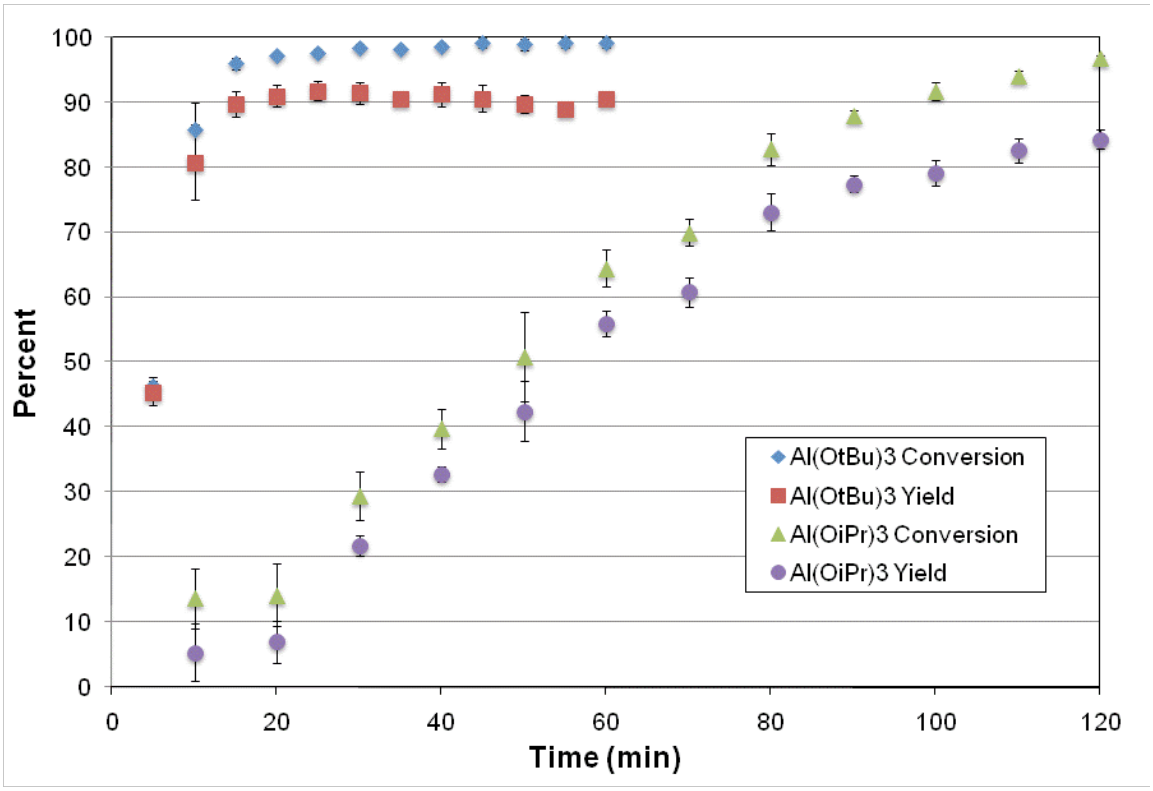

Figure 3.7. Reaction conversion and yield as a function of time for the MPV reduction of (*S*)-CMK in isopropanol catalyzed by Al(O*t*Bu)$_3$ or Al(O*i*Pr)$_3$.

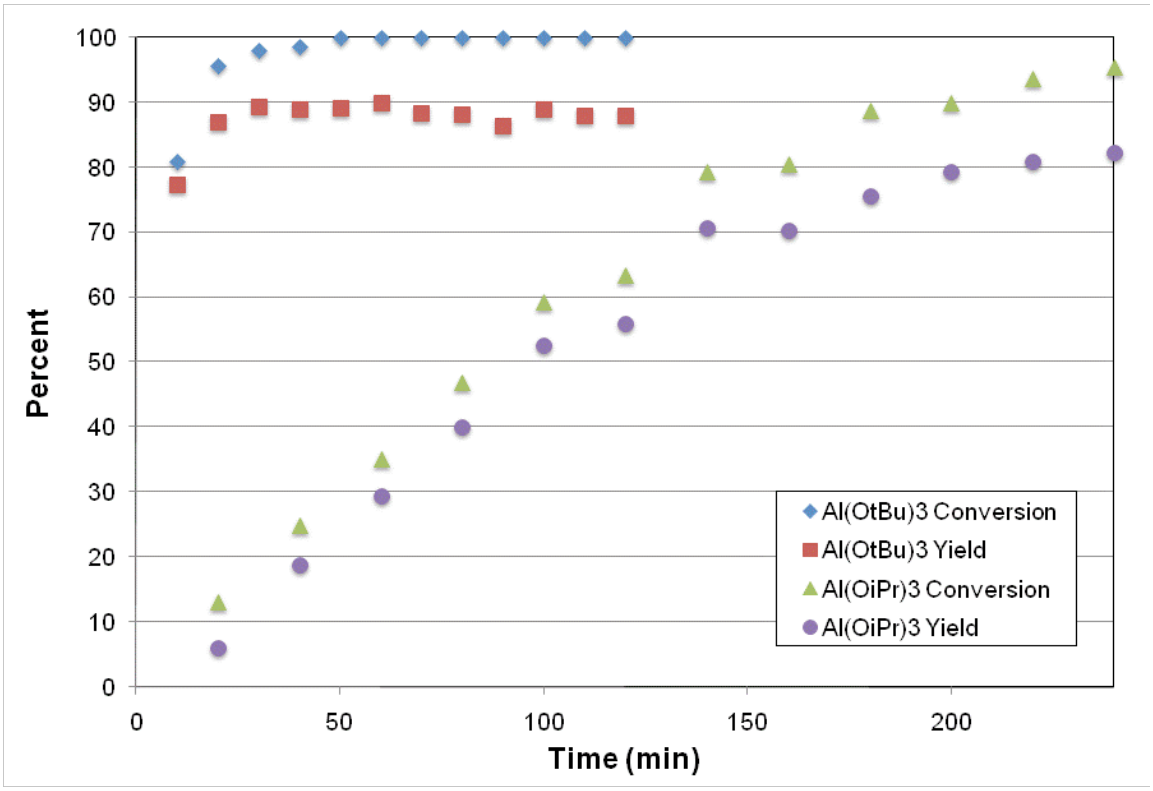

Figure 3.8. Reaction conversion and yield as a function of time for the MPV reduction of (*S*)-CMK in 9:1 toluene/isopropanol catalyzed by Al(O*t*Bu)$_3$ or Al(O*i*Pr)$_3$.

Reduction of Acetophenone

The kinetics of the MPV reduction of acetophenone and benzaldehyde were also investigated. For the reduction of acetophenone to *sec*-phenylethanol, the reactions with aluminum *tert*-butoxide and aluminum isopropoxide were conducted at 50°C in anhydrous isopropanol. The reactions with aluminum *tert*-butoxide were stopped every fifteen minutes for three hours and the reactions with aluminum isopropoxide ran for seven hours with reactions stopped every 35 minutes. Figure 3.9 shows the results of these reactions run in triplicate with the percent yield of *sec*-phenylethanol plotted over time. The reduction with aluminum *tert*-butoxide yields about 75% product after three hours while it takes the aluminum isopropoxide reactions seven hours to reach the same

level of completion. A similar trend was observed when the same reactions were run in a 9:1 toluene/isopropanol solvent mixture (Figure 3.10).

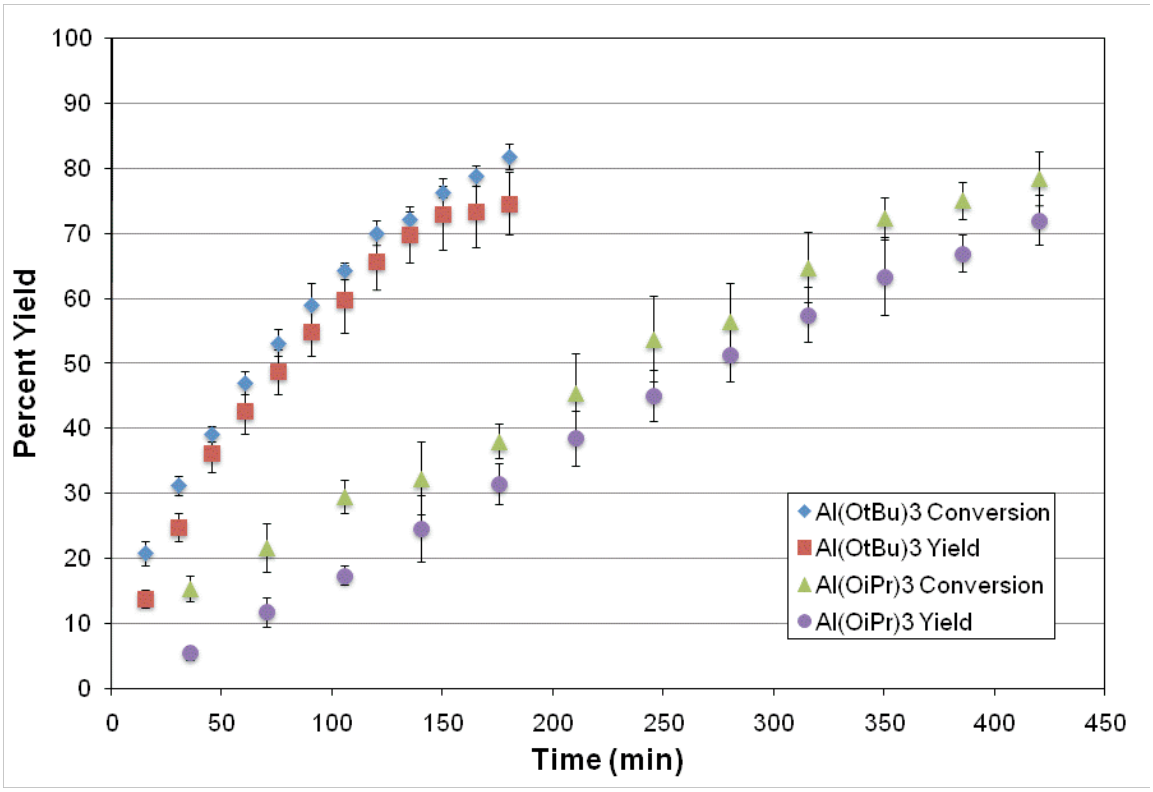

Figure 3.9. Reaction conversion and yield as a function of time for the MPV reduction of acetophenone in isopropanol catalyzed by Al(O*t*Bu)$_3$ and Al(O*i*Pr)$_3$.

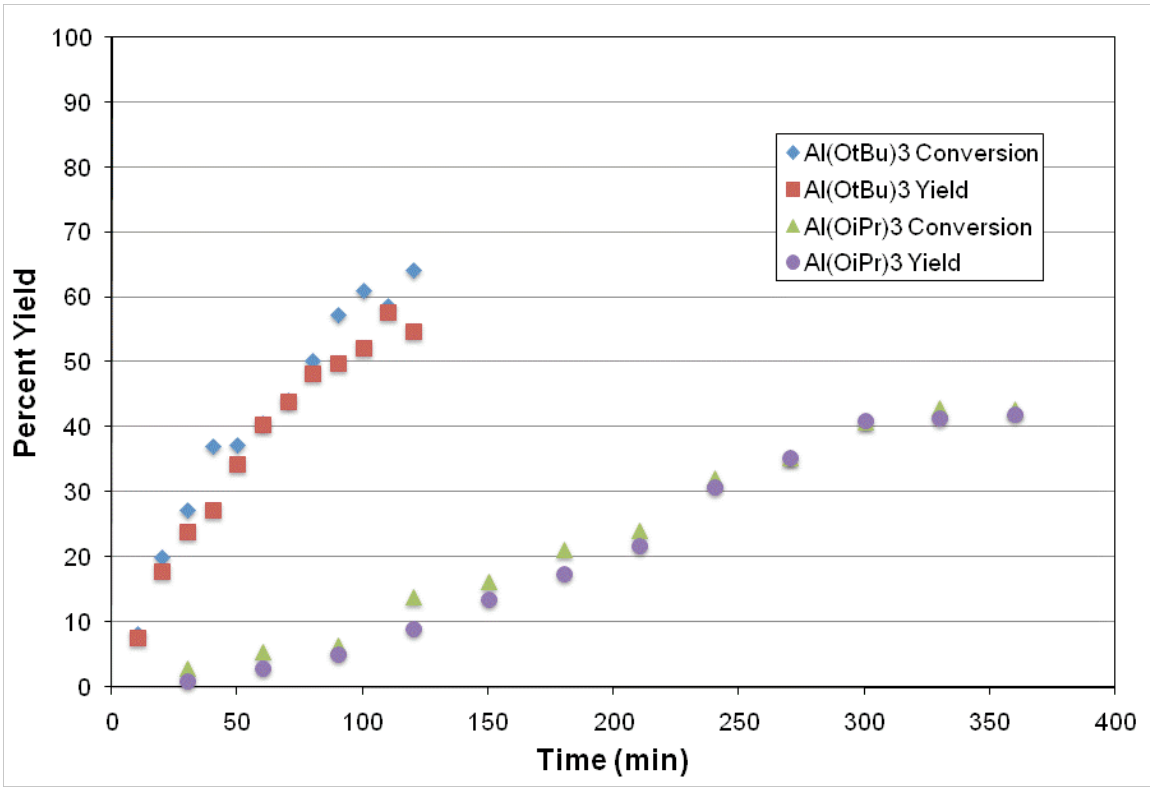

Figure 3.10. Reaction conversion and yield as a function of time for the MPV reduction of acetophenone in 9:1 toluene/isopropanol catalyzed by Al(O*t*Bu)$_3$ and Al(O*i*Pr)$_3$.

Reduction of Benzaldehyde

The MPV reduction of benzaldehyde to benzylalcohol was conducted using both aluminum isopropoxide and aluminum *tert*-butoxide following the same procedure as with acetophenone. Because of the increased reactivity of the aldehyde, the reaction was carried out at 40°C instead of 50°C. Each reaction was run three times. The results of the MPV reductions of benzaldehyde are shown in Figure 3.11. Again, the rate increase using aluminum *tert*-butoxide compared to aluminum isopropoxide is evident from this data. The reduction using aluminum *tert*-butoxide reaches over 80% yield in less than ten minutes, whereas the aluminum isopropoxide reaction requires 90 minutes to achieve the same yield. In addition, the reaction in 9:1 toluene/isopropanol takes three times as long when the catalyst is aluminum isopropoxide instead of aluminum

tert-butoxide (Figure 3.12). These experiments show that the rate enhancement of aluminum *tert*-butoxide over aluminum isopropoxide applies to aldehyde as well as ketone starting materials.

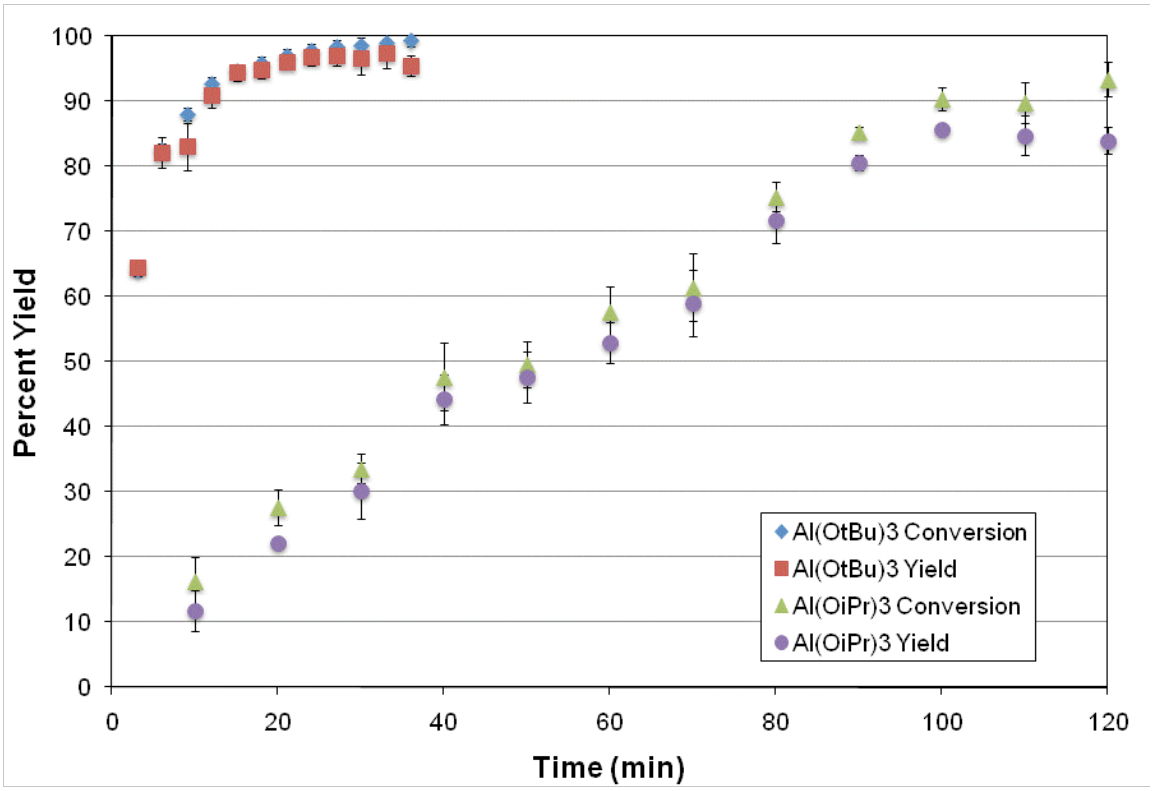

Figure 3.11. Reaction conversion and yield as a function of time for the MPV reduction of benzaldehyde in isopropanol catalyzed by Al(O*t*Bu)$_3$ and Al(O*i*Pr)$_3$.

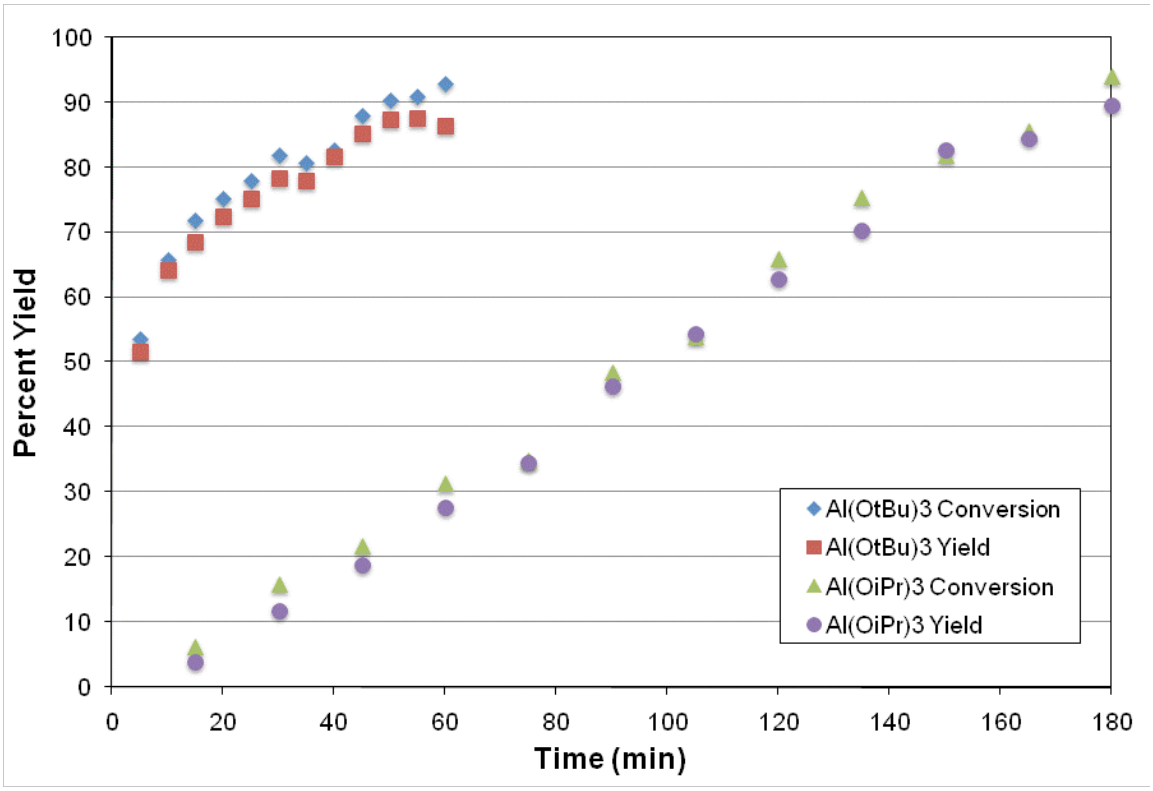

Figure 3.12. Reaction conversion and yield as a function of time for the MPV reduction of benzaldehyde in 9:1 toluene/isopropanol catalyzed by Al(O*t*Bu)$_3$ and Al(O*i*Pr)$_3$.

Aluminum Alkoxide States of Aggregation

The relative rates of reaction between aluminum *tert*-butoxide and aluminum isopropoxide were attributed to their respective states of aggregation. Based on molecular weight studies and ^{1}H NMR experiments, Shiner and coworkers proposed that aluminum *tert*-butoxide exists as a cyclic dimer while aluminum isopropoxide forms the tetrameric complex shown in Figure 3.13.[22] ^{1}H NMR studies that I conducted on aluminum *tert*-butoxide and aluminum isopropoxide in d_6-benzene support the tetrameric nature of aluminum *tert*-butoxide and the dimeric nature of aluminum isopropoxide. This provides a 1:2 ratio of methyl protons in aluminum *tert*-butoxide and a 1:1:2 ratio of methyl groups in aluminum isopropoxide. As Figure 3.13 shows, the dimeric structure proposed for aluminum *tert*-butoxide contains two different types of *tert*-butyl groups in a

1:2 ratio: those on the bridging oxygens and those nonbridging groups highlighted in red. The tetrameric structure of aluminum isopropoxide results in two different types of bridging alkoxide groups, giving a 1:1:2 ratio of the two bridging alkoxide groups to the nonbridging groups. Additionally, increasing equivalents of anhydrous isopropanol were added to a solution of aluminum *tert*-butoxide in d_6-benzene. As each successive equivalent of isopropanol is added, the ^{1}H NMR spectrum became more complex and peaks corresponding to the isopropyl CH group emerged. The NMR spectra are in agreement with the alkoxy groups exchanging only at the nonbridging *tert*-butoxy groups and the aluminum complex overall maintaining its dimeric structure.

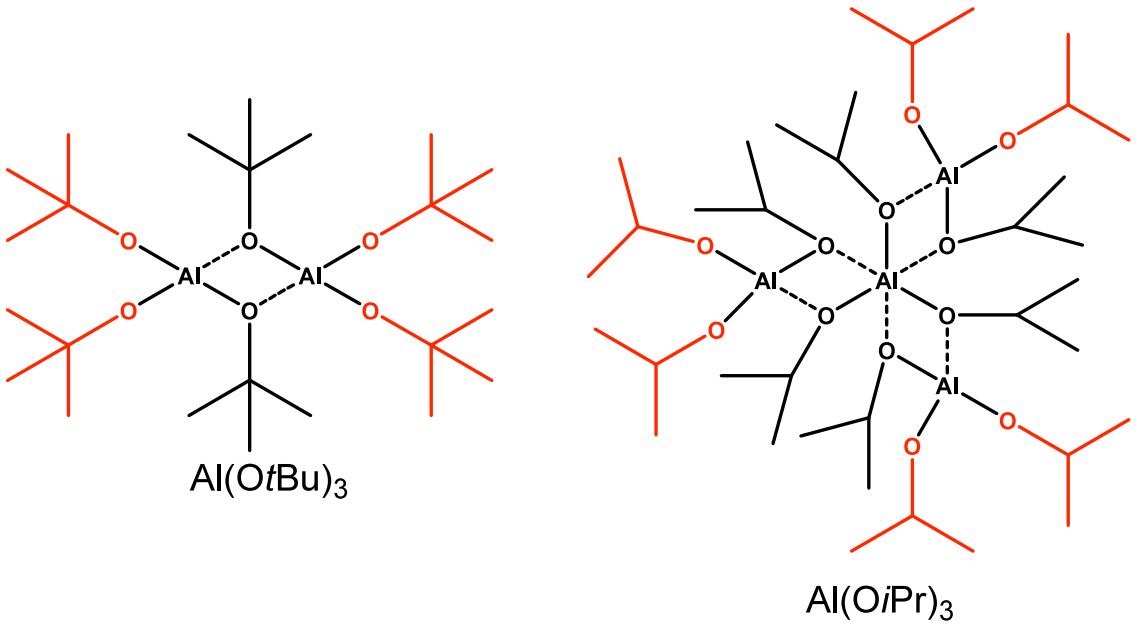

Figure 3.13. States of aggregation of Al(O*t*Bu)$_3$ and Al(O*i*Pr)$_3$. Nonbridging alkoxide groups are highlighted in red.

Furthermore, it has been previously suggested that only the nonbridging alkoxy groups of aluminum alkoxides can perform the hydrogen transfer required in the MPV reduction.[23] Comparing the number of nonbridging groups to bridging groups in the

aluminum *tert*-butoxide and aluminum isopropoxide structures shows a decrease in this ratio between the dimeric and tetrameric complexes (2:1 to 1:1). As a result, the cyclic dimer is expected to be more reactive than the tetramer, which is consistent with the experimental results. The increased steric hindrance of the aluminum isopropoxide complex would also contribute to slowing the MPV reduction rate. Other researchers have also attributed a faster MPV reaction rate to a lower state of aggregation of the aluminum catalyst.[14,24]

Overall, this improvement in the MPV reduction can be easily applied to industrial processes. The procedure for running the reaction, product purification method, and product yield and selectivity do not change from the common reaction using aluminum isopropoxide. However, at least a two-fold decrease in reaction time was observed for each of the starting materials investigated when the MPV catalyst was changed from aluminum isopropoxide to aluminum *tert*-butoxide. Increasing the rate of the reaction not only decreases the time it takes to produce a desired compound but also lowers the energy costs associated with heating a large vessel over a longer period of time. Currently, reducing the amount of aluminum *tert*-butoxide to take advantage of its higher catalyst potency, is being investigated. By reducing the amount of the aluminum species, costs can be reduced (both of the materials as well as disposal of aluminum-contaminated waste) while maintaining productivity.

CONCLUSIONS

In conclusion, techniques have been developed to improve the stereoselectivity and reaction kinetics of the classic MPV reduction. The reaction procedure was modified from batch conditions to improve the reproducibility of the results and an improvement in the diastereoselectivity of the reduction of (*S*)-CMK was observed when

the reaction was run in different solvents. In addition, a significant rate increase was observed when aluminum isopropoxide was replaced with aluminum *tert*-butoxide as an MPV catalyst for (*S*)-CMK, acetophenone, and benzaldehyde. The kinetic effect was attributed to the dimeric state of aggregation of aluminum *tert*-butoxide.

EXPERIMENTAL METHODS

Materials and Equipment

All chemicals were ordered from Aldrich or VWR and used as received, unless otherwise noted. The (*S*)-CMK starting material and samples of (*S,S*)- and (*R,S*)-CMA were obtained from Ampac Fine Chemicals (Sacramento, CA). Acetophenone and benzaldehyde were distilled prior to use.

All solvents used in the batch MPV reductions were dried before being used. Isopropanol was dried over calcium chloride then distilled onto molecular sieves. 2-Butanol and tert-butanol were dried over powdered molecular sieves and distilled before use. Acetonitrile was similarly dried over calcium hydride then distilled onto molecular sieves. I dried DMSO by distillation from sodium hydroxide. Anhydrous THF was purchased from Aldrich and used as received. Ethyl acetate, diethylether, and benzene were dried over molecular sieves before use. All solvents used in the carousel MPV reductions were purchased as anhydrous from Aldrich and used as received except for isopropyl acetate, which was obtained at 99% purity and dried over molecular sieves before use.

^{1}H and ^{13}C NMR spectra were obtained from a Varian-Mercury VX400 MHz spectrometer using $CDCl_3$ as an internal reference, unless otherwise noted. HPLC analysis was run on an Agilent 1100 series LC with a UV detector and an electron spray ionization mass spectrometer (ESI-MS).

Product Analysis

^{1}H NMR Analytical Method

The DR and percent conversion were determined in some reactions from the ^{1}H NMR spectrum. A portion of the ^{1}H NMR spectrum is shown in Figure 3.14 for the (*S*)-

CMK starting material as well as the (*R,S*) and (*S,S*) products. One easily identifiable difference between the spectra is the shift in the NH peak (labeled as "a" in the figure). The peak shows up at about 5.08 ppm in the starting material and shifts downfield to 4.87 and 4.58 ppm in the (*R,S*)-CMA and (*S,S*)-CMA products, respectively. By integrating the area of these peaks, we were able to determine the relative concentration of each component in our product samples, giving us the DR and percent conversion.

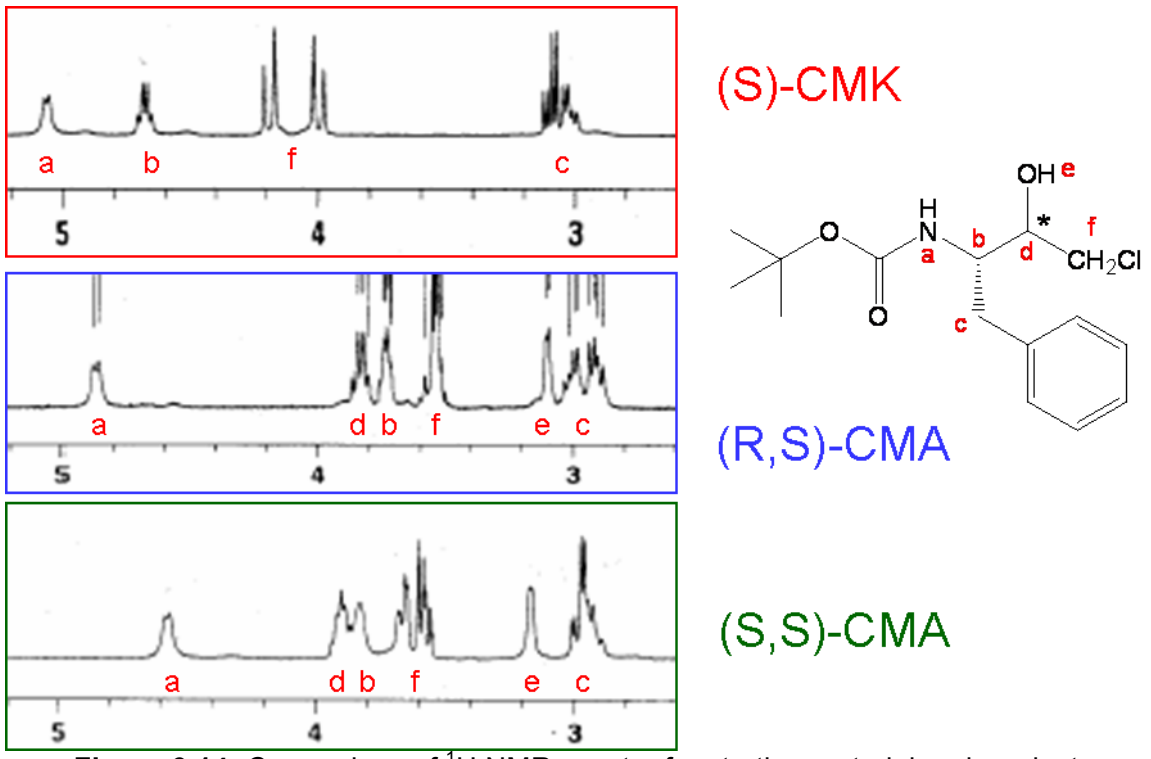

Figure 3.14: Comparison of ^{1}H NMR spectra for starting material and product diastereomers.

HPLC Analytical Method

All samples were run in the HPLC to determine the DR, conversion, and product yield. A Phenomenex Luna 5μ C18(2) reverse phase column was used in conjunction with a guard column to prevent clogging. The solvent system consisted of HPLC grade acetonitrile and HPLC grade water with a 0.1% trifluoroacetic acid buffer. The flow rate

and column temperature were set to 1.5 mL/min and 40°C, respectively. We ran our samples using the solvent gradient shown in Table 3.5. The method ran for fifteen minutes then had a post-run time of four minutes. The UV detector was set to 210 nm.

Table 3.5: HPLC solvent gradient.

Time (min)	MeCN:H_2O
0	48:52
8	48:52
11	80:20
15	80:20

The (*S*)-CMK reduction samples were dissolved in solvents compatible with the HPLC method (methanol and DMSO). We observed a retention time of about 7.8 minutes for the (*S*)-CMK starting material and 4.6 and 5.6 minutes for the (*S,S*)- and (*R,S*)-CMA products, respectively (Figure 3.15). The relative amount of each compound was determined by integrating their respective peaks.

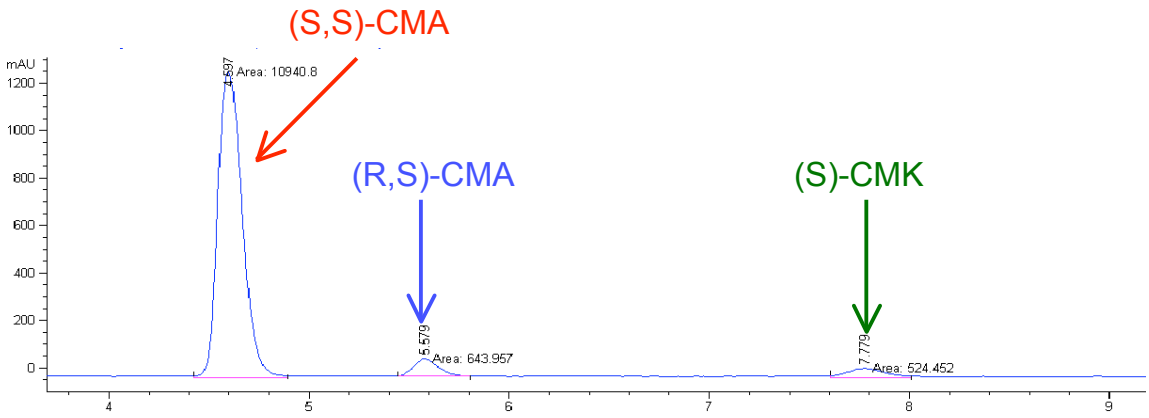

Figure 3.15: HPLC spectrum for sample mixture of (*S,S*)-CMA, (*R,S*)-CMA, and (*S*)-CMK.

In order to determine the percent conversion and yield for the MPV reactions run in the carousel reactor, we made calibration curves for (*S*)-CMK, (*S,S*)-CMA, and (*R,S*)-CMA on the HPLC. Samples of each compound in methanol were made in duplicate at each concentration and the curve was made using the average area between the two samples. The calibration curves are shown in Figure 3.16, Figure 3.17, and Figure 3.18. These calibration curves were used to determine the product yield in the MPV reductions from the HPLC spectra.

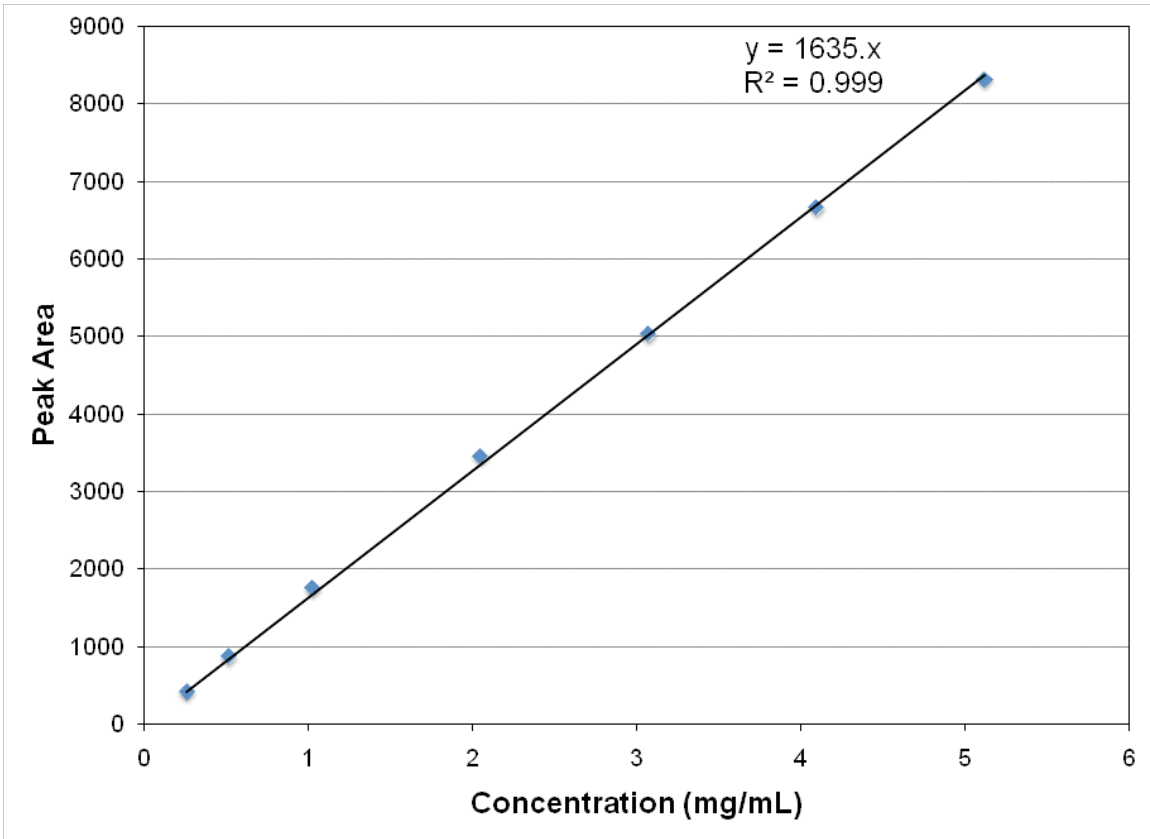

Figure 3.16: HPLC calibration curve of (*S*)-CMK in methanol.

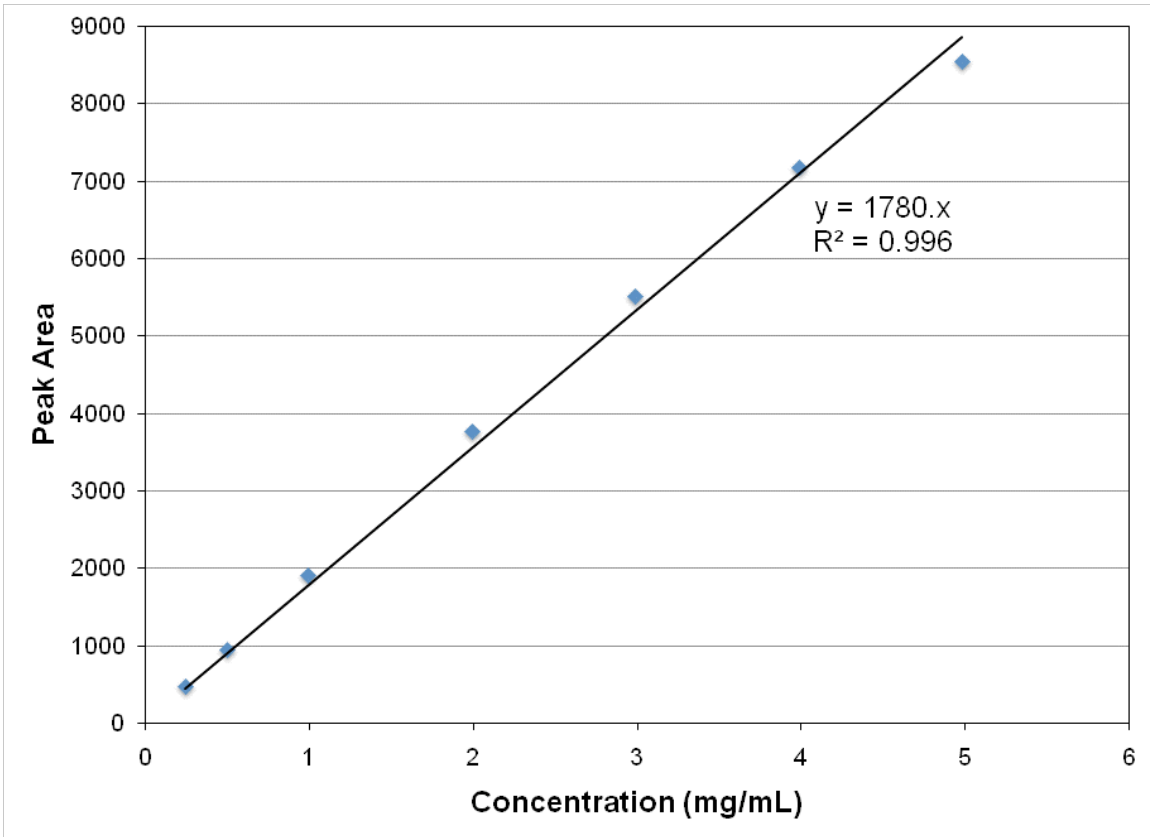

Figure 3.17: HPLC calibration curve for (*S,S*)-CMA in methanol.

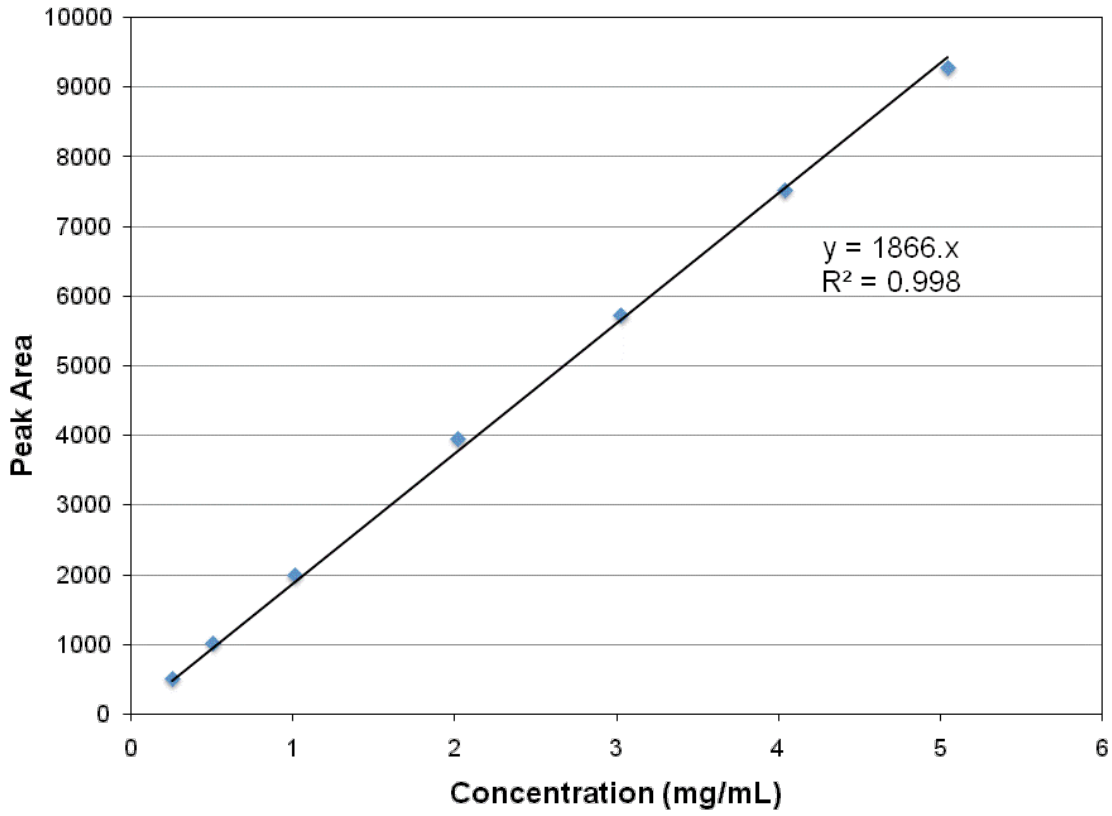

Figure 3.18: HPLC calibration curve of (*R,S*)-CMA in methanol.

Batch Scale MPV Reductions

General Reaction Procedure

(*S*)-CMK was reduced following the MPV reduction procedure used in literature.[16] (*S*)-CMK (1.9 g, 6.4 mmol) was dissolved in anhydrous isopropanol (20 mL) and heated to 50°C. Aluminum isopropoxide (0.68 g, 3.4 mmol) was added and allowed to react for two hours. The product precipitated out of solution to form a white slurry. The reaction mixture was cooled to room temperature. Then, the aluminum isopropoxide was quenched with water (~50 mL) and acetic acid (~5 mL). The organics were extracted into ethyl acetate. The organic phase was washed with a saturated sodium bicarbonate solution then brine. The organics were dried over magnesium sulfate and the solvent was removed under vacuum. This yielded a white powder in 89% yield.

The same reaction procedure described above was used with other alcohol solvents (2-butanol, *tert*-butanol, and 1:1 isopropanol/*tert*-butanol) and different aluminum alkoxides (aluminum-tri-*sec*-butoxide and aluminum *tert*-butoxide), keeping the molar ratios constant. The reaction time varied with the alcohols used.

Synthesis of Aluminum Isopropoxide

Aluminum isopropoxide was synthesized according to a standard procedure.[21] Aluminum foil (2.7 g, 0.1 mol), anhydrous isopropanol (30 mL, 0.39 mol) and mercury (II) chloride (0.05 g, 0.1 mmol) were stirred together. This mixture was heated to reflux at 90°C. Once at reflux, carbon tetrachloride (0.2 mL, 2 mmol) was added to initiate the reaction. Bubbles formed on the aluminum and the mixture started to turn grey. More isopropanol (30 mL, 0.39 mol) was added to wash the carbon tetrachloride off the sides of the flask. The reaction was allowed to react under reflux. After all the foil had reacted (3-4 hours), the reaction was removed from heat and cooled to room temperature. The reaction mixture had black suspended particles in it. This mixture was used in the MPV reaction without further purification or characterization. The concentration was calculated assuming 100% yield of aluminum isopropoxide from the aluminum foil.

Reductions in Various Organic Solvents

The MPV reductions in various organic solvents were done in a similar manner to the general reaction procedure above. All the organic solvents used in the MPV reductions were dried before being used according to literature procedure. (*S*)-CMK (1.9 g, 6.4 mmol) and anhydrous isopropanol (0.5 mL, 6.5 mmol) were stirred in the anhydrous organic solvent (19.5 mL) and heated to 50°C. Aluminum isopropoxide (0.68 g, 3.4 mmol) was added and allowed to react overnight. The reaction mixture was cooled to room temperature. Then, the aluminum isopropoxide was quenched with

water (~50 mL) and acetic acid (~5 mL). Any organic precipitate was extracted into ethyl acetate. The organic phase was washed with a saturated sodium bicarbonate solution then brine. The organics were dried over magnesium sulfate and the solvent was removed under vacuum. This yielded a white powdery product, which was analyzed by HPLC.

Reduction with Hydrogen Bonding Additives

The reaction was run following the same general reaction procedure above. The additives (either TBAF or lithium fluoride) were added to the (*S*)-CMK solution at the beginning of the reaction. A solution of TBAF in THF (0.75 mL of 1 M solution, 0.75 mmol) was used while the lithium fluoride (0.17 g, 6.5 mmol) was added as a solid. The starting solution was yellow in both cases. The reactions were run in anhydrous isopropanol overnight at 50°C. When TBAF was used, the organics could not be easily extracted following the above procedure because the aqueous and organics were one phase. However, when brine was added to the reaction mixture, the phases split and the product could be isolated. The lithium fluoride reaction product was obtained by the standard workup.

Carousel MPV Reductions

General Reaction Workup

Depending on the amount of conversion of (*S*)-CMK in each reaction, the various post-reaction mixtures required different dilution volumes to make the solutions homogeneous. When the reactions proceeded past about 80% conversion to the desired products, the resulting heterogeneous reaction mixtures required more ethyl acetate or methanol to dissolve the products and create a homogeneous solution. The sample volumes were subsequently adjusted to maintain approximately the same

concentrations for HPLC analysis and they were all diluted with methanol to a total sample volume of 1 mL.

Reduction with Aluminum Alkoxides

(*S*)-CMK (0.475 g, 1.59 mmol) was stirred together with aluminum isopropoxide (0.170 g, 0.83 mmol), aluminum *tert*-butoxide (0.205 g, 0.83 mmol), or aluminum ethoxide (0.135 g, 0.83 mmol) in anhydrous isopropanol (5 mL). The reaction mixtures were heated to 50°C under argon atmosphere for two hours. The reactions were removed from heat and diluted with ethyl acetate. Hydrochloric acid (5 mL of a 2 M solution) was added to quench the reactions and the organics were extracted into ethyl acetate. Each solution was sampled twice and diluted with methanol before being analyzed by HPLC. Table 3.6 shows the volume dilutions used in the different reactions.

Table 3.6: Reaction workup with aluminum alkoxides.

	Ethyl Acetate Added	Sample Volume
$Al(O\textit{i}Pr)_3$	10 mL	0.150 mL
$Al(O\textit{t}Bu)_3$	20 mL	0.300 mL
$Al(OEt)_3$	10 mL	0.150 mL

Reduction in Various Organic Solvents

(*S*)-CMK (0.475 g, 1.59 mmol) and aluminum isopropoxide (0.170 g, 0.83 mmol) were dissolved in a mixture of an anhydrous organic solvent (4.5 mL) and anhydrous isopropanol (0.5 mL). The organic solvents used were ethyl acetate, THF, isopropyl acetate, 2-butanol, *tert*-butanol, DCM, and toluene. The solutions were heated to 50°C and the reactions were run overnight (18 hours). The reaction mixtures were then cooled in an ice bath. They were diluted with methanol and quenched with hydrochloric

acid (2 mL of a 2 M solution). Each solution was sampled twice and analyzed by HPLC. Table 3.7 shows the volume dilutions used in the different reactions.

Table 3.7: Reaction workup for various organic solvent solutions.

	Methanol Added	Sample Volume
EtOAc	20 mL	0.250 mL
THF	20 mL	0.250 mL
iPrOAc	30 mL	0.350 mL
2-BuOH	30 mL	0.350 mL
t-BuOH	30 mL	0.350 mL
DCM	30 mL	0.350 mL
Toluene	30 mL	0.350 mL

Kinetics of (*S*)-CMK Reduction

(*S*)-CMK (0.475 g, 1.59 mmol) was dissolved in anhydrous isopropanol (5 mL) at 50°C under argon. Aluminum isopropoxide (0.170 g, 0.83 mmol) or aluminum *tert*-butoxide (0.205 g, 0.83 mmol) was added to start the reaction. The solutions were homogeneous at the start of the reaction but as the reaction progressed, the product precipitated out of solution. When aluminum *tert*-butoxide was used as the catalyst, the products precipitated in less than ten minutes. When aluminum isopropoxide was used, the products precipitated after an hour. After the specified reaction time, the reactions were removed from heat and placed in an ice bath. The reactions were quenched cold with hydrochloric acid (2 mL of a 2 M solution) and diluted with methanol (20 mL or 30 mL). Each reaction mixture was sampled (0.250 mL or 0.350 mL) twice and further diluted with methanol (0.750 mL or 0.650 mL). These crude solutions were run directly on the HPLC without further purification.

The same kinetics experiment was run in a 9:1 toluene/isopropanol solvent mixture. (*S*)-CMK (0.475 g, 1.59 mmol) was dissolved in anhydrous toluene (4.5 mL)

and anhydrous isopropanol (0.5 mL) at 50°C under argon. Aluminum isopropoxide (0.170 g, 0.83 mmol) or aluminum *tert*-butoxide (0.205 g, 0.83 mmol) was added to start the reaction. The solutions were all homogeneous at the start of the reaction and became heterogeneous as the reaction progressed. The aluminum *tert*-butoxide reactions were run for two hours with reactions quenched every ten minutes; the aluminum isopropoxide reactions ran for four hours and the reactions were quenched every twenty minutes. After the allotted reaction times, the reaction tubes were placed in an ice bath to stop the reaction. The post-reaction mixtures were diluted with methanol (20 mL or 30 mL) and quenched cold with hydrochloric acid (2 mL of a 2 M solution). Each solution was sampled (0.250 mL or 0.350 mL) twice, diluted with methanol, and analyzed by HPLC.

Kinetics of Acetophenone Reduction

Aluminum isopropoxide (0.170 g, 0.83 mmol) or aluminum *tert*-butoxide (0.205 g, 0.83 mmol) was stirred under argon in anhydrous isopropanol (5 mL) at 50°C. Acetophenone (190 μL, 1.59 mmol) was added to start the reaction. The solutions were homogeneous throughout the reaction. After the allotted reaction time, each reaction was quenched with hydrochloric acid (2 mL of a 2 M solution) and diluted with methanol (10 mL). The reactions were cooled in an ice bath and sampled twice to run on the HPLC.

Kinetics of Benzaldehyde Reduction

Aluminum isopropoxide (0.170 g, 0.83 mmol) or aluminum *tert*-butoxide (0.205 g, 0.83 mmol) was stirred under argon in anhydrous isopropanol (5 mL) at 50°C to dissolve the aluminum alkoxide. The temperature was lowered to 40°C before benzaldehyde (165 μL, 1.59 mmol) was added to start the reaction. The solutions were homogeneous

throughout the reaction time. After the allotted reaction time, each reaction was quenched with hydrochloric acid (2 mL of a 2 M solution) and diluted with methanol (10 mL). The reactions were cooled in an ice bath and sampled twice to run on the HPLC.

Al(O*i*Pr)$_3$ State of Aggregation

^{1}H NMR (C_6D_6) δ 1.32 (d, 36H), 1.38 (d, 18H), 1.68 (d, 18H), 4.41 (m, 6H), 4.67 (m, 6H). ^{13}C NMR (C_6D_6) δ 25.4, 26.7, 28.0, 28.2, 63.6, 66.4.

Al(O*t*Bu)$_3$ State of Aggregation

^{1}H NMR (C_6D_6) δ 1.38 (s, 12H), 1.48 (s, 6H). ^{13}C NMR (C_6D_6) δ 31.2, 31.4, 33.8, 94.5.

Al(O*t*Bu)$_3$ and Isopropanol State of Aggregation

Four separate solutions were made containing Al(OtBu)$_3$ (0.034 g, 0.140 mmol) dissolved in C_6D_6 (1.5 mL). Anhydrous isopropanol was added to each solution in the following amounts: 0 μL, 10 μL, 20 μL, and 30 μL. The solutions were all heated to 50°C and stirred for 2 hours then analyzed by ^{1}H NMR.

REFERENCES

(1) Meerwein, H.; Schmidt, R. *Justus Liebigs Annalen der Chemie* **1925**, *444*, 221-238.

(2) Verley, M. *Bulletin de la Societe Chimique de France* **1925**, *37*, 871-874.

(3) Ponndorf, W. *Angewandte Chemie* **1926**, *39*, 138-143.

(4) Wilds, A. *Organic Reactions* **1944**, *2*, 178-223.

(5) Djerassi, C. *Organic Reactions* **1951**, *6*, 207-272.

(6) de Graauw, C.; Peters, J.; van Bekkum, H.; Huskens, J. *Synthesis* **1994**, 1007-1017.

(7) Cha, J. S. *Organic Process Research & Development* **2006**, *10*, 1032-1053.

(8) Namy, J. L.; Souppe, J.; Collin, J.; Kagan, H. B. *Journal of Organic Chemistry* **1984**, *49*, 2045-2049.

(9) Fukuzawa, S.; Nakano, N.; Saitoh, T. *European Journal of Organic Chemistry* **2004**, 2863-2867.

(10) Nishide, K.; Node, M. *Chirality* **2002**, *14*, 759-767.

(11) Doering, W.; Young, R. *Journal of the American Chemical Society* **1950**, *72*, 631-631.

(12) Ooi, T.; Ichikawa, H.; Maruoka, K. *Angewandte Chemie-International Edition* **2001**, *40*, 3610-+.

(13) Liu, Y. C.; Ko, B. T.; Huang, B. H.; Lin, C. C. *Organometallics* **2002**, *21*, 2066-2069.

(14) Graves, C. R.; Zhou, H. Y.; Stern, C. L.; Nguyen, S. T. *Journal of Organic Chemistry* **2007**, *72*, 9121-9133.

(15) Campbell, E. J.; Zhou, H. Y.; Nguyen, S. T. *Angewandte Chemie-International Edition* **2002**, *41*, 1020-+.

(16) Malik, A. A.; Clement, T. E.; Palandoken, H.; Robinson III, J.; Stringer, J. A. US Patent, 2003.

(17) Malik, A. A.; Clement, T. E.; Palandoken, H.; Robinson III, J.; Stringer, J. A. US Patent, 2005.

(18) Cohen, R.; Graves, C.; Nguyen, S.; Martin, J.; Ratner, M. *Journal of the American Chemical Society* **2004**, *126*, 14796-14803.

(19) Oppenauer, R. *Recueil des Travaux Chimiques des Pays-Bas* **1937**, *56*, 137-144.

(20) Hoffman, R. V.; Maslouh, N.; Cervantes-Lee, F. *Journal of Organic Chemistry* **2002**, *67*, 1045-1056.

(21) Vogel, A. I.; Furniss, B. S. *Vogel's Textbook of Practical Organic Chemistry*; 5th ed.; Longman Scientific & Technical ; Wiley: London New York, 1989.

(22) Shiner, V.; Whittaker, D.; Fernande, V. *Journal of the American Chemical Society* **1963**, *85*, 2318-2322.

(23) Kow, R.; Nygren, R.; Rathke, M. *Journal of Organic Chemistry* **1977**, *42*, 826-827.

(24) Campbell, E.; Zhou, H.; Nguyen, S. *Organic Letters* **2001**, *3*, 2391-2393.

CHAPTER 4 ASYMMETRIC TRANSFER HYDROGENATION REACTIONS

INTRODUCTION

The reduction of prochiral ketones by a hydrogen donor, such as isopropanol or sodium formate, in the presence of a homogeneous catalyst and a chiral ligand is known as asymmetric transfer hydrogenation (ATH).[1-3] Metals which have been used to catalyze transfer hydrogenation reactions include rhodium, iridium, and ruthenium. Historically, catalytic hydrogenation with molecular hydrogen was used to reduce carbonyl compounds to the corresponding alcohols. The use of chiral ligands in coordination with the transition metal catalysts can result in very high enantioselectivity.[4,5] The field of ATH reactions is relatively new, with the first discovery being the cyclopentadienyl ruthenium (II) catalyst system for the reduction of ketones by Shvo and co-workers just over twenty years ago.[6,7] Instead of using reagents like molecular hydrogen or boranes, this method uses air-stable transition metal catalysts in conjunction with a benign hydrogen source like isopropanol (Figure 4.1). Much of the progress in ATH reactions has been done by Noyori and co-workers,[8,9] which, in addition to his work with heterogeneous catalytic hydrogenation, led to his Nobel Prize in 2001.[10]

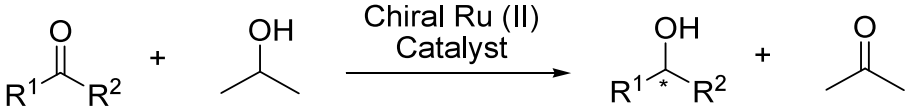

Figure 4.1: General ATH reaction scheme.

Although the ATH reaction is a powerful technique in organic chemistry, there are a few drawbacks to the system. First, the hydrogen transfer is reversible and the reaction efficiency is determined by the relative structures of the ketone starting material and the hydrogen donor. Not only can this limit the conversion of the reaction, but it may also decrease the enantioselectivity towards the desired product. Formic acid was proposed as an alternative inexpensive hydrogen source that would improve the reaction conversion through the irreversible evolution of carbon dioxide. Using a 5:2 formic acid/triethylamine azeotropic mixture led to improved product yields in the ATH reaction.[11] Another potential downside to the ATH reaction is the high cost of the transition metal catalysts and chiral ligands. To decrease the process cost as well as the environmental impact, researchers have investigated recyclable ATH catalyst systems. The first attempt at a recyclable catalyst involved its immobilization on silica,[12-14] polymers,[15] or dendrimers.[16] Catalyst recycling was also achieved by modifying the catalyst and running the reaction in an ionic liquid[17,18] or aqueous solvent system.[19,20]

ATH has been investigated previously as a method to prepare both (*S,S*)- and (*R,S*)-CMA from the corresponding ketone (*S*)-CMK. Combining a rhodium catalyst with the chiral ligands (1*R*,2*R*)-*N*-(*p*-toluenesulfonyl)-1,2-diphenylethylenediamine [(1*R*,2*R*)-TsDPEN] or (1*S*,2*S*)-*N*-(*p*-toluenesulfonyl)-1,2-diphenylethylenediamine [(1*S*,2*S*)-TsDPEN], researchers produced the (*R,S*) and (*S,S*) diastereomeric products, respectively, in up to 80% diastereomeric excess each.[21] Unfortunately, as mentioned above, both the rhodium catalyst and the chiral ligands are expensive and not viable for industrial scale application of this process.

I proposed to explore cost-effective methods of reduction to produce (*R,S*)-CMA. The reduction of (*S*)-CMK was carried out under heterogeneous catalytic hydrogenation conditions where molecular hydrogen was used as the hydrogen source. Then I compared this classic reduction technique with the ATH method. Getting reproducible

results is paramount to research; therefore, my efforts were first devoted to controlling all variables. Once I established a reliable procedure, the reaction was optimized by varying reaction conditions such as solvent, hydrogen source, reagent concentrations, ligand, and metal catalyst center.

BACKGROUND

Heterogeneous Catalytic Hydrogenation

Heterogeneous catalytic hydrogenation (Figure 4.2) of double bonds is efficient and allows for easy product purification with low cost reagents.[4,5,22,23] Molecular hydrogen is used as the hydrogen source and the reaction is run in the presence of a heterogeneous transition metal catalyst. The reaction occurs through a four step mechanism: (1) the dihydrogen is adsorbed onto the metal surface, (2) the dihydrogen is cleaved by the metal into two metal-hydrogen bonds, (3) the ketone approaches the hydrogen-metal on the surface, and (4) the carbonyl reacts with the hydrogen atoms to yield the product. Noyori and coworkers developed several novel hydrogenation systems that involved various chiral ligands complexed with transition metal catalysts to reduce aromatic ketones.[24-27]

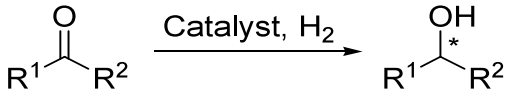

Figure 4.2: General heterogeneous catalytic hydrogenation reaction scheme.

The reduction of (*S*)-CMK is presented with the following heterogeneous catalysts: platinum oxide, palladium on carbon, and nickel nanoparticles. In addition to looking at the effect of different catalysts, the effects of solvent, pressure, temperature,

and time on the product yield and diastereoselectivity were also explored. These results were used as a basis of comparison for the ATH reactions.

Asymmetric Transfer Hydrogenation

(*S*)-CMK was previously reduced via ATH to its diastereomeric products.[21] My aim was mainly to utilize an achiral catalyst, taking full advantage of the adjacent chiral center in the (*S*)-CMK as the sole source for chiral induction. As the reaction scheme in Figure 4.3 shows, the catalyst is made of a dichloro(*p*-cymene)ruthenium(II) dimer {[Ru(*p*-cymene)Cl_2]$_2$} complexed with a diamine ligand like (1*R*,2*R*)-TsDPEN[28] or the achiral version, *N*-tolylsulfonylethylenediamine (TsEN)[29,30]. The structures of the ligands are shown in Figure 4.4.

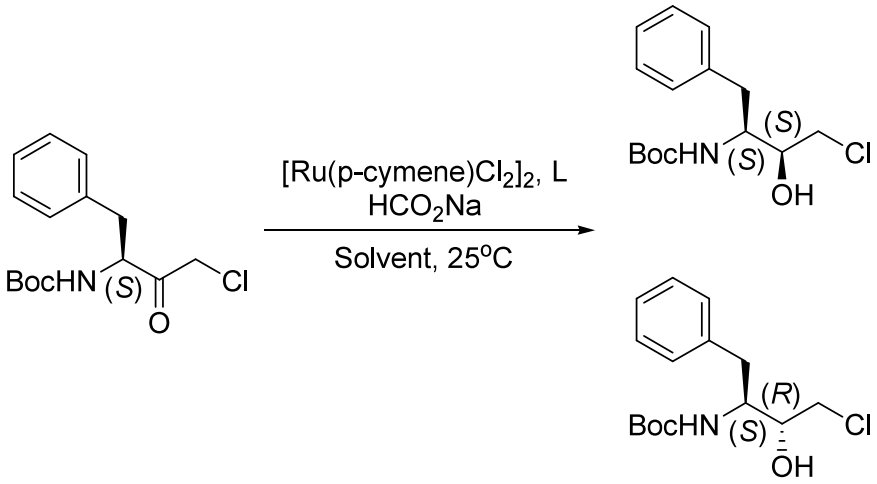

Figure 4.3: ATH reaction on (*S*)-CMK.

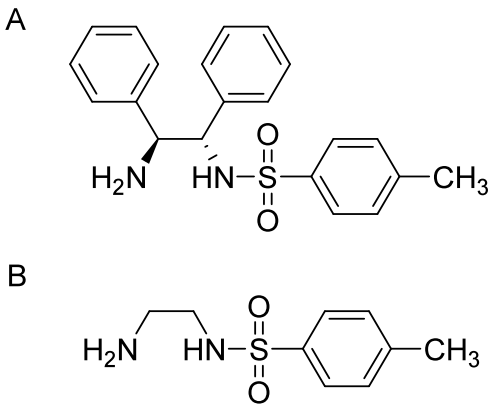

Figure 4.4: ATH reaction ligands. A: (1*R*,2*R*)-*N*-(*p*-Toluenesulfonyl)-1,2-diphenylethylenediamine [(1*R*,2*R*)-TsDPEN].[28] B: *N*-Tolylsulfonylethylenediamine (TsEN).[29,30]

The *in situ* synthetic scheme of catalyst formation is shown in Figure 4.5 and the catalytic cycle for the reduction is depicted in Figure 4.6. The catalyst and diamine ligand are first combined to form the pre-catalyst. The active catalyst is formed *in situ* from the reaction of the hydrogen source (such as sodium formate) with the pre-catalyst. The active catalyst can then coordinate with the starting material and transfer a proton to the ketone, forming the alcohol product. Reaction of the oxidized catalyst with another formate molecule reforms the active catalyst to continue the catalytic cycle.

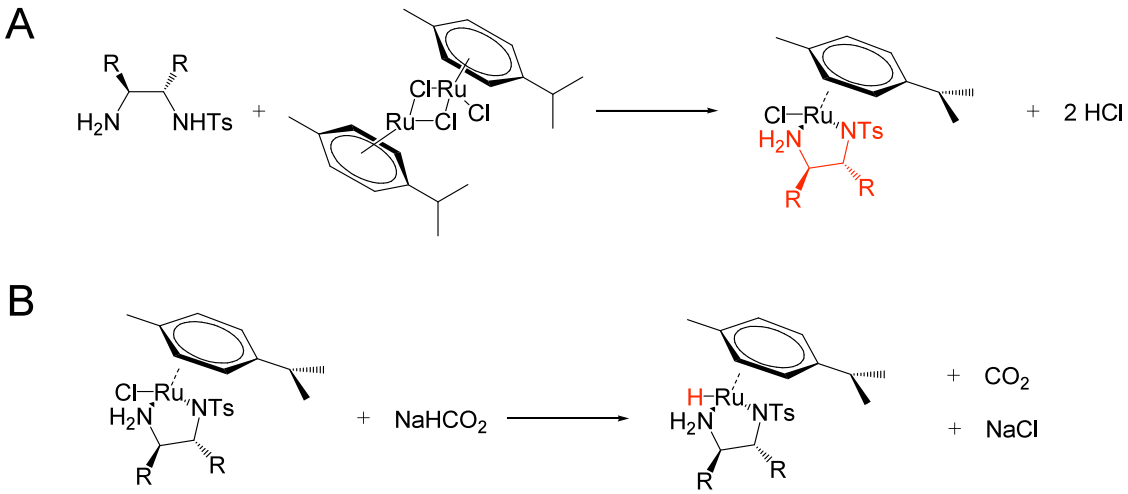

Figure 4.5: ATH catalyst formation mechanism. A: Pre-catalyst formation. B: *In situ* active catalyst formation.

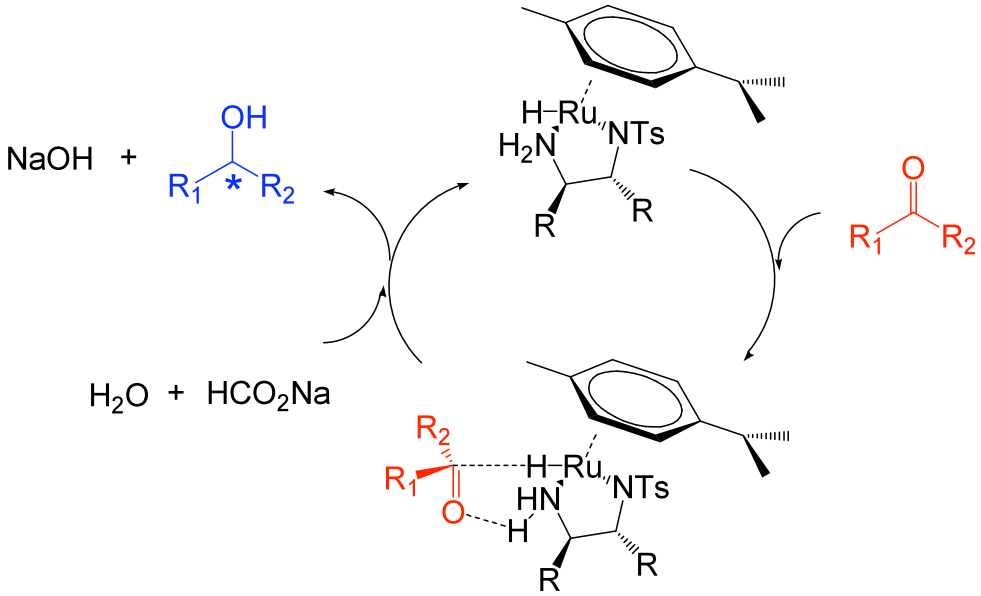

Figure 4.6: ATH catalytic cycle.

RESULTS AND DISCUSSION

Heterogeneous Catalytic Hydrogenation

Adams' catalyst (platinum oxide) was tested as a heterogeneous catalyst for the reduction of (*S*)-CMK with 30 psi pressure of hydrogen gas. After three hours at room temperature, the pressure was vented. The reaction mixture was filtered through a Celite pad, and the organics were extracted into diethylether. The crude products were analyzed by HPLC. The hydrogenation was run in a variety of solvents including methanol, ethanol, ethyl acetate, acetonitrile, THF, dimethylformamide (DMF), and water. The best results were found in acetonitrile, which gave 54% conversion and a DR of about 0.9:1 in three repeated reactions.

Table 4.1: Catalytic hydrogenation of (*S*)-CMK with platinum oxide.

Solvent	Conversion	DR
MeCN	54%	0.9:1
THF	2%	0.8:1
EtOAc	3%	0.7:1
MeOH	35%	0.5:1
EtOH	29%	0.5:1
DMF	6%	0.3:1
H_2O	0%	[a]

[a] No products were detectable by HPLC

Although the induced diastereoselectivity was encouraging, the high conversions shown in Table 4.1 can be misleading. Most of the conversion was due to the formation of byproducts, mostly due to hydrogenolysis of the chlorine group. The hydrogenolysis results in a mixture of the dechlorinated ketone (referred to as MK) and both diastereomers of the dechlorinated alcohol product [referred to as (*S,S*)-MA and (*R,S*)-

MA, respectively] (Figure 4.7 and Figure 4.8). In an attempt to favor the desired reaction, the reaction vessel was pressurized to 50 psi of hydrogen and vented three times. Then, the vessel was pressurized to 100 psi and left to react overnight. The analysis of the product mixture showed a similar level of dechlorination to our previous reactions.

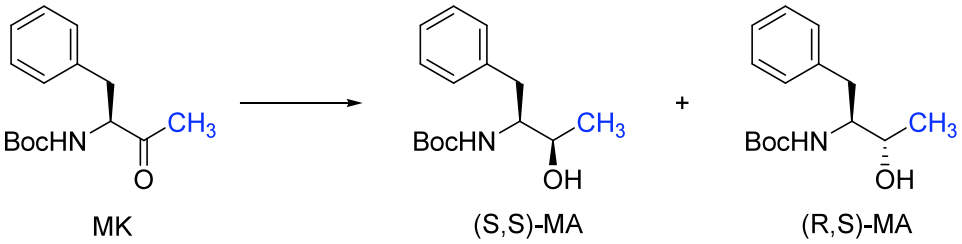

Figure 4.7: Possible dehalogenation products.

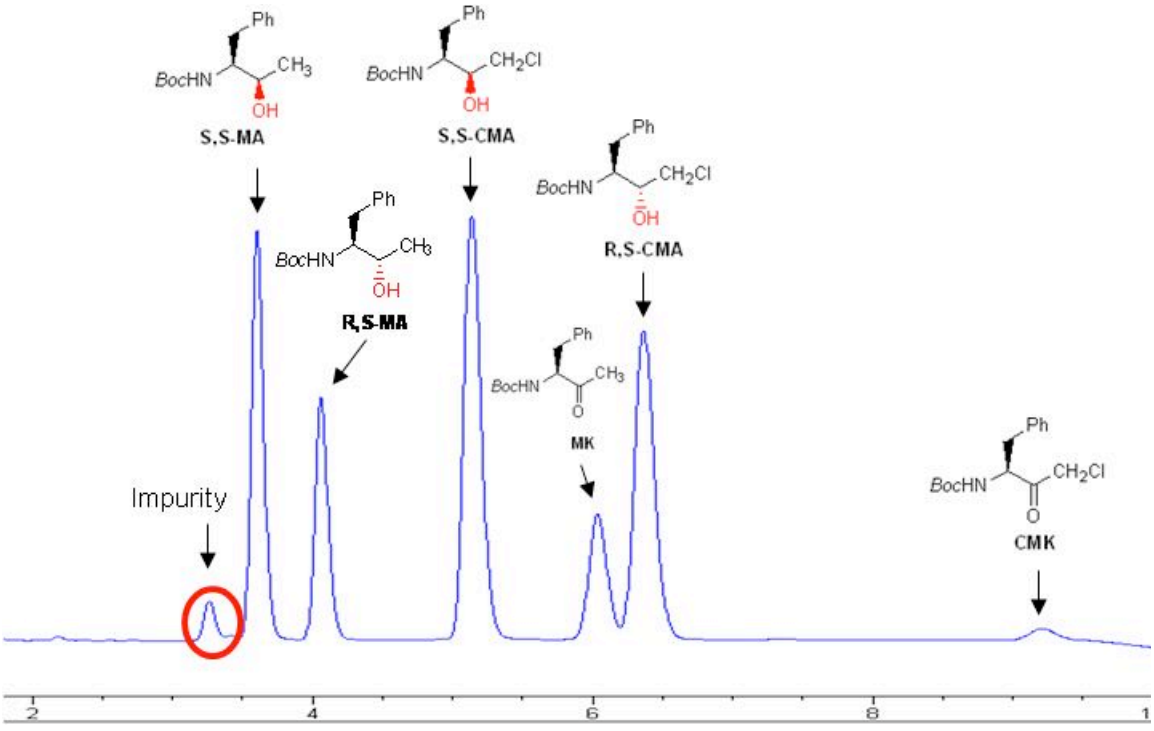

Figure 4.8: Sample HPLC spectrum of hydrogenation of (*S*)-CMK showing starting material, desired products, and dechlorinated side products.

The results from other heterogeneous catalysts were similar to the reductions with Adam's catalyst. Another catalyst investigated was 5 weight% palladium on carbon. After reaction with 30 psi of hydrogen in ethanol, the HPLC analysis showed very little conversion of (*S*)-CMK and no sign of the desired products, (*R,S*)- and (*S,S*)-CMA. The only conversion of (*S*)-CMK resulted in dehalogenation. When the reaction was run using nickel nanoparticles as the catalyst, the analysis showed only 1% conversion of the starting material.

Asymmetric Transfer Hydrogenation

The ATH reaction was carried out with the achiral ligand TsEN in a wide range of solvents, including mixed aqueous and organic solvent systems. Sodium formate and triethylammonium formate were both explored as hydrogen sources. Getting reproducible results is paramount to research; therefore, my efforts were first devoted to controlling all variables.

Original Reaction Apparatus

I originally began running the ATH reactions in a homemade apparatus consisting of an oil bath with an incoming nitrogen line split into eight outlets, which were connected to reaction tubes. The homemade apparatus was designed to run eight reactions at one time with similar conditions, making it an ideal tool to screen a wide variety of conditions. The reactions were run on a 1 mL scale overnight at 40°C. The catalyst precursor and ligand were stirred in the solvent for one hour to form the pre-catalyst before the sodium formate was added. Finally, (*S*)-CMK was added to start the reaction. The reactions were quenched with saturated ammonium chloride, extracted with diethylether, and filtered through a silica plug. The solvent was removed under a stream of nitrogen and the resulting residues were analyzed by HPLC and ^{1}H NMR.

ATH in "Wet" Organic Solvents with the Achiral Catalyst (TsEN)

The first ATH reactions used a small amount of water in an organic solvent (THF, DMSO, DMF, and ethanol) to increase solubility of the sodium formate and thereby maintain a practical reaction rate. I added water (0.1 mL) to the original volume of organic solvent (1 mL) but otherwise used the same reaction conditions described above. The HPLC and ^{1}H NMR results are shown in Table 4.2. In all cases, the reactions proceeded to almost complete conversion. Analyses were done by HPLC or ^{1}H NMR. These reactions were shown to favor the desired (*R,S*) diastereomer with a DR as high as 2.5:1.

Table 4.2: ATH in "wet" organic solvents with achiral catalyst.

Solvent	Conversion	DR (HPLC)	DR (NMR)
THF	95%	1.3:1	0.8:1
DMSO	92%	1.0:1[a]	1.7:1[a]
DMF	92%	2.5:1	2.4:1
EtOH	95%	1.2:1	1.1:1

[a]Estimated DR (overlapping peaks in HPLC or ^{1}H NMR)

ATH in Pure Organic Solvents with the Achiral Catalyst (TsEN)

ATH reactions were carried out in the same solvents used above (THF, DMSO, DMF, and ethanol) without the addition of water. The reactions were all heterogeneous and ran overnight. The HPLC and ^{1}H NMR results (Table 4.3) showed a decrease in the DR compared to the "wet" solvents. In the case of THF, the conversion was also significantly decreased from 95% to 22%, which is believed to result from the heterogeneous nature of the reactions (due to very low sodium formate solubility in organic solvents). In all cases, it seems that the addition of a small amount of water to the organic solvents favors the production of (*R,S*)-CMA.

Table 4.3: ATH reaction in pure organic solvents with achiral catalyst.

Solvent	Conversion	DR (HPLC)	DR (NMR)
THF	22%	0.8:1	0.8:1
DMSO	100%	0.2:1[a]	0.4:1
DMF	94%	0.1:1[a]	0.4:1[a]
EtOH	93%	0.9:1	0.8:1

[a]Estimated DR (overlapping peaks in HPLC or ^{1}H NMR)

ATH in Water with the Achiral Catalyst (TsEN)

I next investigated the ATH reaction in pure water using the same achiral catalyst (TsEN). The reaction mixture was heterogeneous as the (*S*)-CMK starting material's solubility in water is negligible. The reaction was run under the same conditions as in the case of the organic solvents. Although 50% of the starting material was recovered, the DR was promising at 2.1:1 and 1.8:1 by HPLC and ^{1}H NMR, respectively. Encouraged by this favorable DR, the reaction was repeated in water for two days to increase the conversion. Although the conversion was much higher at 89%, the DR dropped to 0.9:1 and 0.8:1.

ATH in 1:1 Water/Organic Solvent Mixtures with the Achiral Catalyst (TsEN)

ATH reactions in a 1:1 mixture of water and organic solvents were investigated. Again, the reactions were heterogeneous as the (*S*)-CMK starting material did not completely dissolve in any of the solvent systems. The results of these reactions are listed in Table 4.4. In all cases except the reaction run in DMSO and water, the DR was improved from the reactions in the "wet" solvents with only 10% water.

Table 4.4: ATH reaction in 1:1 organic solvent/water mixture with achiral catalyst.

Solvent	Conversion	DR (HPLC)	DR (NMR)
THF/H_2O	93%	1.7:1	1.3:1
DMSO/H_2O	83%	0.7:1	0.9:1
DMF/H_2O	79%	3.2:1	3.9:1
EtOH/H_2O	81%	2.4:1	2.4:1

ATH in "Wet" Organic Solvents with the Chiral Catalyst [(1R,2R)-TsDPEN]

The ATH reaction on (*S*)-CMK was carried out under conditions identical to the reactions described above with the exception of the ligand being replaced with chiral (1*R*,2*R*)-TsDPEN. The reactions were run in the "wet" solvent systems (10% water) investigated previously. The chiral catalyst gave significantly better diastereoselectivities than the catalyst utilizing the achiral ligand, TsEN. Table 4.5 shows an increase in DR of up to four times, in the case of THF. The conversions in these reactions were above 90%, except for the reaction in DMSO, which resulted in a conversion of 77%. I also ran the reaction with (1*R*,2*R*)-TsDPEN in water for two days. This reaction again shows an increase in diastereoselectivity from the reaction with TsEN.

Table 4.5: ATH reaction in "wet" organic solvents and water with chiral catalyst.

Solvent	Conversion	DR (HPLC)	DR (NMR)
H_2O (2 days)	92%	2.5:1	2.9:1[a]
THF	98%	5.5:1	5.1:1
DMSO	77%	[b]	5.1:1
DMF	97%	4.4:1	4.0:1[a]
EtOH	96%	3.6:1	4.7:1

[a]Estimated DR (overlapping peaks in HPLC or ^{1}H NMR)
[b]Peak areas could not be estimated due to impurities in sample

(1*R*,2*R*)-TsDPEN has been used in the reduction of (*S*)-CMK previously in literature. However, the reaction has not been run in these solvent systems. Instead, the literature reports the ATH reaction on (*S*)-CMK in pure ethyl acetate, toluene, DCM, or isopropanol with triethylammonium formate as the hydrogen source.[21] These novel ATH reaction systems give good conversions and high diastereoselectivities (DR ~9:1). However, the downside to using the chiral catalyst is a much greater expense.

Reproducibility of ATH Reactions

After a couple of reactions in "wet" organic solvents (THF and DMSO) and in 1:1 water/organic solvent mixtures (THF, DMSO, DMF, and ethanol) were repeated, it became evident that reproducibility was poor. The DRs of the repeated reactions as well as the reactions reported above are given in Table 4.6 and Table 4.7 below, as analyzed by HPLC.

Table 4.6: Repeated ATH reactions in "wet" organic solvents with achiral catalyst.

Solvent	DR, Run 1	DR, Run 2
THF	1.3:1	2.3:1
DMSO	1.0:1	0.7:1

Table 4.7: Repeated ATH reactions in 1:1 water/organic solvent mixtures with achiral catalyst.

Solvent	DR, Run 1	DR, Run 2
THF/H_2O	1.7:1	2.6:1
DMSO/H_2O	0.7:1	1.9:1
DMF/H_2O	3.2:1	1.2:1
EtOH/H_2O	2.4:1	1.2:1

The repeated reactions gave very different results and the data were scattered, showing improvements in some cases and decreased ratios in others. Clearly, my reaction conditions and apparatus were not providing satisfactory reproducibility. The setup does not have a temperature controller or consistent stirring in all reaction tubes, which could make it very difficult to achieve identical reaction conditions.

New Reaction Apparatus

A twelve-reaction carousel apparatus designed specifically for running simultaneous identical reactions was purchased from Brinkmann (see Chapter 3). The apparatus consists of a temperature controller with a stir plate, a water-cooled condenser, and a nitrogen source for each of the twelve reactions.

I repeated some of the reactions run previously in my homemade apparatus. The same reaction procedure was followed. The reactions were run in DMSO, DMF, and THF with no water, 10% water, 20% water, or 50% water (except for THF). The reactions with no water and 10% water were repeated and sampled twice to give a total of four data points for each solvent system. The reactions run with 20% or 50% water were run twice but only sampled once each. These results are plotted in Figure 4.9. The data were relatively consistent in the pure organic solvents but variations still occurred in the systems with water added, especially in DMF with 10% water. Although reproducibility was improved as I changed apparatus, data scattering was still observed.

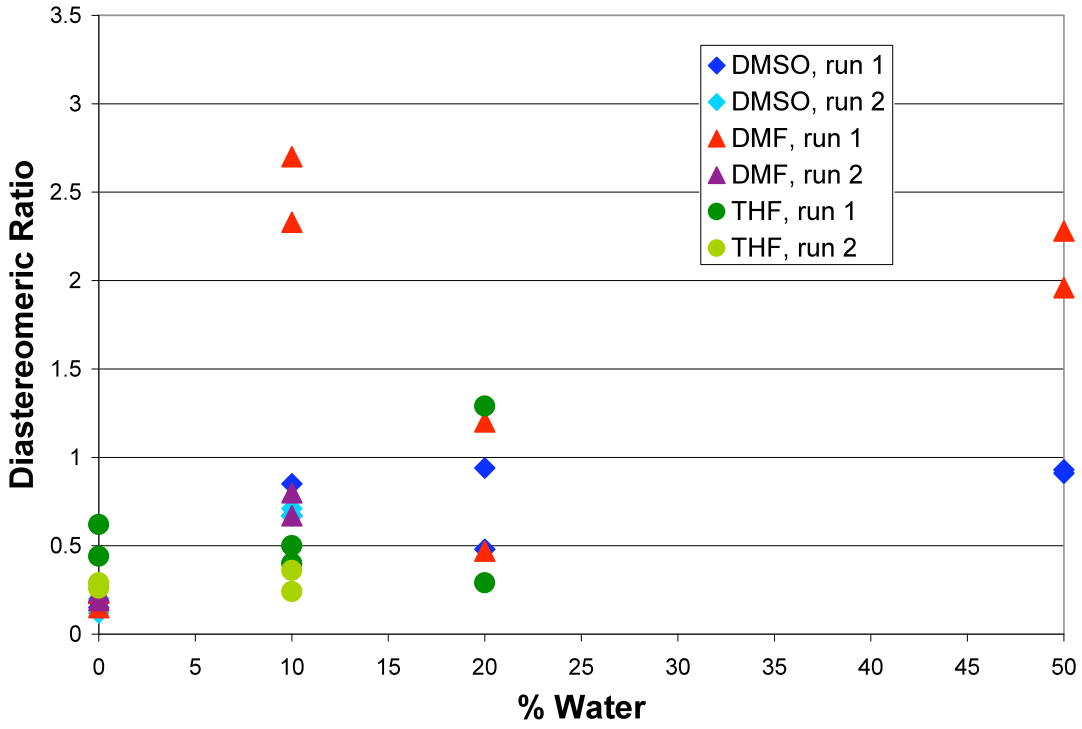

Figure 4.9: ATH results in new apparatus.

Optimization of Workup Procedures

The inconsistency of my results may have risen from a partial and/or preferential extraction of the products [(*R,S*)- and (*S,S*)-CMA] in the diethylether phase. To directly determine if the workup procedures were or were not altering the data, aliquots of the same reaction mixture were taken at three different stages: crude product mixture, diethylether extraction, and DCM extraction. Twelve identical reactions were all run in DMF with 10% water. I first took an aliquot from each reaction, centrifuged, and diluted the supernatant in methanol to make HPLC samples. Next, the reaction mixtures were subjected to the same diethylether extraction technique used previously. The organic phase was not completely homogeneous so I also tried extracting the organics into another solvent, DCM. The DCM workup resulted in two homogeneous phases: an aqueous phase and an organic phase. The organic phase was decanted and the

solvent removed under reduced pressure. The product residue was dissolved in methanol and analyzed by HPLC. All of these results are compared in Table 4.8.

Table 4.8: Comparison of workup procedures in ATH reaction.

	DR	% Conversion
Crude	0.45 ± 0.04	91 ± 9.3
Ether Extract	1.21 ± 0.44	91 ± 9.4
DCM Extract	0.33 ± 0.11	96 ± 7.7

As I expected, the crude sampling gave the most consistent results. The DR was much lower than the results measured in the old apparatus. The diethylether workup again gave high DRs with a significant amount of error. The (*S,S*) diastereomer is probably much less soluble in diethylether than the (*R,S*) product, leading to preferential extraction. This explains the previously misleading results. The DCM seemed to extract more of both products and results in DRs more comparable to the crude samples. I concluded that the reaction procedure must be improved to enable me to gather accurate and reproducible data.

Optimized Reaction Apparatus with Product Sampling

Rather than quenching the reaction and extracting the products, I switched my reaction procedure to dissolving the crude product mixture in a solvent (DMSO or methanol) and injecting these samples directly into the HPLC. DMSO and methanol were chosen because the starting material as well as both products had high solubility in these solvents. Each experiment was consistently sampled twice. The concentrations of the starting material and product diastereomers were calculated from calibration curves of each compound in DMSO or methanol. As before, the DRs were determined

by dividing the concentration of (*R,S*)-CMA by that of (*S,S*)-CMA. The percent conversion was determined based on the disappearance of the starting material (utilizing the HPLC calibration curve). Finally, the yield was calculated based on the appearance of the products, also utilizing HPLC calibration curves.

Test of Reproducibility

In addition to changing the sampling procedure, I also increased the scale of my reactions to 5 mL to reduce the effect of experimental errors. Half of the reactions (six) were run in DMF and the other half (six) were run in DMF with 10% water ("wet" DMF). The ruthenium catalyst precursor and TsEN were stirred for one hour at 40°C before the sodium formate and (*S*)-CMK were added. After running overnight, half of the reaction mixtures were dissolved in DMSO and the other half in methanol. The data from these reactions are shown in Table 4.9.

Table 4.9: Reproducibility of ATH reaction in pure and "wet" DMF.

		DR	% Conversion	% Yield
DMSO Workup	0% Water	0.14 ± 0.01	100 ± 0.0	42 ± 0.4
	10% Water	0.21 ± 0.05	100 ± 0.0	87 ± 3.7
MeOH Workup	0% Water	0.17 ± 0.01	100 ± 0.0	35 ± 0.9
	10% Water	0.39 ± 0.01	100 ± 0.0	85 ± 2.2

The new sampling technique greatly reduced the amount of error in my data. The most notable feature of this data set is the precision; the DRs vary by less than 0.05 and the yields by less than 4% in all cases. Another important trend is the increase in both DR and product yield upon the addition of a small amount of water. The same

trends occur when the reactions are sampled in DMSO or methanol. The methanol results were slightly more consistent than those results in DMSO.

Reproducibility with Triethylammonium Formate

The ATH reactions with formic acid and triethylamine, which form triethylammonium formate *in situ*, were run in ethyl acetate at room temperature. The previous literature reported experimental procedures utilizing a higher concentration of (*S*)-CMK and a lower concentration of catalyst, leading to a substrate-to-catalyst ratio (S/C) of 1000:1.[21] This ratio is ten times higher than the procedure I used in the reactions discussed above, which had a S/C of 100:1. Twelve reactions were run with triethylammonium formate; six reactions used a S/C of 100:1 and six used a S/C of 1000:1. The reactions were all run on a 5 mL scale. The ruthenium catalyst percursor and TsEN ligand were stirred together in the solvent for thirty minutes then triethylamine and formic acid were added before the (*S*)-CMK was added to start the reaction. The reaction mixtures were all homogeneous at the beginning of the reaction. After the reactions were run overnight, they were diluted in DMSO or methanol and the samples were analyzed by HPLC.

The results were very consistent with respect to the DRs, which ranged between 0.26:1 and 0.29:1. The results of the reactions, worked up in either DMSO or methanol, are summarized in Table 4.10. The rows in the tables refer to a S/C of 1000:1 and a S/C of 100:1. These reactions showed an increase in DR as well as product yield from the previously run reactions using sodium formate. This improvement in reaction results is most likely due to the increased solubility of the triethylammonium formate in the solvent as compared to sodium formate.

Table 4.10: Reproducibility of ATH reactions with triethylammonium formate in ethyl acetate.

		DR	% Conversion	% Yield
DMSO Workup	S/C = 1000:1	0.29 ± 0.00	100 ± 0.0	64 ± 2.3
	S/C = 100:1	0.26 ± 0.01	100 ± 0.0	89 ± 2.3
MeOH Workup	S/C = 1000:1	0.29 ± 0.01	100 ± 0.0	56 ± 0.9
	S/C = 100:1	0.27 ± 0.01	100 ± 0.0	74 ± 1.2

Although the DR did not significantly change with the different substrate-to-catalyst ratios, the higher catalyst loading improved the product yields. A higher catalyst concentration most certainly favors the desired reaction and minimizes the generation of side products. The starting material was not present in any of the samples. At a lower catalyst loading (S/C = 1000:1), many side products were formed, explaining the relatively low yield. The HPLC-MS spectra showed peaks consistent with the dechlorinated analogues of (*S*)-CMK, (*R,S*)-CMA, and (*S,S*)-CMA. In all cases, the results were very reproducible with very small experimental errors.

Effect of Different Reaction Conditions on ATH Reaction

Once a reliable and reproducible procedure was established, I moved on to improving my reaction results. The effect of each variable investigated is summarized in Table 4.11. These experiments will be discussed in more detail below.

Table 4.11: Effect of different reaction conditions on ATH reaction.

Variable	Reaction Conditions	Results
Organic Solvents	THF, Ethyl acetate, DMF, Ethanol, Methanol, and DMSO	High yields (~80%) for all Highest DR in methanol (0.45:1)
Substrate-to-Catalyst Ratio	From 25:1 to 400:1	No effect on yield or DR
Ratio of Ammonium Formate to (*S*)-CMK	From 0.5:1 to 5:1	< 2:1 ratio: decreased yields and conversions > 2:1 ratio: conversion and yield high No effect on DR
Ratio of Formic Acid to Triethylamine	From 0.4:1 to 2.5:1	< 1:1 ratio: many side products and low yields > 1:1 ratio: no side products and high yields No effect on DR
Substrate Concentration	From 0.05 M to 0.8 M	No effect on yield or DR
1:1 Water/Organic Mixed Solvents	THF, Ethyl acetate, DMF, Ethanol, Methanol, and DMSO	Increase in DR (as compared to pure solvents) Highest DR in DMF (from 0.34:1 to 0.55:1) Slight increase in yields
Time	Reaction quenched at 10, 20, 30, 40, 50, and 60 minute intervals	No effect on DR
Ligand	(1*R*,2*R*)-TsDPEN and (-)-Ephedrine	**(1*R*,2*R*)-TsDPEN** Improved DR to 1.89:1 No effect on yield (78%) **(-)-Ephedrine** DR of 1.32:1 (methanol) and 0.95:1 (THF/water) Many side products Low yields (57%)
Metal Catalyst	Ru(II), Rh(III), and Ir(III)	**TsEN Ligand** DR – 0.45:1 (Ru), 0.73:1 (Rh), and 0.80:1 (Ir) **(1*R*,2*R*)-TsDPEN** DR – 1.89:1 (Ru), 9.50:1 (Rh), and 2.85:1 (Ir)

ATH Reaction with Triethylammonium Formate in Various Organic Solvents

The ATH reaction, using triethylammonium formate, was run in a variety of organic solvents: THF, ethyl acetate, DMF, ethanol, methanol, and DMSO. One set of reactions was run with a S/C of 100:1 and a lower concentration of (*S*)-CMK and one set with a S/C of 1000:1 and a higher starting material concentration. Not all of the reaction mixtures were completely homogeneous prior to reaction. At a S/C of 1000:1, the methanol and ethanol mixtures were heterogeneous. With a S/C of 100:1, only the ethanol reaction mixture was heterogeneous. All of the reactions were run at room temperature overnight.

The DRs, conversions, and product yields of the reactions in various solvents are shown in Figure 4.10 and Figure 4.11. Figure 4.10 shows the results of the reactions run with a S/C of 1000:1 and Figure 4.11 represents the reactions run with a S/C of 100:1. The solvents are listed by increasing DR with methanol and DMSO giving the highest DR. Interestingly, although these two solvents gave the highest DR, the overall product yields when run with a S/C of 1000:1 were low, indicative of a large amount of side products. The DR was not affected much by the change in catalyst loading, but the yields increased significantly with the addition of larger amounts of catalyst. Again, this was attributed to the catalyst favoring the desired reaction. The catalyst loading corresponding to a S/C of 100:1 was utilized in subsequent reactions as it minimized the formation of side products.

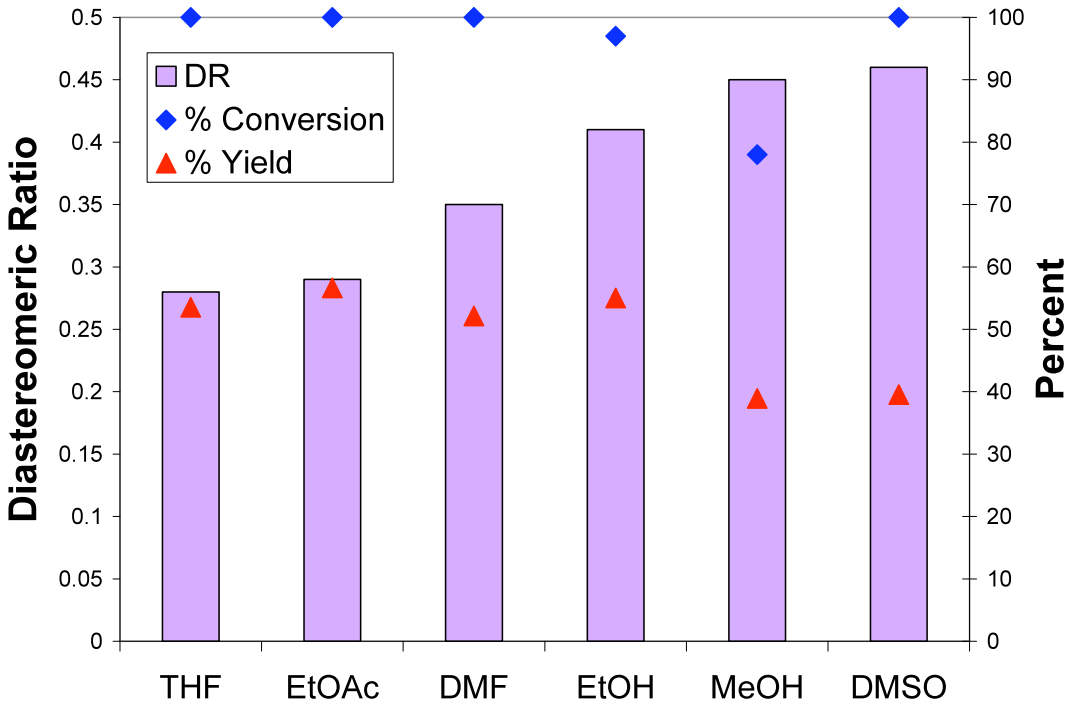

Figure 4.10: ATH with triethylammonium formate in various organic solvents using a S/C of 1000:1.

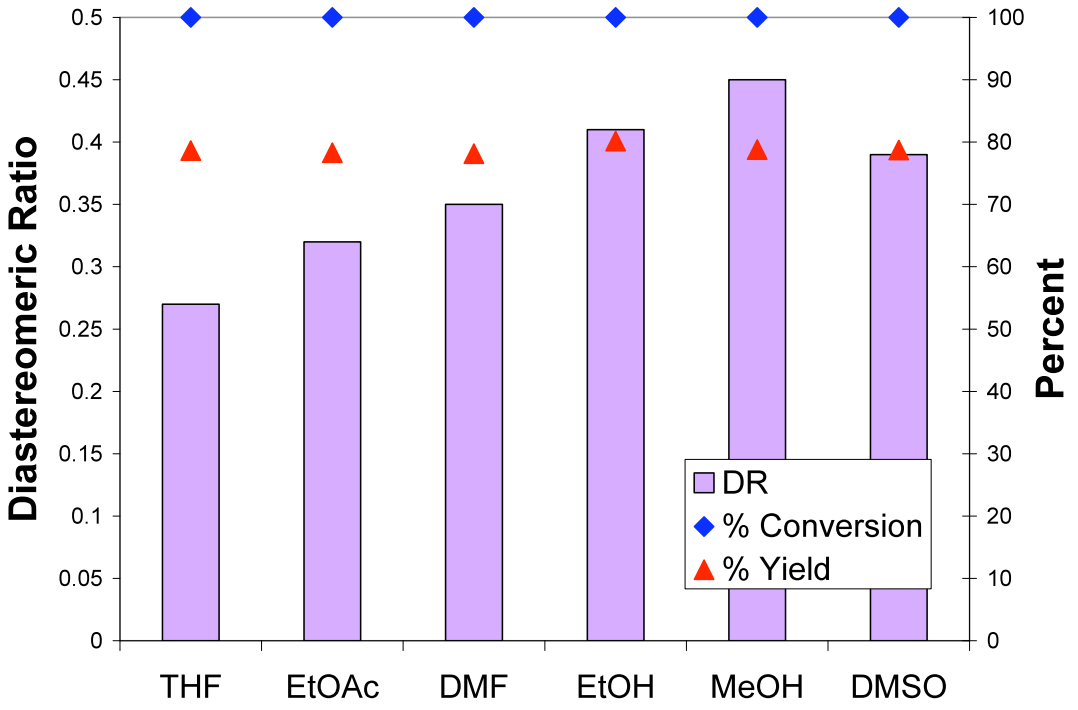

Figure 4.11: ATH with triethylammonium formate in various organic solvents using a S/C of 100:1.

Effect of Temperature and Water on ATH Reaction with Triethylammonium Formate

The reactions carried out with triethylammonium formate were run in the same organic solvents (THF, ethyl acetate, DMF, ethanol, methanol, and DMSO) and temperature (40°C) as described above with sodium formate. In addition, one set of reactions was run in the same solvents with the addition of 10% water. The reaction conditions and workup procedure were otherwise kept identical. The results are shown in Figure 4.12 and Figure 4.13. The most significant effects of increasing the temperature can be seen in the reactions run in THF and DMF. The yield of the reaction in THF decreases dramatically from that of about 80% at room temperature to 45% at 40°C. However, the reaction in DMF shows an improvement in DR, going from about 0.35:1 at room temperature to 0.40:1 at 40°C. Figure 4.13 shows that water had the effect of evening out the results in different solvents. Overall, the best results still occur when methanol is used as the reaction solvent.

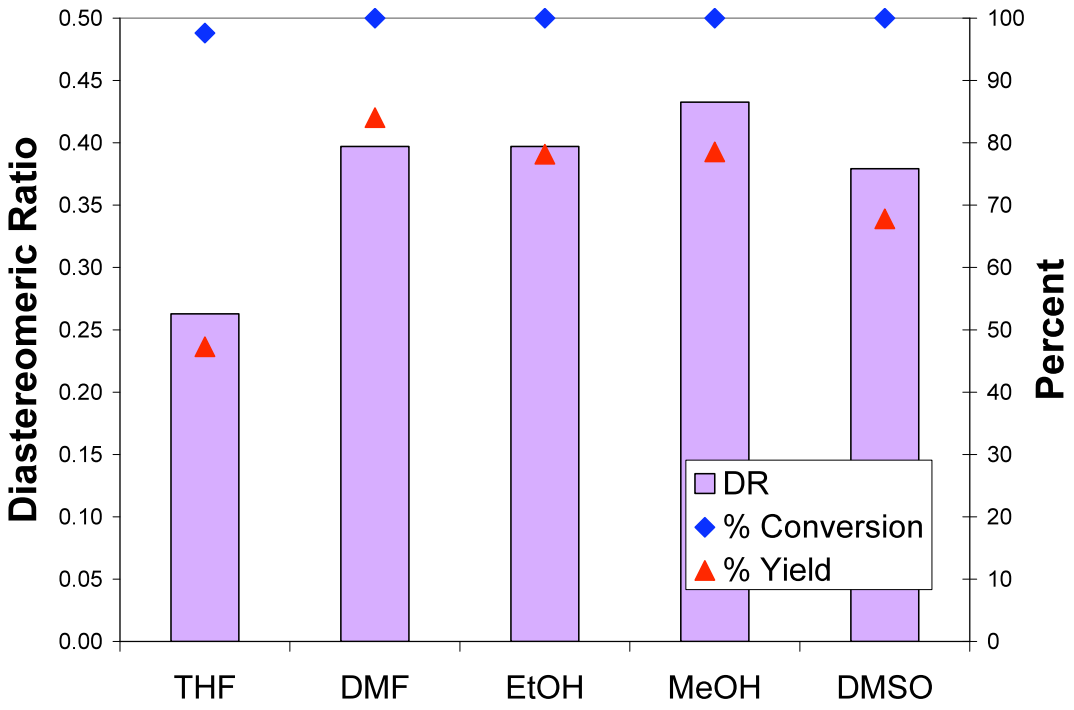

Figure 4.12: ATH with triethylammonium formate in various organic solvents at 40°C.

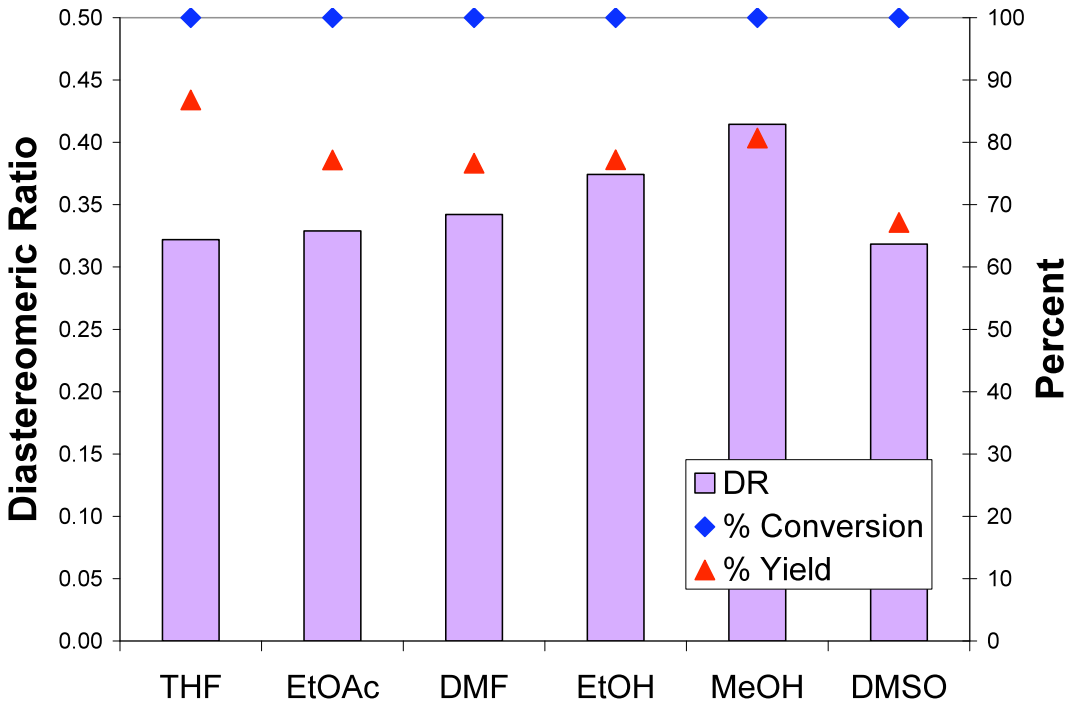

Figure 4.13: ATH reaction with triethylammonium formate in various solvents with 10% water at 40°C.

Effect of Substrate-to-Catalyst Ratio

The effect of the ratio of (*S*)-CMK substrate to ruthenium catalyst was investigated. Keeping the amounts of (*S*)-CMK, triethylamine, and formic acid constant, the amounts of catalyst precursor and ligand were varied from 0.04 equivalents (S/C = 25:1) to 0.0025 equivalents (S/C = 400:1). The ratio of ligand to catalyst precursor was kept constant. The reactions were all run in duplicate in methanol at room temperature. Table 4.12 summarizes the results of these experiments. The small amount of deviation in the DR and yield between the various catalyst loadings falls within experimental error. Overall, the substrate-to-catalyst ratio appears to have no effect on either DR or yield. This means that low catalyst and ligand loadings (S/C = 400:1) can be used to decrease the cost of the reaction without any impact on the product yield.

Table 4.12: Effect of substrate-to-catalyst ratio on ATH reaction.

	DR	% Conversion	% Yield
25:1	0.45 ± 0.01	100 ± 0.0	82 ± 3.1
50:1	0.43 ± 0.00	100 ± 0.0	83 ± 0.5
100:1	0.45 ± 0.01	100 ± 0.0	83 ± 1.4
150:1	0.45 ± 0.01	100 ± 0.0	83 ± 1.6
200:1	0.44 ± 0.00	100 ± 0.0	79 ± 1.5
400:1	0.45 ± 0.02	100 ± 0.0	78 ± 1.1

Effect of Formate-to-Substrate Ratio

The ratio of triethylammonium formate to substrate was investigated. All the reaction vessels were loaded with the same amounts of catalyst, ligand, and starting material in methanol. While maintaining the same ratio of triethylamine to formic acid, I decreased the amount of triethylammonium formate from five equivalents down to 0.5 equivalents. A decline in yield as the amount of formate decreased was expected since the formate is the hydrogen source for the reduction. The yields and conversion

decreased for a formate-to-substrate ratio less than 2:1 (Table 4.13). The DRs, however, remained unchanged.

Table 4.13: Effect of formate-to-substrate ratio on ATH reaction.

	DR	% Conversion	% Yield
5:1	0.43 ± 0.02	100 ± 0.0	86 ± 3.4
4:1	0.43 ± 0.01	100 ± 0.0	86 ± 1.8
3:1	0.43 ± 0.01	100 ± 0.0	84 ± 4.0
2:1	0.44 ± 0.01	100 ± 0.0	86 ± 2.1
1:1	0.45 ± 0.01	93 ± 3.5	63 ± 8.6
0.5:1	0.46 ± 0.03	53 ± 10.1	27 ± 6.8

Effect of Triethylamine-to-Formic Acid Ratio

I explored the effects of the triethylamine-to-formic acid ratio by keeping the catalyst, ligand, (*S*)-CMK, and formic acid loadings constant while decreasing the amount of triethylamine used from 2.5 equivalents relative to formic acid to 0.4 equivalents. These reactions were again run in methanol at room temperature. As Table 4.14 shows, the DR was unaffected by the changes in triethylamine-to-formic acid ratio. However, the yields significantly decreased from 98% down to 20% in the presence of an excess of triethylamine. I attribute this decrease in yield to a number of side reactions that occur in the basic solution, further evidenced by the large number of extra peaks detected in the HPLC spectrum. In order to maintain high yields, an excess of formic acid must be used.

Table 4.14: Effect of triethylamine-to-formic acid ratio on ATH reaction.

	DR	% Conversion	% Yield
2.5:1	0.43 ± 0.01	100 ± 0.0	20 ± 8.0
2:1	0.42 ± 0.01	100 ± 0.0	53 ± 22
1.5:1	0.43 ± 0.03	100 ± 0.0	46 ± 28
0.67:1	0.45 ± 0.01	100 ± 0.0	91 ± 3.5
0.5:1	0.46 ± 0.01	100 ± 0.0	88 ± 3.9
0.4:1	0.48 ± 0.01	100 ± 0.0	98 ± 4.5

Effect of Substrate Concentration

The effect of (*S*)-CMK concentration on the diastereoselectivity and yield of the ATH reaction was investigated. The catalyst was prepared on a batch scale by stirring the ruthenium precatalyst and TsEN ligand in methanol for one hour at room temperature. Each reaction tube was then loaded with a set volume of the catalyst solution. Triethylamine, formic acid, and increasing amounts of (*S*)-CMK were added to start the reactions. All reactions were initially homogeneous except for the experiment using an initial (*S*)-CMK concentration of 0.8 M. The results of these experiments are given in Table 4.15. The DR did not vary as a function of the (*S*)-CMK concentration. The yield did decrease slightly (about 10%) at higher substrate concentrations. This could be due to a decrease in formate-to-substrate ratio at higher concentrations or the heterogeneous nature of the 0.8 M reaction.

Table 4.15: Effect of varying (*S*)-CMK concentration on ATH reaction.

	DR	% Conversion	% Yield
0.05 M	0.48 ± 0.02	100 ± 0.0	89 ± 1.4
0.1 M	0.45 ± 0.03	100 ± 0.0	85 ± 3.3
0.2 M	0.45 ± 0.01	100 ± 0.0	86 ± 2.1
0.4 M	0.44 ± 0.01	100 ± 0.0	82 ± 1.7
0.6 M	0.45 ± 0.01	100 ± 0.0	83 ± 7.1
0.8 M	0.45 ± 0.01	100 ± 0.0	73 ± 2.0

Effect of Time on ATH Reaction

In order to determine how the diastereoselectivity changes as a function of time, two sets of six identical reactions were prepared and quenched at ten minute intervals for one hour. First, the catalyst was prepared by mixing the ruthenium precatalyst and TsEN in methanol for one hour. Then, triethylamine and formic acid were added. Finally, a solution of (*S*)-CMK in methanol was added, triggering the beginning of the reaction. After 10, 20, 30, 40, 50, or 60 minutes, the reactions were quenched with a saturated ammonium chloride solution. The organics were extracted into DCM. The solvent was removed from each solution and the residue dissolved in methanol and analyzed by HPLC. Throughout the time interval investigated, the DR remained constant at 0.42:1. After one hour, the reaction yield was about 60% (Figure 4.14), indicating that running these reactions overnight is unnecessary. The reaction is likely complete in less than two hours.

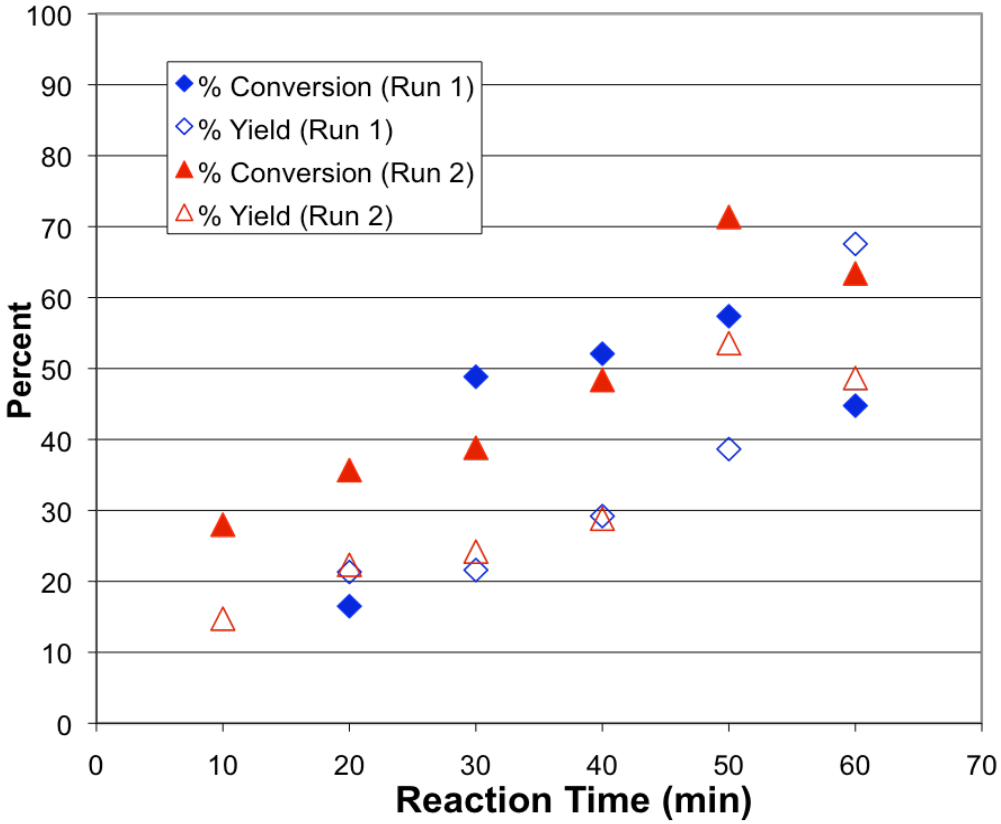

Figure 4.14: Effect of time on ATH reaction.

Investigation of Various ATH Ligands

One of the most influential variables to the ATH reaction is the ligand surrounding the transition metal catalyst. In the reactions described above, TsEN was used with a ruthenium metal center. The reactions were carried out with other ligands [ethylenediamine, ethanolamine, and (-)-ephedrine] or without any ligand. The same general reaction procedure was used. All of the reactions were run in methanol at room temperature overnight. The results of these reactions are given in Table 4.16. In all cases the yields were significantly lower than that with TsEN (80%). In the case of ethylenediamine, the HPLC spectrum showed no peaks corresponding to the desired reduction products. The use of ethanolamine as the ligand resulted in a slight increase

in DR (0.56:1) but yielded very little product (5%). The reaction using (-)-ephedrine also increased the DR but a large number of side reactions led to a decrease in yield (23%). (-)-Ephedrine was also used as a ligand in a 1:1 water/THF solvent system, which resulted in a DR of 0.95:1 with a higher yield of 57%. However, there were still a large number of side products present.

Table 4.16: Effect of ligand on ATH reaction.

	DR	% Conversion	% Yield
No ligand	0.44 ± 0.01	56 ± 3.4	23 ± 3.0
Ethylenediamine		34 ± 1.3	0
Ethanolamine	0.56 ± 0.02	39 ± 1.9	5.4 ± 0.9
(-)-Ephedrine		40 ± 5.0	0

In addition to using the reference ligands in the ATH reaction, the commonly used chiral ligand (1*R*,2*R*)-TsDPEN was tested for the ATH reduction of (*S*)-CMK. Researchers found that the use of (1*R*,2*R*)-TsDPEN in conjunction with ruthenium, rhodium, or iridium catalyst precursors gave high yields and diastereoselectivity in the reduction of various ketones.[8,9] When the chiral ligand (1*R*,2*R*)-TsDPEN was used in place of TsEN, it was found that the DR increased to 1.89:1 from 0.45:1. The yield remained around 80%, comparable to my previous reactions. Although I improved the diastereoselectivity of the ATH reaction, the chiral ligand is ten times more expensive than the achiral version.

Effect of Various Metal Catalysts

I finally chose to focus on the use of different transition metal catalyst precursors. The most commonly used compounds in the literature ATH reactions are [Ru(*p*-cymene)Cl_2]$_2$, [Rh(C_5Me_5)Cl_2]$_2$, and [Ir(C_5Me_5)Cl_2]$_2$. I followed the same procedure used

previously, stirring the different catalyst precursors together with either TsEN or (1*R*,2*R*)-TsDPEN in methanol for one hour and then adding the remaining reagents to start the reaction. Table 4.17 summarizes the results of these experiments. Both the rhodium and iridium catalyst precursors improved the diastereoselectivity of the reaction with either of the ligands. The use of the rhodium catalyst in conjunction with the chiral ligand resulted in the highest DR of 9.5:1. Unfortunately, the rhodium catalyst precursor is ten times more expensive than the ruthenium precursor so the increase in selectivity would have to be weighed against the increased cost of the reaction.

Table 4.17: ATH reaction with Ru, Rh, and Ir catalyst precursors.

		Catalyst Precursor					
		$[\mathbf{Ru}(\text{p-cymene})Cl_2]_2$		$[\mathbf{Rh}(C_5Me_5)Cl_2]_2$		$[\mathbf{Ir}(C_5Me_5)Cl_2]_2$	
		DR	% Yield	DR	% Yield	DR	% Yield
Ligand	No ligand	0.44	23				
	Ethylenediamine		0				
	Ethanolamine	0.56	5				
	TsEN	0.45	80	0.73	85	0.80	79
	(1R,2R)-TsDPEN	1.89	78	9.50	82	2.85	85
	(-)-Ephedrine	1.32	44	0.54	58		

Because of the significant improvements in diastereoselectivity observed with the rhodium catalyst, this catalyst was studied in different solvents. Figure 4.15 shows the results of the ATH reaction with rhodium and TsEN in ten pure organic solvents. As with the ruthenium catalyst, it was found that methanol gave the best results in terms of both DR and yield. Again, mixed water/organic solvent systems were investigated. Choosing six organic solvents (methanol, ethanol, isopropanol, DMF, DMSO, and acetonitrile), the experiments were conducted with rhodium and TsEN in a mixed 10% water/organic solvent mixture. These results are illustrated in Figure 4.16. Interestingly, the DR decreased upon addition of water to the alcohol solvents. However, the other three

solvents (DMF, DMSO, and acetonitrile) all showed an increase in diastereoselectivity with the increase in water content. In addition, a significant increase in yield occurred when 10% water was added to DMSO. I speculate that the reaction proceeds faster in a water/DMSO system, reducing the number of side reactions.

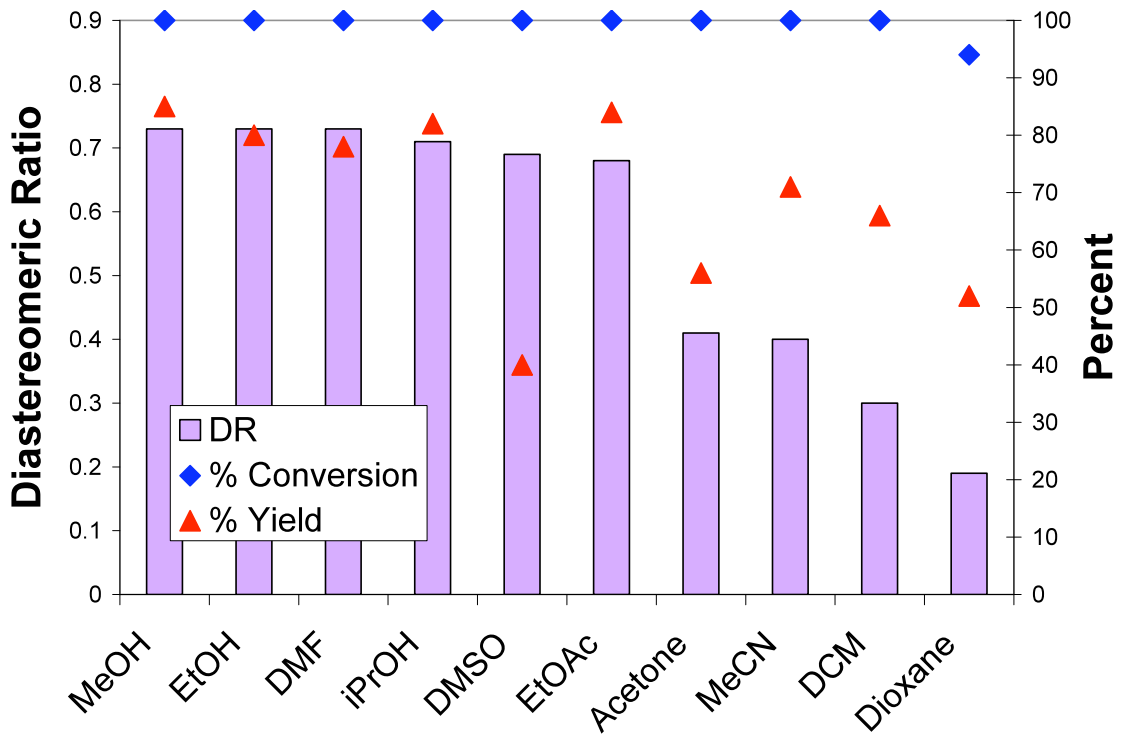

Figure 4.15: ATH reaction with Rh catalyst in various organic solvents.

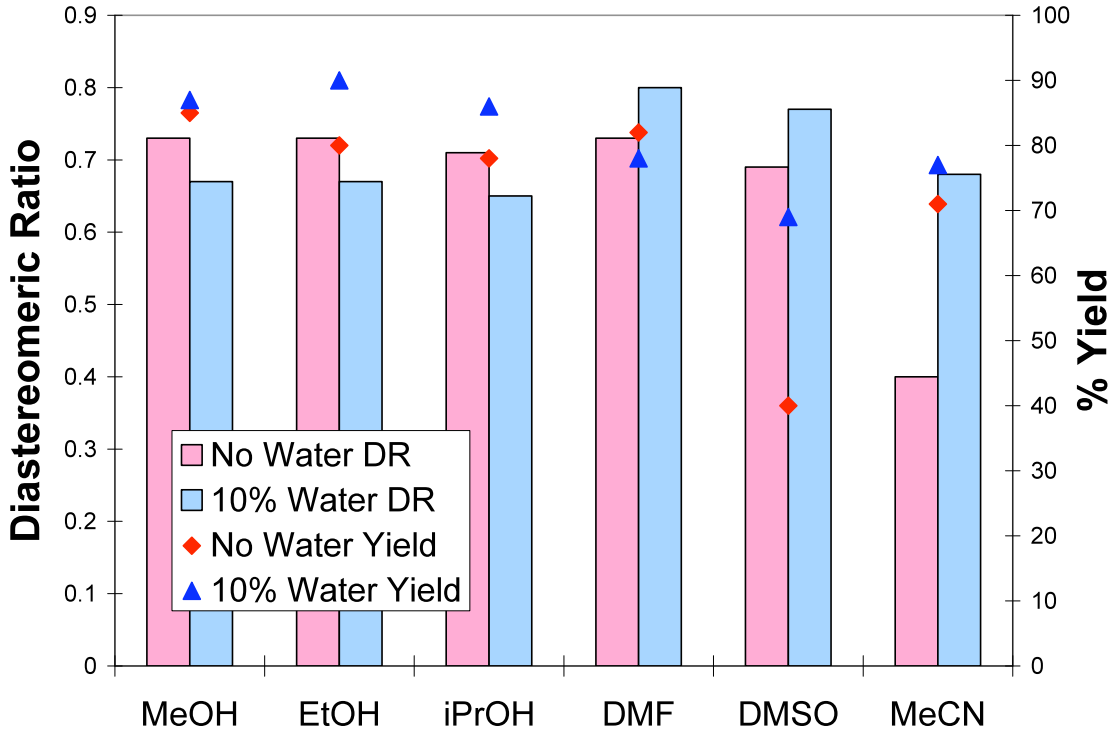

Figure 4.16: ATH reaction with Rh catalyst in pure organic solvents and in organic solvents with 10% water.

CONCLUSIONS

In conclusion, I have investigated many aspects of the ATH reaction to optimize the reaction conditions for diastereoselective production of (*R,S*)-CMA. I first focused on obtaining reproducible and reliable results. Then, by varying the reaction conditions, I was able to increase the DR from 0.06:1 in the standard MPV reduction to as high as 9.5:1 using a chiral rhodium catalyst. The transition metal used as the catalyst and the structure of the ligand were found to be the most important variables in the ATH reaction.

EXPERIMENTAL METHODS

Materials and Equipment

All chemicals were ordered from Sigma-Aldrich or VWR and used as received, unless otherwise noted. The (*S*)-CMK starting material and samples of (*S,S*)- and (*R,S*)-CMA were obtained from Ampac Fine Chemicals (Sacramento, CA). ^{1}H and ^{13}C NMR spectra were obtained from a Varian-Mercury VX400 MHz spectrometer using $CDCl_3$ as an internal reference, unless otherwise noted. HPLC analysis was run on an Agilent 1100 series LC with a UV detector and an ESI-MS.

Product Analysis

The products were analyzed using the same ^{1}H NMR techniques as in the MPV reductions. The same HPLC method was also used to analyze the ATH product samples but new calibration curves were made.

HPLC Analysis: DMSO Calibration Curves

Samples of (*S*)-CMK, (*S,S*)-CMA, and (*R,S*)-CMA were used to make calibration curves on the HPLC. A stock solution at the highest concentration (~5 mg/mL) was made for each compound and diluted to make the remainder of the samples. The peak areas from the HPLC spectra were plotted against the sample concentrations and fitted to a straight line going through the origin. The resulting calibration curves all gave high correlation values ($R^2 > 0.99$). These curves are given in Figure 4.17, Figure 4.18, and Figure 4.19. The (*R,S*)-CMA sample was only 90% pure, with 10% of (*S,S*)-CMA as the impurity. The sample concentrations were corrected by subtracting the concentration of (*S,S*)-CMA in the samples. I determined this concentration from the (*S,S*)-CMA

calibration curve based on the corresponding peak areas in the (*R,S*)-CMA calibration samples. These curves were used to obtain the product yield from the ATH reactions based on the HPLC spectra peak areas.

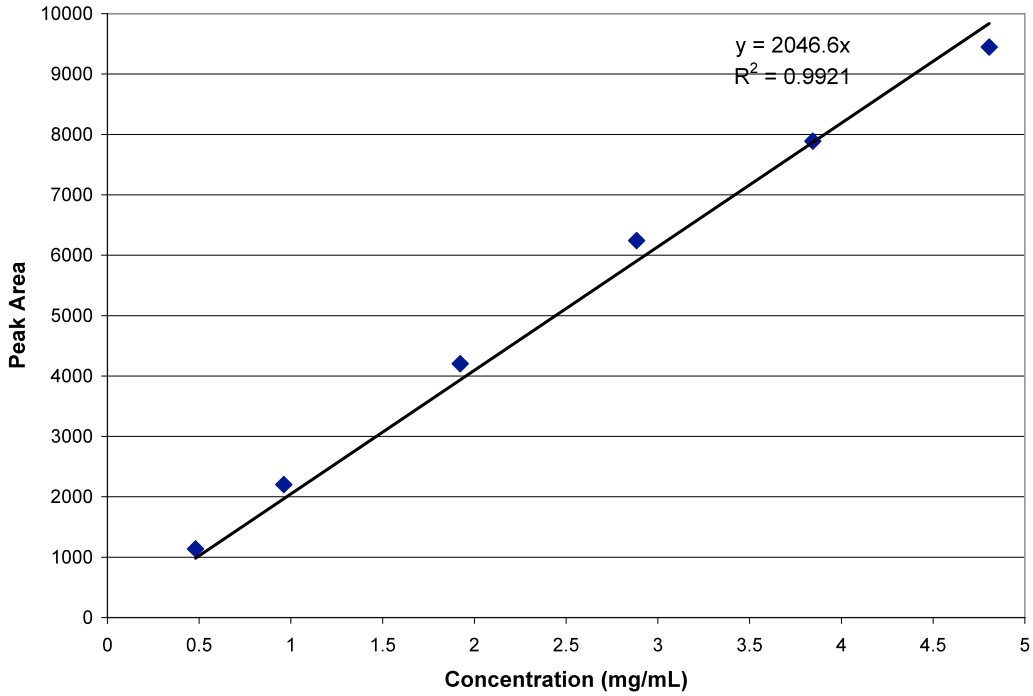

Figure 4.17: (*S*)-CMK calibration curve in DMSO.

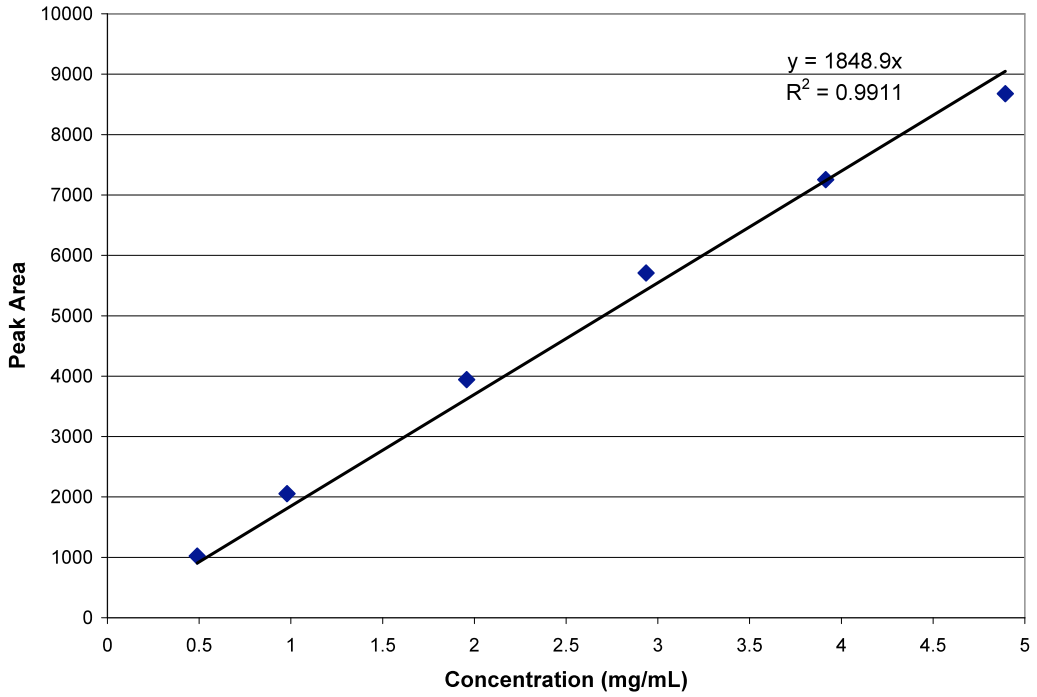

Figure 4.18: (*S,S*)-CMA calibration curve in DMSO.

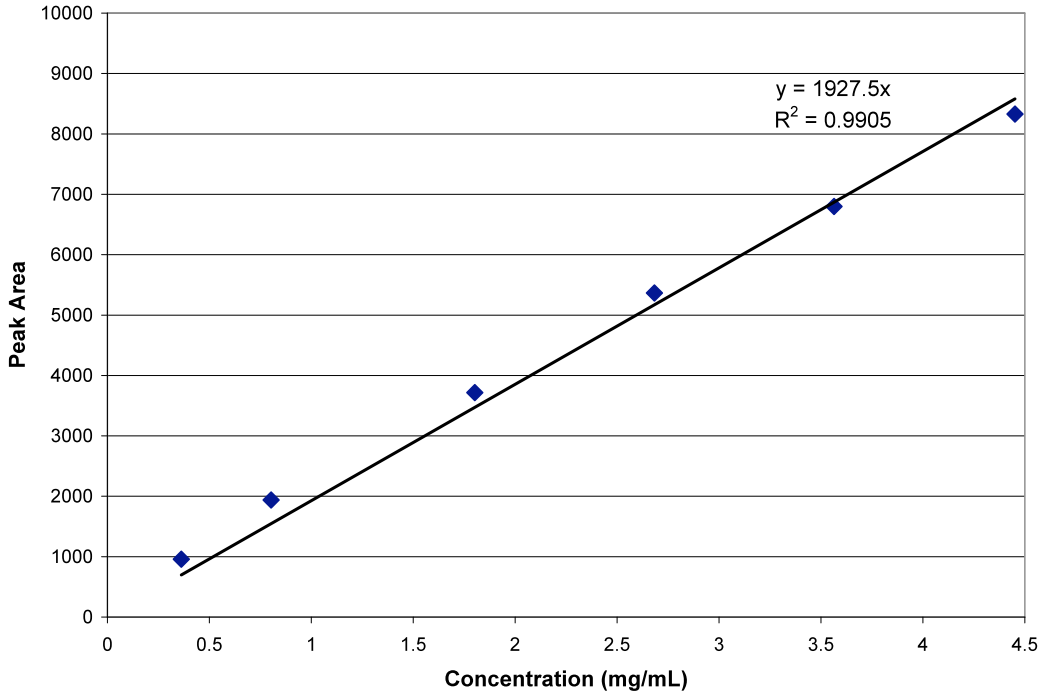

Figure 4.19: (*R,S*)-CMA calibration curve in DMSO.

HPLC Analysis: Methanol Calibration Curves

The calibration curves for (*S*)-CMK, (*S,S*)-CMA, and (*R,S*)-CMA in methanol were obtained in a manner identical to that for the same curves in DMSO. The samples for the methanol calibration curves were made in duplicate and the curve was made using the average area between the two samples. Error bars are shown in the (*S*)-CMK and (*S,S*)-CMA curves but they were generally smaller than the representative points. The concentrations in the (*R,S*)-CMA samples were again corrected using the (*S,S*)-CMA calibration curve. The calibration curves are shown in Figure 4.20, Figure 4.21, and Figure 4.22. These calibration curves were used to determine the product yield in the AHT reactions from the HPLC spectra.

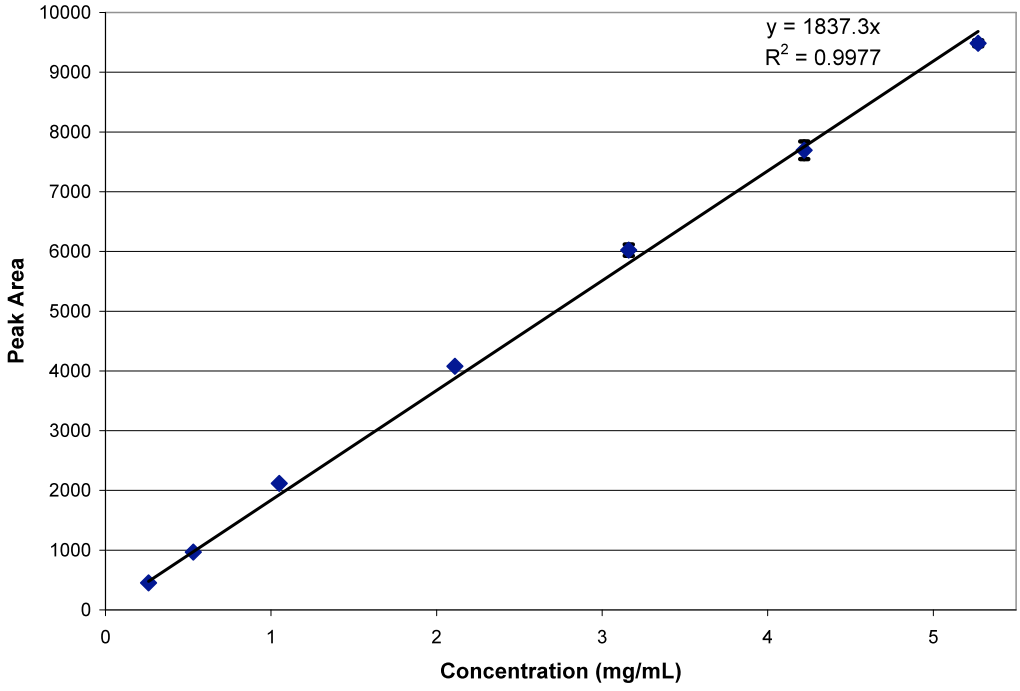

Figure 4.20: (*S*)-CMK calibration curve in methanol.

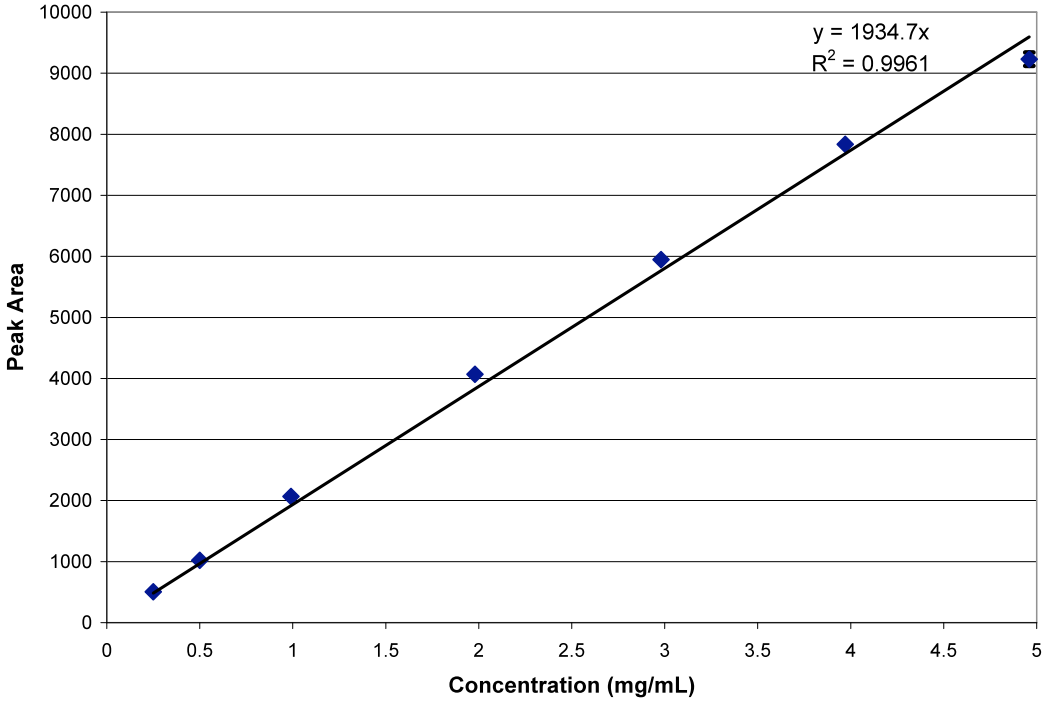

Figure 4.21: (*S,S*)-CMA calibration curve in methanol.

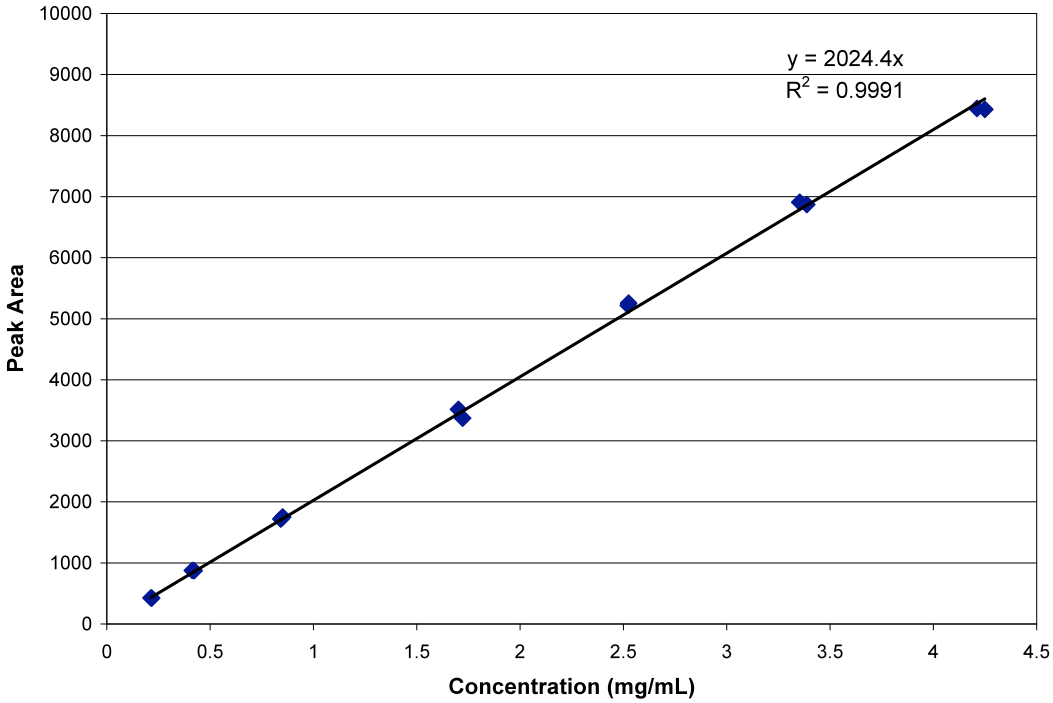

Figure 4.22: (*R,S*)-CMA calibration curve in methanol.

Heterogeneous Catalytic Hydrogenation

The catalytic hydrogenation reactions were run in a Bucchi shaker hydrogenation apparatus as shown in Figure 4.23. This setup allows for good mixing while running reactions under pressure.

Figure 4.23: Shaker type hydrogenation apparatus.

Hydrogenation with Platinum Oxide

(*S*)-CMK (2.5 g, 8.4 mmol) was added to a suspension of platinum oxide (0.1 g, 0.4 mmol) in a solvent (25 mL). The organic solvents used include acetonitrile, THF, ethyl acetate, methanol, ethanol, DMF, and water. The reaction vessel was flushed with nitrogen then 50 psi of hydrogen was added and vented. This cycle was repeated three times. The reaction vessel was then filled with 30 psi of hydrogen and left to run at room temperature for three hours. The reaction vessel was vented to stop the reaction and the solution was filtered on a Celite pad to remove the catalyst. The solution was diluted with water and extracted into diethylether. The ethyl acetate was removed under vacuum and the resulting residue was analyzed by HPLC.

Hydrogenation with Palladium on Carbon

The same procedure was used for the palladium on carbon catalyst as was described above for the platinum oxide. The only difference was the amount of palladium on carbon (0.045 g of 5 weight% loading, 0.02 mmol).

Hydrogenation with Nickel Nanoparticles

The same procedure was used for the nickel nanoparticle catalyst as was described above for the platinum oxide. The nickel nanoparticles were previously synthesized by Hillary Huttenhower.

Asymmetric Transfer Hydrogenation

Synthesis of (1*R*,2*R*)-TsDPEN

(1*R*,2*R*)-*N*-(*p*-toluenesulfonyl)-1,2-diphenylethylenediamine was synthesized according to literature procedure.[31] (1*R*,2*R*)-1,2-diphenylethylenediamine (0.81 g, 3.8 mmol) was stirred in anhydrous THF (32 mL) at 0°C. Anhydrous triethylamine (1.6 mL) was added to this solution. Then a solution of 4-methylbenzene-1-sulfonyl chloride (0.73 g, 3.8 mmol) in anhydrous THF (8 mL) was added over thirty minutes. The reaction mixture was stirred overnight at 0°C. The solvent was removed under vacuum to afford a white solid. This solid was treated with a sodium bicarbonate solution (60 mL) and extracted with DCM (4 x 15 mL). The combined organic layers were washed with brine (20 mL), dried over magnesium sulfate and concentrated under vacuum. The crude product was purified by flash chromatography in ethyl acetate on a silica column. This afforded the pure product as a white solid. This compound is also commercially available from Aldrich.

^{1}H ($CDCl_3$): 2.30 (s, 3H), 4.11 (d, 2H), 4.26 (m, 1H), 6.94 (d, 2H), 7.14 (m, 10H), 7.27 (d, 2H).

Synthesis of TsEN

The achiral ligand (*N*-tolylsulfonylethylenediamine) was synthesized following the same procedure as above for the chiral ligand. The only modification was to change the starting diamine material to 1,2-ethylenediamine. The product was a white powdery solid. This compound is also commercially available from Aldrich.

^{1}H ($CDCl_3$): 2.40 (s, 3H), 2.76 (m, 2H), 2.93 (m, 2H), 7.29 (d, 2H), 7.72 (d, 2H).

Original Reaction Apparatus

The original reaction apparatus used for the ATH reactions consisted of an oil bath on a hot plate with a nitrogen line split into eight outlets, which could be connected to reaction tubes. A cold water line was wrapped around the top of each tube to act as a makeshift condenser. The temperature was monitored by a thermometer placed in the oil bath and maintained using the hot plate controls. Each reaction tube was equipped with a magnetic stir bar to enhance mixing of the contents.

Original Reaction Procedure

The ATH reaction was originally performed as follows. The catalyst precursor, dichloro(*p*-cymene)ruthenium (II) dimer (3 mg, 0.005 mmol), and the chiral or achiral ligand (0.018 mmol) were stirred in the organic solvent or water (1 mL) for one hour at 40°C. In the case of the "wet" organic solvents, an additional amount of water (0.1 mL) was used. I also tried 1:1 mixtures of water and organic solvents, in which case 0.5 mL of both water and organic solvent were added to the reaction mixture in place of the 1 mL of organic solvent. Sodium formate (0.26 g, 3.9 mmol) was then added to the reaction mixture, followed by the (*S*)-CMK (0.15 g, 0.50 mmol). The reaction was allowed to run overnight at 40°C. The reaction was removed from heat and quenched with a saturated ammonium chloride solution (~1 mL). The organics were extracted into

ether and filtered through a Celite pad. The ether solvent was removed by drying under nitrogen and this crude product was analyzed by HPLC and ^{1}H NMR.

New Reaction Apparatus

A 12-reaction carousel apparatus from Brinkmann with built-in temperature controller and stir plate (see Chapter 3) was purchased. This apparatus has connections for all twelve reactions to be run under an inert gas with consistent stirring and heating. The set up also includes a condenser, which was hooked up to a cold water line. The temperature controller kept the temperature of each reaction to ±1°C of the set point.

Comparison of Workup Methods

Twelve identical reactions in DMF with 10% water were set up and run according to the standard procedure above. After reacting overnight, the reactions were removed from heat and a small sample (~0.2 mL) was removed from each reaction. These samples were centrifuged and the supernatant decanted and diluted in methanol. The crude samples were run directly in the HPLC. Using the same reaction mixtures, I next repeated my ether extract procedures as before. The reactions were quenched using saturated ammonium chloride, extracted into ether, and filtered through a Celite pad. The ether was removed under inert gas and the solid residue was dissolved in methanol to make HPLC samples. The reaction mixtures were extracted again using DCM. This extraction resulted in two clear phases with no precipitates. The DCM extraction was repeated and the organic phase decanted and dried. HPLC samples of the residue were made in methanol.

Product Sampling Test of Reproducibility

The reproducibility of my crude sampling method was tested using the ATH reactions run in DMF, with six reactions in pure DMF and six reactions in "wet" DMF. The scale of the reactions was increased to 5 mL to also improve the reproducibility. The ruthenium catalyst precursor (15 mg, 0.025 mmol) and TsEN (21 mg, 0.085 mmol) were stirred in the solvent (either 5 mL DMF, or 4.5 mL DMF and 0.5 mL water) for one hour at 40°C. Sodium formate (1.3 g, 19 mmol) and then (*S*)-CMK (0.75 g, 2.5 mmol) was added to start the reaction. The reactions were run overnight at 40°C. At the conclusion of the reaction, the reaction mixtures were removed from heat and half of them dissolved in methanol (15 mL) while the other half were dissolved in DMSO (15 mL). Small samples (0.125 mL) were taken from each flask and diluted to 1 mL with their respective solvents. These samples were analyzed by HPLC.

Reproducibility with Triethylammonium Formate

I ran one set of six reactions using the literature conditions and one set of six reactions using the reagent concentrations used in the previous ATH reactions. In the case of the literature reactions, smaller amounts of the ruthenium catalyst precursor (2.6 mg, 0.0042 mmol) and TsEN (3.7 mg, 0.015 mmol) were used while larger amounts of (*S*)-CMK (1.2 g, 4.0 mmol) were added. Under our reactions conditions, the ruthenium catalyst (16 mg, 0.026 mmol) and TsEN (21 mg, 0.083 mmol) to substrate (0.74 g, 2.5 mmol) ratio was much higher. In all cases, the catalyst and ligand were stirred in ethyl acetate for thirty minutes at room temperature. Then, the triethylamine (0.56 mL, 4.0 mmol) and formic acid (0.18 mL, 4.9 mmol) were added. Condensation was formed on the walls of the reaction tubes after addition of the acid but they cooled after a few minutes. After waiting for ten minutes, the (*S*)-CMK starting material was added. The reactions were all completely homogeneous at the beginning of the reaction and were

left to run overnight at room temperature. Half of the reactions were dissolved in methanol (25 mL) and half in DMSO (25 mL). Two samples (0.25 mL) were taken from each reaction and diluted to 1 mL with their respective solvents. These samples were analyzed by HPLC.

ATH General Reaction Procedure

ATH reactions were run according to the following general reaction procedure. $[Ru(p\text{-cymene})Cl_2]_2$ (2.6 mg, 0.0042 mmol) and the TsEN ligand (3.7 mg, 0.015 mmol) were first loaded into the reaction tubes, dissolved in the reaction solvent (5 mL) and stirred at room temperature for one hour to form the precatalyst. Next, the triethylamine (0.56 mL, 4.0 mmol) and formic acid (0.18 mL, 4.9 mmol) were added. The (*S*)-CMK (0.75 g, 2.5 mmol) was added last to start the reaction. After running overnight, the reaction mixtures were all dissolved in methanol (25 mL) and stirred for approximately thirty minutes until the solutions were homogeneous. Two samples (0.25 mL) were taken from each solution and diluted with methanol to a total volume of 1 mL. The samples were analyzed by HPLC using the procedure described above.

Reaction in Various Organic Solvents

ATH reactions were run in six organic solvents: ethyl acetate, DMSO, THF, DMF, methanol, and ethanol. One set was run using literature conditions with a substrate-to-catalyst ratio of 1000:1; the other set of reactions was run using my previous conditions with a substrate-to-catalyst ratio of 100:1. In the first case, the ruthenium catalyst precursor (2.6 mg, 0.0042 mmol) and TsEN (3.7 mg, 0.015 mmol) loadings were much lower and the amount of (*S*)-CMK substrate (1.19 g, 4.00 mmol) was high. With a substrate-to-catalyst loading of 100:1, we used larger amounts of catalyst (16 mg, 0.025 mmol) and ligand (21 mg, 0.085 mmol) with a smaller amount of (*S*)-CMK (0.75 g, 2.5

mmol). In both cases, the catalyst and ligand were first loaded in the reaction tubes and stirred in the reaction solvent (5 mL) for one hour. Next, the triethylamine (0.56 mL, 4.0 mmol) and formic acid (0.18 mL, 4.9 mmol) were added. The (*S*)-CMK was added last to start the reaction. Not all of the reactions were homogeneous, the worst being the alcohol solvents. The reactions were all run at room temperature overnight and analyzed following the general procedure above.

Effect of Temperature and Water

The effect of temperature and water concentration was evaluated by running the ATH reaction at 40°C with one set of reactions in pure organic solvents and one with a 1:9 water/organic solvent mixture. The organic solvents tested were the same as above: ethyl acetate, DMSO, THF, DMF, methanol, and ethanol. The ruthenium catalyst precursor (16 mg, 0.025 mmol) and TsEN ligand (21 mg, 0.085 mmol) were stirred together in the reaction solvent for thirty minutes at 40°C. Triethylamine (0.56 mL, 4.0 mmol) and formic acid (0.18 mL, 4.9 mmol) were added to the mixtures. Finally, (*S*)-CMK (0.75 g, 2.5 mmol) was added to start the reaction. The reactions were run at 40°C overnight. Following the same workup procedure as above, the reactions were dissolved in methanol (25 mL) and sampled twice before being run on the HPLC.

Effect of Substrate-to-Catalyst Ratio

Following the same general reaction procedure described above, the effect of the substrate-to-catalyst ratio was investigated by varying the amount of catalyst and ligand while everything else remained the same. The reactions were all run in methanol (5 mL). The amount of ruthenium catalyst precursor was decreased from a S/C of 25:1 (62 mg, 0.10 mmol) to a S/C of 400:1 (3.7 mg, 0.006 mmol). The ratio of TsEN ligand to the ruthenium catalyst precursor remained the same so it also decreased from 84 mg (0.34

mmol) to 5.3 mg (0.02 mmol). The reactions were run at room temperature overnight and analyzed as described above.

Effect of Formate-to-Substrate Ratio

Following the same general reaction procedure described above, the effect of the formate-to-substrate ratio was investigated by varying the amount of triethylamine and formic acid while everything else remained the same. The reactions were all run in methanol (5 mL). The amount of formic acid was decreased from a formate-to-substrate ratio of 5:1 (0.47 mL, 13 mmol) to a formate-to-substrate ratio of 0.5:1 (0.05 mL, 1.2 mmol). The ratio of triethylamine to formic acid remained the same so it also decreased from 1.4 mL (10 mmol) to 0.14 mg (1.0 mmol). The reactions were run at room temperature overnight and analyzed as described above.

Effect of Triethylamine-to-Formic Acid Ratio

Following the same general reaction procedure described above, the effect of the triethylamine-to-formic acid ratio was investigated by varying the amount of triethylamine while everything else remained the same, including the amount of formic acid. The reactions were all run in methanol (5 mL). The amount of triethylamine was decreased from a triethylamine-to-formic acid ratio of 2.5:1 (1.7 mL, 12 mmol) to a triethylamine-to-formic acid ratio of 0.4:1 (0.27 mL, 2.0 mmol). The reactions were run at room temperature overnight and analyzed as described above.

Effect of Substrate Concentration

Following the same general reaction procedure described above, the effect of the (*S*)-CMK substrate concentration was investigated by varying the amount of (S)-CMK while everything else remained the same. The reactions were all run in methanol (5

mL). The concentration of (*S*)-CMK was decreased from 0.8 M (1.2 g, 4.0 mmol) to 0.05 M (0.074 g, 0.25 mmol). The reactions with 0.8 M (*S*)-CMK were not homogeneous at the start of the reaction. The reactions were run at room temperature overnight and analyzed as described above.

Effect of Time on ATH Reaction

The ruthenium catalyst precursor and TsEN ligand were stirred in methanol (2 mL) at room temperature for one hour. Triethylamine and formic acid were added. (*S*)-CMK (10 g, 34 mmol) was dissolved in methanol (36 mL) at 50°C. The (*S*)-CMK solution (3 mL) was added to each reaction tube to start the reaction. The reactions were run for 10, 20, 30, 40, 50, and 60 minutes at room temperature. At the end of the allotted time interval, the reactions were quenched with saturated ammonium chloride (3 mL) and extracted into DCM (3 mL). The DCM solutions were dried overnight and analyzed by HPLC.

Investigation of Various ATH Ligands

Following the same general reaction procedure described above, the effect of the ligand was investigated by substituting other compounds [ethylenediamine, ethanolamine, (-)-ephedrine, or (1*R*,2*R*)-TsDPEN] for TsEN or running the reaction without a ligand. The ruthenium catalyst precursor was stirred with either no ligand, ethylenediamine (6.0 µL, 0.090 mmol), ethanolamine (6.0 µL, 0.099 mmol), (-)-ephedrine (15 mg, 0.088 mmol), or (1*R*,2*R*)-TsDPEN (31 mg, 0.085 mmol) in methanol (5 mL) for one hour at room temperature. Triethylamine, formic acid, and then (*S*)-CMK were added to start the reactions. The reactions were all run at room temperature overnight and analyzed as described above.

Effect of Catalyst Metal Center

Following the same general reaction procedure described above, the effect of the catalyst metal center was investigated by switching the catalyst precursor from [Ru(*p*-cymene)Cl_2]$_2$ to [Rh(C_5Me_5)Cl_2]$_2$ or [Ir(C_5Me_5)Cl_2]$_2$. The rhodium (16 mg, 0.026 mmol) or iridium (20 mg, 0.025 mmol) catalyst precursors were stirred with TsEN (18 mg, 0.083 mmol) or (1*R*,2*R*)-TsDPEN (31 mg, 0.083 mmol) in methanol (5 mL) at room temperature for one hour. The reactions were started by adding triethylamine, formic acid, and (*S*)-CMK. Although the rhodium reactions were run in duplicate, the iridium reactions were only run once with each ligand. The reactions were run at room temperature overnight and analyzed as described above. The rhodium reactions were also run in various solvent systems following the same general procedure.

REFERENCES

(1) Wang, C.; Wu, X.; Xiao, J. *Chemistry - An Asian Journal* **2008**, *3*, 1750-1770.

(2) Zassinovich, G.; Mestroni, G.; Gladiali, S. *Chemical Reviews* **1992**, *92*, 1051-1069.

(3) Palmer, M.; Wills, M. *Tetrahedron - Asymmetry* **1999**, *10*, 2045-2061.

(4) Noyori, R. *Chemical Society Reviews* **1989**, *18*, 187-208.

(5) Noyori, R. *Science* **1990**, *248*, 1194-1199.

(6) Blum, Y.; Czarkie, D.; Rahamim, Y.; Shvo, Y. *Organometallics* **1985**, *4*, 1459-1461.

(7) Shvo, Y.; Czarkie, D.; Rahamin, Y.; Chodosh, D. *Journal of the American Chemical Society* **1986**, *108*, 7400-7402.

(8) Noyori, R.; Hashiguchi, S. *Accounts of Chemical Research* **1997**, *30*, 97-102.

(9) Ikariya, T.; Blacker, A. *Accounts of Chemical Research* **2007**, *40*, 1300-1308.

(10) Noyori, R. *Angewandte Chemie - International Edition* **2002**, *41*, 2008-2022.

(11) Fujii, A.; Hashiguchi, S.; Uematsu, N.; Ikariya, T.; Noyori, R. *Journal of the American Chemical Society* **1996**, *118*, 2521-2522.

(12) Liu, P.; Gu, P.; Wang, F.; Tu, Y. *Organic Letters* **2004**, *6*, 169-172.

(13) Saluzzo, C.; Lemaire, M. *Advanced Synthesis and Catalysis* **2002**, *344*, 915-928.

(14) Li, X.; Wu, X.; Chen, W.; Hancock, F.; King, F.; Xiao, J. *Organic Letters* **2004**, *6*, 3321-3324.

(15) Polborn, K.; Severin, K. *European Journal of Inorganic Chemistry* **2000**, 1687-1692.

(16) Chen, Y.; Wu, T.; Jiang, L.; Deng, J.; Liu, H.; Zhu, J.; Jiang, Y. *Journal of Organic Chemistry* **2005**, *70*, 1006-1010.

(17) Geldbach, T.; Dyson, P. *Journal of the American Chemical Society* **2004**, *126*, 8114-8115.

(18) Kawasaki, I.; Tsunoda, K.; Tsuji, T.; Yamaguchi, T.; Shibuta, H.; Uchida, N.; Yamashita, M.; Ohta, S. *Chemical Communications* **2005**, 2134-2136.

(19) Ma, Y.; Liu, H.; Chen, L.; Cui, X.; Zhu, J.; Deng, J. *Organic Letters* **2003**, *5*, 2103-2106.

(20) Bubert, C.; Blacker, J.; Brown, S.; Crosby, J.; Fitzjohn, S.; Muxworthy, J.; Thorpe, T.; Williams, J. *Tetrahedron Letters* **2001**, *42*, 4037-4039.

(21) Hamada, T.; Torii, T.; Onishi, T.; Izawa, K.; Ikariya, T. *Journal of Organic Chemistry* **2004**, *69*, 7391-7394.

(22) Noyori, R.; Takaya, H. *Accounts of Chemical Research* **1990**, *23*, 345-350.

(23) Noyori, R. *Tetrahedron* **1994**, *50*, 4259-4292.

(24) Ohkuma, T.; Ooka, H.; Hashiguchi, S.; Ikariya, T.; Noyori, R. *Journal of the American Chemical Society* **1995**, *117*, 2675-2676.

(25) Ohkuma, T.; Ooka, H.; Yamakawa, M.; Ikariya, T.; Noyori, R. *Journal of Organic Chemistry* **1996**, *61*, 4872-4873.

(26) Doucet, H.; Ohkuma, T.; Murata, K.; Yokozawa, T.; Kozawa, M.; Katayama, E.; England, A.; Ikariya, T.; Noyori, R. *Angewandte Chemie - International Edition* **1998**, *37*, 1703-1707.

(27) Ohkuma, T.; Doucet, H.; Pham, T.; Mikami, K.; Korenaga, T.; Terada, M.; Noyori, R. *Journal of the American Chemical Society* **1998**, *120*, 1086-1087.

(28) Hashiguchi, S.; Fujii, A.; Takehara, J.; Ikariya, T.; Noyori, R. *Journal of the American Chemical Society* **1995**, *117*, 7562-7563.

(29) Soleimannejad, J.; Sisson, A.; White, C. *Inorganica Chimica Acta* **2003**, *352*, 121-128.

(30) Dijksman, A.; Elzinga, J. M.; Li, Y. X.; Arends, I.; Sheldon, R. A. *Tetrahedron-Asymmetry* **2002**, *13*, 879-884.

(31) Kirkham, J. E. D.; Courtney, T. D. L.; Lee, V.; Baldwin, J. E. *Tetrahedron* **2005**, *61*, 7219-7232.

CHAPTER 5 BORON REDUCING AGENTS

INTRODUCTION

Asymmetric reduction of carbonyl compounds is of fundamental importance in the synthesis of chiral secondary alcohols, such as (*S,S*)-CMA and (*R,S*)-CMA, which are central to biologically-active substances. As a result, reducing agents used to perform such a chemical transformation are numerous; however, obtaining both a high yield and high selectivity remains a challenge. The use of a boron reducing agent and/or a boron catalyst is one of the approaches used to achieve stereo- and chemo-selective reduction of carbonyls to alcohols.

The use of boron or boron based compounds as a catalyst for reduction reactions started in 1936 with the use of triethylborane to reduce benzaldehyde to its corresponding boronic ester (Figure 5.1).[1,2] The subsequent discovery of sodium borohydride as a reducing agent in 1952 changed how chemists performed reductions of aldehydes and ketones because of its high chemoselectivity and increased stability compared to its lithium counterparts.[3] This discovery led to the development of other boron reducing agents, including 9-borabicyclo[3.3.1]-nonane (9-BBN),[4,5] diisopinocampheylboranes,[6] and the Selectride reagents. Unfortunately, although these reagents are mild and highly selective for the reduction of carbonyls, they are not stereoselective in the reduction of prochiral ketones.

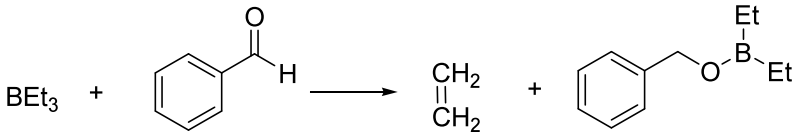

Figure 5.1: Reduction of benzaldehyde with triethylborane.[2]

The asymmetric reduction of carbonyls using oxazaborolidine catalysts is an effective tool for the stereoselective synthesis of chiral alcohols.[7] These reactions are run under mild conditions, are operationally simple, and result in high selectivity and yield, making them well-suited for industrial applications. The oxazaborolidine catalyst is formed from the reaction of an amino alcohol (chiral or achiral) and a borane complex, boronic acid, or boroxine. Oxazaborolidines with a *B*-H moiety are usually formed *in situ* and used immediately. Due to the moisture and air sensitivity of the *B*-H oxazaborolidines,[8-10] methods to produce the more chemically stable *B*-alkyl[11-13] and *B*-aryl[14] catalysts have been developed. For example, the commercially available (*R*)-(+)-CBS and (*S*)-(-)-CBS have proven to be effective catalysts in the reduction of many different carbonyl compounds.[8,15-20]

Previous work using boron reducing agents in the reduction of (*S*)-CMK has been reported (Table 5.1).[21,22] The highest DR (5:1) was achieved using the chiral reagent (+)-Dip chloride. While an excellent DR was achieved, this reagent is expensive for use on an industrial scale.

Table 5.1: Summary of boron reagents used in the reduction of (*S*)-CMK.[21,22]

Reagent(s)	Solvent	Temp (ºC)	Time (h)	DR
(+)-Dip Chloride (1.4 eq.)	THF	5 → 25	12	5:1
K-Selectride®/$MgBr_2$*OEt_2	THF	25	0.5	2.6:1
K-Selectride®	THF	reflux	2	2:1
K-Selectride®/Ti(O*i*Pr)$_4$	THF	25	0.5	2:1
KS-Selectride®	THF	25	2	2:1
R-Alpine borane (conc.)	THF	reflux	216	1:1
L-Selectride®	THF	25	1	0.9:1
$NaBH_4$/$CeCl_3$ (anhydrous)	THF	25	2	0.8:1
N-Selectride®	EtOH/THF	25	2	0.7:1
$NaBH_4$/$CeCl_3$·$7H_2O$	THF	25	18	0.7:1
$NaBH_4$/EDTA (Na_2·$2H_2O$)	THF	25	0.5	0.7:1
$NaCNBH_3$	THF	25	36	0.7:1
(+)-2-Butanol/$NaBH_4$	THF	25	1	0.6:1
Cp_2TiBH_4	Glyme	25	0.5	0.6:1
$NaBH_4$	THF	25	2	0.6:1
(-)-2-Butanol/$NaBH_4$	THF	25	0.5	0.6:1
$NaBH_4$/Al(O*i*Pr)$_4$	THF	reflux	2	0.6:1
$NaBH_4$/Diacetone-D-glucose	THF	25	12	0.6:1
$NaBH_4$/EDTA	THF	25	12	0.6:1
$NaBH_4$/L-Tartaric Acid	THF	5	1	0.6:1
$NaBH_4$/$MgBr_2$·OEt_2	THF	25	1	0.6:1
BH_3-*t*-butylamine	THF	25	1	0.5:1
LS-Selectride®	THF	25	1	0.5:1
$NaBH_4$/D-Tartaric Acid	THF	25	0.5	0.5:1
(+)-2-Butanol·BH_3	THF	25	1	0.4:1
$NaBH_4$/$CaCl_2$	MeOH	25	1	0.4:1
AminoAlcohol Borane	THF	25	12	0.3:1
Na(PEG)$_2BH_2$	THF	25	0.5	0.3:1
BH_3·THF	EtOH/THF	25	2	0.2:1

The goal of this work was to explore boron reducing agents in the reduction of (*S*)-CMK to optimize the yield and DR while minimizing the reaction cost. The research initially focused on the use of sodium borohydride and boron triisopropoxide to then be

extended to chiral oxazaborolidines, which proved to yield the best results. The objective of this investigation was to identify boron reducing agents that stereoselectively produce (*R,S*)-CMA in high yields.

BACKGROUND

Boron Triisopropoxide Reduction Mechanism

As Figure 5.2 shows, the mechanism of the boron triisopropoxide reduction of ketones is analogous to that of the MPV reduction with aluminum isopropoxide. First, the carbonyl compound coordinates with the boron of the boron triisopropoxide. The reaction proceeds through a six member ring transition state by hydride transfer to the carbonyl from the α-carbon of the isopropoxide group. Acetone is released and the boronic ester is cleaved to the product alcohol, regenerating the boron triisopropoxide catalyst.

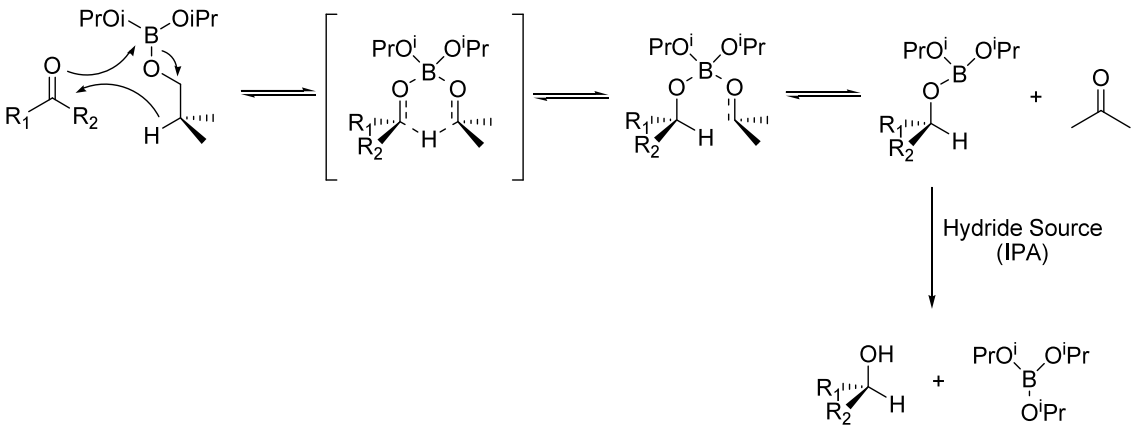

Figure 5.2: Mechanism of the boron triisopropoxide reduction of ketones.

Oxazaborolidine Reduction Mechanism

The mechanism of the oxazaborolidine-catalyzed reduction of ketones is known in the literature (Figure 5.3).[23] The oxazaborolidine first complexes with a borohydride molecule to form a charged species, which then coordinates with the ketone to mediate the hydride transfer from the borohydride to the ketone. Upon addition of another borohydride molecule, the alcohol product is released. The resulting catalyst can undergo another catalytic cycle. This mechanism has been used extensively to help researchers understand the high stereoselectivity of the reduction.[24-31]

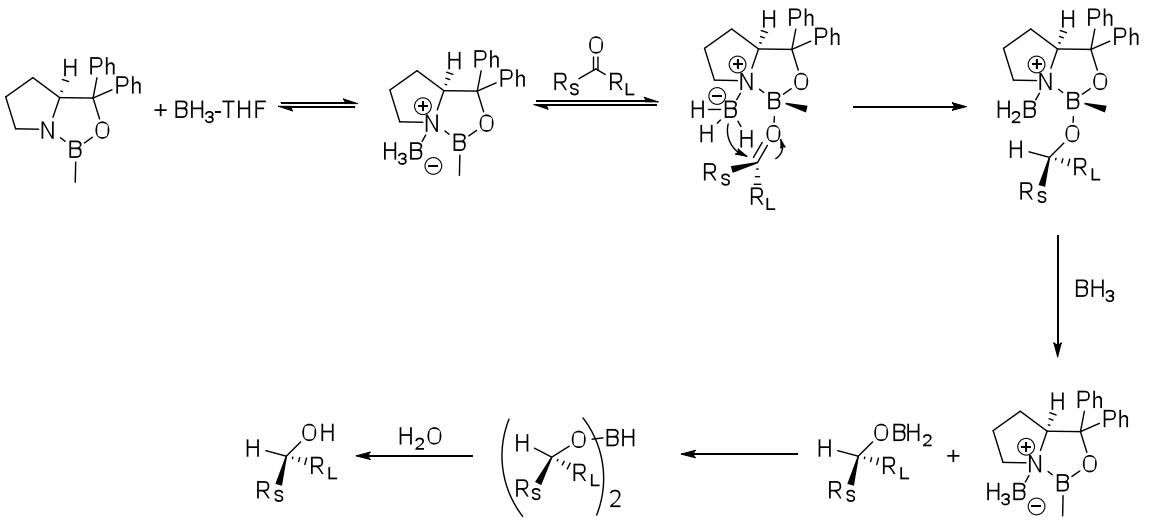

Figure 5.3: Mechanism of the reduction of ketones by 2-methyl-CBS-oxazaborolidine.[23]

RESULTS AND DISCUSSION

Reduction with Sodium Borohydride

The reduction of (*S*)-CMK was investigated with sodium borohydride. Sodium borohydride was previously used for the reduction of (*S*)-CMK to give a DR of 0.6:1.[21,22] These experiments were repeated in our laboratory with similar results: a DR of 0.6:1

and 100% conversion. Sodium borohydride does not appear to be a promising reducing agent for the selective production of (*R,S*)-CMA.

Reduction with Boron Triisopropoxide

The diastereoselective reduction of (*S*)-CMK was carried out with boron triisopropoxide. The reagent was purchased from Aldrich and was also prepared and used *in situ* following literature procedures.[32-34] The reduction of (*S*)-CMK was performed using both the purchased reagent and the reagent prepared *in situ*. When the reduction was run with the purchased reagent for 48 hours in refluxing THF, no reaction was consistently observed. The solvent was changed to toluene so that a higher reaction temperature could be achieved but again, no reaction occurred. In contrast, when the reaction was run with the reagent synthesized *in situ*, after reacting overnight in THF at room temperature, 38% conversion of (*S*)-CMK was observed with a DR of 0.38:1.

The two boron triisopropoxide reagents (bought or prepared) were characterized by ^{11}B NMR to explain the results of the reduction reactions. The coupling of protons with the boron nuclei can complicate the spectrum by increasing the multiplicity of the peaks, but they give important information regarding the number of protons attached to each boron atom.[35] Analysis of the purchased boron reagent showed a single peak (δ 17.2 ppm) which remained a singlet when run without proton decoupling, indicative of no hydrogen atoms present on the boron nucleus.

Three different samples of boron triisopropoxide prepared *in situ* were made: (1) BH_3•THF with one equivalent of isopropanol in an NMR tube, (2) BH_3•THF with 3.2 equivalent of isopropanol (as used above) in an NMR tube, and (3) BH_3•THF with 3.2 equivalent of isopropanol on a batch scale (sampled directly from the round-bottom flask). The mixtures made in the NMR tubes were allowed to equilibrate for two hours

before the NMR spectra were recorded. The batch scale preparation was stirred for 24 hours before a sample was analyzed by ^{11}B NMR. As a comparison, the ^{11}B NMR spectrum of BH_3•THF was obtained, which showed a single peak (δ -0.47 ppm) as a singlet with proton decoupling and a quartet without the decoupling. When one equivalent of isopropanol was used, four boron species (δ 26.79, 18.93, 17.60, -0.34 ppm) were observed. In contrast, when 3.2 equivalents of isopropanol were used, there were three different boron peaks in the ^{11}B NMR spectrum (δ 26.79, 18.47, 17.54, -0.34 ppm). The batch mixture with 3.2 equivalents of isopropanol was analyzed after 24 hours and showed two boron species (δ 18.48, 17.54 ppm).

Although the desired boron triisopropoxide is formed in each of the above samples, there are other boron species present that may also perform the reduction. Also, the formation of the desired boron triisopropoxide reducing agent takes longer than the time reported in the literature, as evidenced by the BH_3•THF peak present in the samples after two hours. Overall, boron triisopropoxide does not seem to be a promising reducing agent for the synthesis of (*R,S*)-CMA.

Reduction with Borane Catalyzed by Oxazaborolidines

Four different oxazaborolidines were investigated: (1) (4*R*,5*S*)-4,5-diphenyl-1,3,2-oxazaborolidine [abbreviated (*R,S*)-DPO] made and used *in situ*, (2) 1,3,2-oxazaborolidine made and used *in situ*, and (3) two commercially available catalysts [(*R*)-(+)-CBS and (*S*)-(-)-CBS] (Figure 5.4). The first two catalysts were synthesized and characterized. All four catalysts were applied to the reduction of (*S*)-CMK.

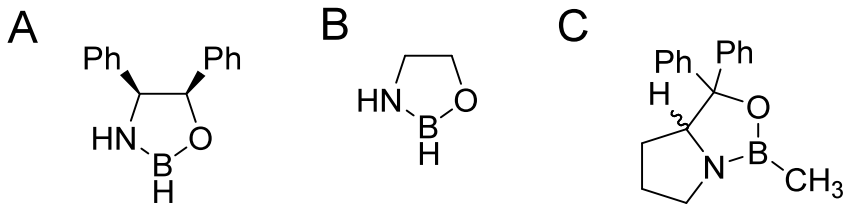

Figure 5.4: Structures of oxazaborolidine catalysts. A: (4*R*,5*S*)-4,5-Diphenyl-1,3,2-oxazaborolidine [(*R,S*)-DPO]. B: 1,3,2-Oxazaborolidine. C: (*R*)-(+)-CBS or (*S*)-(-)-CBS.

The reduction reactions were originally run under "batch" conditions in a standard round-bottom flask apparatus as a screening tool to identify promising reaction conditions. The reactions were repeated on the same scale as the batch conditions in the carousel apparatus used extensively in Chapters 3 and 4. One difficulty that arose in the carousel setup was the challenge of drying the reaction tubes and keeping them under an inert atmosphere. The seals of the carousel reactor are made with Teflon, which melts at elevated temperatures. Although the glass reaction tubes were dried in the oven, the remaining parts of the apparatus were not dried, which may have allowed moisture into the reaction tubes. Since the borane reducing agent is water sensitive, even small amounts of water could affect the reproducibility of the reaction.

As this work was an initial screening of reagents for future application to an industrial process, the main focus was to identify the best performing catalysts in terms of high yields and diastereoselectivity. Reaction variables, such as temperature and concentration, were investigated briefly without optimization of the reaction conditions.

Synthesis and Characterization of Oxazaborolidines

(*R,S*)-DPO was prepared from (1*R*,2*S*)-1,2-diphenyl-2-aminoethanol and borane according to a literature procedure (Figure 5.5).[36-38] Attempts to characterize the *in situ* catalyst by ^{1}H and ^{13}C NMR and mass spectrometry were unsuccessful due to the

instability of the oxazaborolidine catalyst when isolated from the solvent. However, proton decoupled ^{11}B NMR showed a singlet at δ -19.6 ppm consistent with the formation of one boron containing specie. Without proton decoupling, the peak appeared as a doublet, indicating that one proton was attached to the boron, supporting the formation of the desired catalyst.

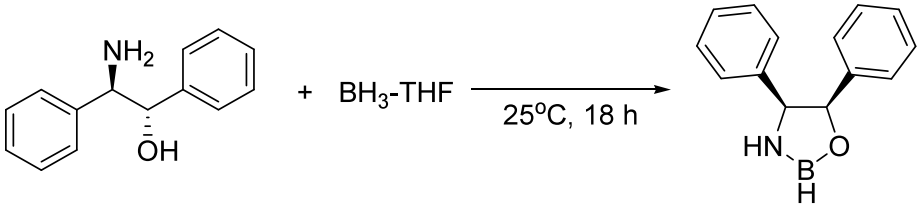

Figure 5.5: Synthesis of (*R,S*)-DPO.

The achiral catalyst, 1,3,2-oxazaborolidine, was synthesized in the same manner as the chiral (*R,S*)-DPO above. 2-Aminoethanol and borane were reacted in THF to form the achiral catalyst (Figure 5.6). The ^{1}H and ^{13}C NMR spectra were again difficult to interpret because of the catalyst instability when isolated. The proton decoupled ^{11}B NMR spectrum showed a single peak as a singlet at δ -19.4 ppm. Without proton decoupling, the peak appeared as a doublet, evidencing the presence of one hydrogen atom on the boron nucleus, consistent with the formation of the desired catalyst.

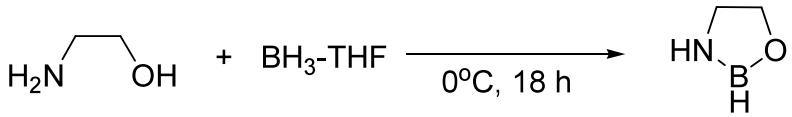

Figure 5.6: Synthesis of 1,3,2-oxazaborolidine.

Reduction with Borane without Catalyst

The reduction of (*S*)-CMK using borane alone in a mixture of THF and ethanol has been reported with a DR of 0.2:1.[21,22] The reaction was investigated as a function of temperature, with the reaction temperature varying from -20°C to 25°C. This reaction was carried out as a control experiment under batch conditions at 0°C in THF (Figure 5.7). Then the reaction was carried out once each at 10°C and -20°C under batch conditions and three times at 25°C in the carousel reactor. The HPLC analyses of these reactions are given in Table 5.2. All of the reactions went to completion after eight hours. The DR was slightly higher in all cases (between 0.30:1 and 0.45:1) than the previously reported value (0.2:1). However, since the DR is within experimental error, the temperature does not seem to have a significant influence on the diastereoselectivity of the reaction.

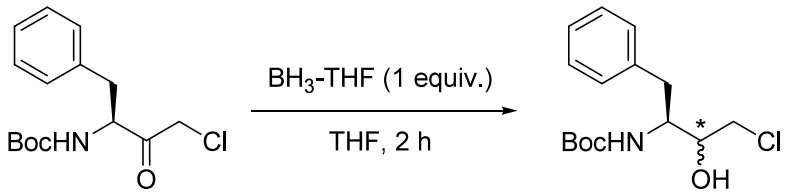

Figure 5.7: Reduction of (*S*)-CMK with borane without catalyst.

Table 5.2: Reduction of (*S*)-CMK with borane.

Reagent	Batch/Carousel	Temp (ºC)	% Yield	DR
BH_3-THF	Batch	0	98 ± 3	0.45 ± 0.04
BH_3-THF	Batch	10	100[a]	0.40
BH_3-THF	Batch	-20	100[a]	0.40
BH_3-THF	Carousel	25	98 ± 3	0.30 ± 0.05

[a]Yields estimated from total peak area in HPLC

Reduction with Borane Catalyzed by (*R,S*)-DPO or 1,3,2-Oxazaborolidine

(*R,S*)-DPO and 1,3,2-oxazaborolidine were formed as described above and used as *in situ* catalysts for the reduction of (*S*)-CMK. The reducing agent in these reactions was borane. One equivalent of either catalyst was formed *in situ* with BH_3•THF. A solution of (*S*)-CMK in THF was added to start the reaction. These reactions were analyzed by HPLC and the results are given in Table 5.3. The *in situ* catalysts were originally used on a batch scale with six equivalents of borane to give DRs of 1.2:1 with (*R,S*)-DPO and 0.86:1 with 1,3,2-oxazaborolidine. However, when these reactions were repeated in the carousel setup, the DR decreased by half and the yield also decreased. This decrease has been attributed to possible water contamination in the carousel reactor that caused the degradation of the oxazaborolidine compounds. To investigate the effect of the excess of borane, carousel reactions were run using 1.1 equivalents of borane to form each of the oxazaborolidines, which results in only 0.1 excess equivalents of borane assuming complete yield of the oxazaborolidine catalysts. Interestingly, these reactions resulted in DRs of 0.34:1 with (*R,S*)-DPO and 0.59:1 with 1,3,2-oxazaborolidine, similar to that of pure borane. An excess of borane is probably necessary to achieve complete conversion of the aminoalcohols to the oxazaborolidine catalysts.

Table 5.3: Reduction of (*S*)-CMK with (*R,S*)-DPO or 1,3,2-oxazaborolidine.

Catalyst	Batch/Carousel	Time (h)	% Yield	DR
(*R,S*)-DPO	Batch	18	97[a]	1.2 ± 0.1
(*R,S*)-DPO	Carousel	18	85 ± 4	0.59 ± 0.05
(*R,S*)-DPO (1.1 eq BH_3)	Carousel	18	97 ± 13	0.34 ± 0.01
1,3,2-Oxazaborolidine	Batch	24	90[a]	0.86 ± 0.02
1,3,2-Oxazaborolidine	Carousel	18	85 ± 8	0.48 ± 0.05
1,3,2-Oxazaborolidine (1.1 eq BH_3)	Carousel	18	75 ± 9	0.59 ± 0.08

[a]Yields estimated from total peak area in HPLC

Reduction with Borane Catalyzed by (*R*)-(+)-CBS or (*S*)-(-)-CBS

The reduction of (*S*)-CMK was attempted using the commercially available oxazaborolidine compounds originally synthesized by Corey [(*R*)-(+)-CBS and (*S*)-(-)-CBS].[7] The reactions were all run three times using a 2 M solution of either catalyst in THF at room temperature either on a batch scale or in the carousel reactor. The results of these reactions are summarized in Table 5.4. Significant changes in DR occurred upon going from a batch scale to the carousel reactor. With (*S*)-(-)-CBS, the DR dropped from 0.49:1 on a batch scale to 0.17:1 in the carousel. Similarly, the DR increased from 3.8:1 in the batch reaction to 6.3:1 in the carousel. One possible explanation for this difference is the solubility of the oxazaborolidine catalysts in THF. The catalysts were purchased from Aldrich as a 2 M solution but the catalyst was observed to precipitate around the rim of the bottle, especially in the case of (*R*)-(+)-CBS. A different bottle of the reagents were used for the batch reactions as for the carousel reactions, which may have caused the discrepancy.

Table 5.4: Reduction of (*S*)-CMK with commercially available (*R*)-(+)-CBS and (*S*)-(-)-CBS.

Catalyst	Batch/Carousel	Time (h)	% Yield	DR
(*S*)-(-)-CBS	Batch	24	90*	0.49 ± 0.06
(*S*)-(-)-CBS	Carousel	18	91 ± 2	0.17 ± 0.01
(*S*)-(-)-CBS (no BH_3)	Carousel	18	0 ± 3	---
(*R*)-(+)-CBS	Batch	24	85*	3.8 ± 0.3
(*R*)-(+)-CBS	Carousel	18	72 ± 8	6.3 ± 0.2
(*R*)-(+)-CBS (no BH_3)	Carousel	18	0 ± 3	---

[a]Yields estimated from total peak area in HPLC

Since the reproducibility was poor when the reactions were run with the (*R*)-(+)-CBS and (*S*)-(-)-CBS solutions in THF, (*R*)-(+)-CBS and (*S*)-(-)-CBS were purchased as solids so the amount of catalyst in each reaction could be accurately controlled. The results of the reaction with the solid (*R*)-(+)-CBS are given in Table 5.5 as a comparison

with the catalyst as a solution in THF. The DR (5.2:1) is closer to that of the batch reactions (3.8:1).

Table 5.5: Comparison of (*R*)-(+)-CBS as a solution or as a solid.

Catalyst	Time (h)	% Yield	DR
(*R*)-(+)-CBS (2 M soln.)	18	72 ± 8	6.3 ± 0.2
(*R*)-(+)-CBS (solid)	18	89 ± 5	5.2 ± 0.4

Reproducibility of Oxazaborolidine-Catalyzed Reactions

In an effort to improve the reproducibility of the oxazaborolidine reactions, a stock solution of each oxazaborolidine catalyst [(*R,S*)-DPO, 1,3,2-oxazaborolidine, (*R*)-(+)-CBA, and (*S*)-(-)-CBS] was prepared with BH_3•THF and loaded directly into each carousel reaction tube. Each reaction was run six times at room temperature and the results of these reactions are given in Table 5.6. Each reaction showed slightly improved yields compared to the previous results. In addition, the diastereoselectivity improved for (*R,S*)-DPO and 1,3,2-oxazaborolidine (DR of 0.80:1 and 0.61:1, respectively). The reaction with (*S*)-(-)-CBS also became more stereoselective with a DR of 0.07:1, although in this case the reaction is selective for the (*S,S*)-CMA product. The most significant result is a DR of 9.5:1 using (*R*)-(+)-CBS. (*R*)-(+)-CBS is the most effective catalyst for the diastereoselective production of (*R,S*)-CMA.

Table 5.6: Reduction of (*S*)-CMK using stock solutions of oxazaborolidine catalysts.

Catalyst	Time (h)	% Yield	DR	DR (previous)
(*R,S*)-DPO	8	90 ± 2	0.80 ± 0.01	0.59 ± 0.05
1,3,2-Oxazaborolidine	8	88 ± 2	0.61 ± 0.02	0.48 ± 0.05
(*S*)-(-)-CBS	8	94 ± 2	0.07 ± 0.01	0.17 ± 0.01
(*R*)-(+)-CBS	8	92 ± 2	9.5 ± 0.2	6.3 ± 0.2

CONCLUSIONS

In conclusion, several boron reducing agents were screened for the diastereoselective reduction of (*S*)-CMK to (*R,S*)-CMA. The most promising reagents investigated are the chiral oxazaborolidine catalysts in conjunction with borane. (*S*)-(-)-CBS stereoselectively produced the (*S,S*) product while (*R*)-(+)-CBS yielded the desired (*R,S*) diastereomer with a DR of 9.5:1.

EXPERIMENTAL METHODS

Materials and Equipment

All chemicals were ordered from Aldrich and used as received, unless otherwise noted. The (*S*)-CMK starting material and samples of (*S,S*)-CMA and (*R,S*)-CMA were obtained from Ampac Fine Chemicals (Sacramento, CA). All solvents used were purchased as anhydrous from Aldrich and used as received. The glassware and apparatus were dried before use in the reactions.

^{1}H and ^{13}C NMR spectra were obtained from a Varian-Mercury VX 400 MHz spectrometer using DMSO-d_6 as an internal reference. ^{11}B NMR spectra were obtained from a Bruker DRX 500 MHz spectrometer using THF- d_6 as an internal reference. Elemental analyses were performed by Atlantic Microlab (Norcross, GA). HRMS experiments were performed by Georgia Institute of Technology Bioanalytical Mass Spectrometry Facility (Atlanta, GA). HPLC analysis was run on an Agilent 1100 series LC with a UV detector and an ESI-MS. The product analysis was performed following the analytical procedure described in Chapters 3 and 4.

Batch Reactions

Reduction with Boron Triisopropoxide Prepared *in situ*

A BH_3•THF solution (5 mL of a 1 M solution, 5 mmol) was charged to a round-bottom flask under argon in an ice bath and allowed to cool for 30 minutes. Anhydrous isopropanol (1.3 mL, 17 mmol) was added dropwise to the borane solution over 30 minutes. After hydrogen evolution ceased (~ two hours) the solution was stirred overnight and allowed to warm to room temperature. (*S*)-CMK (2.0 g, 6.7 mmol) was dissolved in anhydrous THF and added to the reaction mixture. The mixture was allowed to stir overnight. At this time, the solution was quenched with water and the

aqueous layer was saturated with potassium carbonate. The organic layer was isolated, dried over magnesium sulfate, diluted with THF, and analyzed by HPLC.

Reduction with Commercially Available Boron Triisopropoxide

(*S*)-CMK (2.0 g, 6.7 mmol) was dissolved in anhydrous THF. After one hour, boron triisopropoxide (1.9 mL, 8.1 mmol) was added to the reaction flask. The mixture was heated to reflux and allowed to stir for three days. At 24 hour intervals, samples were taken, diluted with THF, and analyzed by HPLC.

Reduction with Borane

(*S*)-CMK (1.5 g, 5.0 mmol) was dissolved in anhydrous THF (10 ml) and cooled to 0°C in an ice bath. A solution of BH_3•THF (5 mL of a 1 M solution, 5 mmol) was added to the (*S*)-CMK solution. The solution was stirred for two hours, quenched with methanol, diluted with THF, and analyzed by HPLC.

Reduction with 4,5-Diphenyl-1,3,2-oxazaborolidine

(1*S*,2*R*)-(+)-2-Amino-1,2-diphenylethanol (0.13 g, 0.60 mmol) was placed in a round bottom flask in an ice bath. BH_3•THF (3.6 mL of a 1 M solution, 3.6 mmol) was slowly added to the flask. The solution was allowed to stir overnight and slowly warm to room temperature. (*S*)-CMK (0.18 g, 0.60 mmol) was dissolved in anhydrous THF (~20 mL) and added to the reaction mixture. After 18 hours, the reaction solution was diluted with THF and analyzed by HPLC.

Reduction with 1,3,2-Oxazaborolidine.

Ethanolamine (0.10 mL, 1.7 mmol) was placed in a round bottom flask in an ice bath. BH_3•THF (10 mL of a 1 M solution, 10 mmol) was slowly added to the flask. The

solution was allowed to stir overnight and to slowly warm to room temperature. (*S*)-CMK (0.5 g, 1.7 mmol) was dissolved in anhydrous THF (~20 mL) and added to the reaction mixture. After 18 hours, the reaction solution was diluted with THF and analyzed by HPLC.

Reduction with (*S*)-(-)-CBS

(*S*)-(-)-CBS (2.0 mL of a 1 M solution in THF, 2.0 mmol) was placed in an ice bath. BH_3•THF (1.7 mL of a 1 M solution, 1.7 mmol) was slowly added to the flask. The solution was allowed to stir for one hour before a solution of (*S*)-CMK (0.5 g, 1.7 mmol) dissolved in anhydrous THF (~20 mL) was added to the reaction mixture. After 18 hours, the reaction solution was diluted with THF and analyzed by HPLC.

Reduction with (*R*)-(+)-CBS

(*R*)-(+)-CBS (2.0 mL of a 1 M solution, 2.0 mmol) was placed in an ice bath. BH_3•THF (1.7 mL of a 1 M solution, 1.7 mmol) was slowly added to the flask. The solution was allowed to stir for one hour before a solution of (*S*)-CMK (0.5 g, 1.7 mmol) dissolved in anhydrous THF (~20 mL) was added to the reaction mixture. After 18 hours, the reaction solution was diluted with THF and analyzed by HPLC.

Carousel Reactions

Reduction with Borane

(*S*)-CMK (0.6 g, 3.0 mmol) was placed in three of the reactor tubes. The tubes were then placed in the carousel and put under an argon atmosphere. Anhydrous THF (2 mL) was added to each reactor tube to dissolve the (*S*)-CMK. After one hour, the BH_3•THF solution (6.0 mL of a 1 M solution, 6.0 mmol) was added to the tube. The

solution was stirred for two hours, quenched with methanol, diluted with THF, and analyzed by HPLC.

Preparation of 1,3,2-Oxazaborolidine Stock Solution

Ethanolamine (1.0 mL, 18 mmol) was placed under an argon atmosphere and cooled to 0ºC in an ice bath. A solution of BH_3•THF (108 mL of a 1 M solution, 108 mmol) was slowly added to the flask. The solution was allowed to stir for 24 hours and slowly warm up to room temperature.

Reduction with 1,3,2-Oxazaborolidine Stock Solution

(*S*)-CMK (0.77 g, 2.6 mmol) was placed in six of the reactor tubes in the carousel reactor. The tubes were then placed in the carousel reactor and put under an argon atmosphere. Anhydrous THF (2 mL) was added to each reactor tube to dissolve the (*S*)-CMK. After one hour, the stock solution of 1,3,2-oxazaborolidine (16 mL) was added to each of the reactor tubes. The solution was allowed to stir for eight hours. At this time the reaction was quenched with methanol (6 mL). The quenched reaction mixture was diluted with THF and analyzed by HPLC.

Preparation of 4,5-Diphenyl-1,3,2-oxazaborolidine Stock Solution

(1*S*,2*R*)-(+)-2-Amino-1,2-diphenylethanol (3.8 g, 18 mmol) was placed under an argon atmosphere and cooled to 0ºC in an ice bath. A solution of BH_3•THF (54 mL of a 1 M solution, 54 mmol) was slowly added to the flask. The solution was allowed to stir for 24 hours and slowly warm up to room temperature.

Reduction with 4,5-Diphenyl-1,3,2-oxazaborolidine Stock Solution

(*S*)-CMK (0.77 g, 2.6 mmol) was placed in six of the reactor tubes in the carousel reactor. The tubes were then placed in the carousel reactor and put under an argon atmosphere. Anhydrous THF (2 mL) was added to each reactor tube to dissolve the (*S*)-CMK. After one hour, the stock solution of 4,5-diphenyl-1,3,2-oxazaborolidine (8 mL) was added to each of the reactor tubes. The solution was allowed to stir for eight hours. At this time the reaction was quenched with methanol (6 mL). The quenched reaction mixture was diluted with THF and analyzed by HPLC.

Preparation of 2-Methyl-CBS-oxazaborolidine Stock Solutions

(*S*)-(-)-CBS or (*R*)-(+)-CBS (3.9 g, 14 mmol) was placed under an argon atmosphere. A solution of BH_3•THF (28 mL of a 1 M solution, 28 mmol) was slowly added to the flask. The solution was allowed to stir overnight.

Reduction with (*S*)-(-)-CBS or (*R*)-(+)-CBS

(*S*)-CMK (0.60 g, 2.0 mmol) was placed in six of the reactor tubes in the carousel reactor. The tubes were then placed in the carousel reactor and put under an argon atmosphere. Anhydrous THF (2 mL) was added to each reactor tube to dissolve the (*S*)-CMK. After one hour, the stock solution of 2-methyl-CBS-oxazaborolidine (4 mL) was added to each of the reactor tubes. The solution was allowed to stir for eight hours. At this time the reaction was quenched with methanol (4 mL). The quenched reaction mixture was diluted with THF and analyzed by HPLC.

REFERENCES

(1) Cha, J. S. *Organic Process Research & Development* **2006**, *10*, 1032-1053.

(2) Meerwien, H.; Hinz, G.; Majert, H.; Sonke, H. J. *Journal for Praktische Chemie* **1963**, *147*, 226-250.

(3) Schlesinger, H.; Brown, H. C.; Hoekstra, H. R.; Rapp, L. R. *Journal of the American Chemical Society* **1953**, *75*, 199-204.

(4) Knights, E.; Brown, H. *Journal of the American Chemical Society* **1968**, *90*, 5281.

(5) Soderquist, J.; Brown, H. *Journal of Organic Chemistry* **1981**, *46*, 4599-4600.

(6) Brown, H.; Prasad, J. *Journal of the American Chemical Society* **1986**, *108*, 2049-2054.

(7) Corey, E. J.; Link, J. O. *Tetrahedron Letters* **1989**, *30*, 6275-6278.

(8) Corey, E. J.; Bakshi, R. K.; Shibata, S.; Chen, C.-P.; Singh, V. K. *Journal of the American Chemical Society* **1987**, *109*, 7925-7926.

(9) Itsuno, S.; Ito, K. *Journal of Organic Chemistry* **1984**, *49*, 555-557.

(10) Itsuno, S.; Sakurai, Y.; Ito, K.; Hirano, A. *Bulletin of the Chemical Society of Japan* **1987**, *60*, 395-396.

(11) Corey, E. J.; Link, J. O. *Journal of Organic Chemistry* **1991**, *56*, 442-444.

(12) Corey, E. J.; Link, J. O. *Tetrahedron Letters* **1992**, 4141-4144.

(13) Mathre, D. J.; Jones, T. K.; Xavier, L. C.; Blacklock, T. J.; Reamer, R. A.; Mohan, J. J.; Jones, E. T. T.; Hoogsteen, K.; Baum, M. W.; Grabowski, E. J. J. *Journal of Organic Chemistry* **1991**, *56*, 751-762.

(14) Jones, T. J.; Mohan, J. J.; Xavier, L. C.; Blacklock, T. J.; Mathre, D. J.; Sohar, P.; Jones, E. T. T.; Reamer, R. A.; Roberts, F. E.; Grabowski, E. J. J. *Journal of Organic Chemistry* **1991**, 2880-2888.

(15) Corey, E. J. *Chemical Society Reviews* **1988**, *17*, 111.

(16) Corey, E. J.; Jardine, P. D. S.; Mohri, T. *Tetrahedron Letters* **1988**, *29*, 6409.

(17) Corey, E. J.; Gavai, A. V. *Tetrahedron Letters* **1988**, *29*, 3201-3204.

(18) Corey, E. J.; Shibata, S.; Bakshi, R. K. *Journal of Organic Chemistry* **1988**, *53*, 2861-2863.

(19) Corey, E. J.; Reichard, G. A. *Tetrahedron Letters* **1989**, *30*, 5207.

(20) Jones, T. K.; Mohan, J. J.; Xavier, L. C.; Blacklock, T. J.; Mathre, D. J.; Sohar, P.; Jones, E. T. T.; Reamer, R. A.; Roberts, F. E.; Grabowski, E. J. J. *Journal of Organic Chemistry* **1991**, *56*, 763-769.

(21) Malik, A. A.; Clement, T. E.; Palandoken, H.; Robinson III, J.; Stringer, J. A. US Patent, 2003.

(22) Malik, A. A.; Clement, T. E.; Palandoken, H.; Robinson III, J.; Stringer, J. A. US Patent, 2005.

(23) Corey, E. J.; Bakshi, R. K.; Shibata, S. *Journal of the American Chemical Society* **1987**, *109*, 5551-5553.

(24) Corey, E. J.; Link, J. O.; Bakshi, R. K. *Tetrahedron Letters* **1992**, *33*, 7107-7110.

(25) Evans, D. A. *Science* **1988**, *240*, 420-426.

(26) Jones, D. K.; Liotta, D. C.; Shinkai, I.; Mathre, D. J. *Journal of Organic Chemistry* **1993**, *58*, 799-801.

(27) Quallich, G. J.; Blake, J. F.; Woodall, T. M. *Journal of the American Chemical Society* **1994**, *116*, 8516-8525.

(28) Nevalainen, V. *Tetrahedron: Asymmetry* **1992**, *3*, 921-932.

(29) Nevalainen, V. *Tetrahedron: Asymmetry* **1992**, *3*, 933-945.

(30) Nevalainen, V. *Tetrahedron: Asymmetry* **1992**, *3*, 1441-1453.

(31) Nevalainen, V. *Tetrahedron: Asymmetry* **1992**, *3*, 1563-1572.

(32) Cha, J. S.; Park, J. H. *Bulletin of the Korean Chemical Society* **2002**, *23*, 1051-1052.

(33) Cha, J. S.; Park, J. H. *Bulletin of the Korean Chemical Society* **2002**, *23*, 1377.

(34) Uysal, B.; Buyukan, B. S. *ARKIVOC* **2007**, *xiv*, 134-140.

(35) Reed, D. *Chemical Society Reviews* **1993**, *22*, 109-116.

(36) Quallich, G. J.; Woodall, T. M. *Tetrahedron Letters* **1993**, *34*, 4145-4148.

(37) Quallich, G. J.; Woodall, T. M. *Synlett* **1993**, 929-930.

(38) Yaozhong, J.; Mi, Q.; Aiqiao, M. *Tetrahedron: Asymmetry* **1994**, *5*, 1211-1214.

CHAPTER 6 REDUCTION OF (*S*)-CMK WITH VARIOUS PROTECTING GROUPS

INTRODUCTION

The diastereoselectivity of the MPV reduction of (*S*)-CMK – induced by the α-chiral carbon of *S* configuration – is influenced by the aluminum alkoxide reagent's capabilities to hydrogen bond with the amide of the Boc-protected (*S*)-CMK. The possible transition state complexes between aluminum isopropoxide and (*S*)-CMK were studied using Spartan® modeling calculations. Based on these models, potential approaches to favor (*R,S*)-CMA selectively were identified, including the replacement of the Boc protecting group. By replacing the Boc protecting group with a phthalimide group, which cannot hydrogen bond with the aluminum isopropoxide, it was hypothesized that the diastereoselectivity toward (*R,S*)-CMA could be improved.

The effect of the amine protecting group on the diastereoselectivity of the (*S*)-CMK reduction was investigated by altering the protecting group. First, (*S*)-CMK was synthesized with two different *N*-protecting groups: phthalimide or trifluoroacetamide (Figure 6.1). In the MPV reduction, the protected amine of the phthalimide-protected (*S*)-CMK cannot hydrogen bond with the aluminum isopropoxide and the diastereoselectivity towards (*R,S*)-CMA was improved. The phthalimide-protected (*S*)-CMK was also reduced under the same ATH reaction or boron reagents conditions used with the Boc-protected (*S*)-CMK.

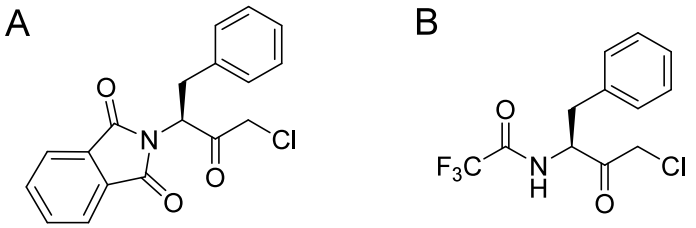

Figure 6.1: Structures of phthalimide-protected (*S*)-CMK (**A**) and trifluoroacetamide-protected (*S*)-CMK (**B**).

BACKGROUND

Spartan® modeling studies (Hartree-Fock level with basis set of 6-31G*) showed that hydrogen bonding between the aluminum isopropoxide and (*S*)-CMK plays an essential role in determining the stereoselectivity of the products (see Chapter 3). Preventing this hydrogen bonding from occurring could favor our desired (*R,S*)-CMA product. One method proposed to prevent this hydrogen bonding is to replace the Boc protecting group with a phthalimide group that does not contain an acidic hydrogen capable of hydrogen bonding. This approach has been shown to improve the stereoselectivity of the MPV reduction of a similar α-aminoketone.[1]

(*S*)-CMK with phthalimide and trifluoroacetamide protecting groups have been previously synthesized[2,3] but the reduction of the ketones to their respective alcohols has not been reported in the literature. The corresponding alcohol products are potentially proprietary compounds.

RESULTS AND DISCUSSION

Synthesis of (*S*)-CMK with Different Amine Protecting Groups

The phthalimide protecting group yields a tertiary amine, precluding possible hydrogen bonding with the alkoxide groups on the aluminum. The trifluoroacetamide protecting group yields a secondary amine with a hydrogen still available for hydrogen bonding. However, the trifluoroacetamide group was investigated to evaluate the electronic effect of the protecting group on the reaction selectivity.

Synthesis of (*S*)-CMK Ammonium Hydrochloride Salt

The Boc protecting group was removed by treating (*S*)-CMK with hydrochloric acid to form the corresponding ammonium hydrochloride salt [(*S*)-4-chloro-3-oxo-1-phenylbutan-2-aminium chloride] (Figure 6.2).[4] ^{1}H and ^{13}C NMR, elemental analysis, and melting point support the formation of the ammonium hydrochloride salt.[5] The free amine analog of (*S*)-CMK could be obtained upon neutralization of the ammonium hydrochloride salt but I observed early on that the free amine was unstable. I hypothesize that this can be due to substitution reactions between the free amine of one molecule and the chlorine group of another molecule.

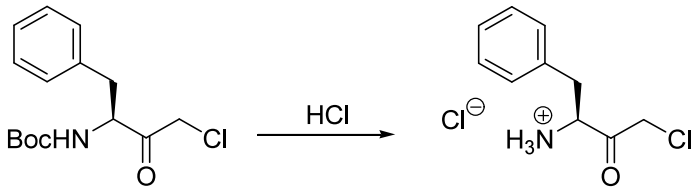

Figure 6.2: Formation of (*S*)-4- chloro-3-oxo-1-phenylbutan-2-aminium chloride through deprotection of (*S*)-CMK.

Synthesis of Phthalimide-Protected (*S*)-CMK

The synthesis of a phthalimide-protected version of (*S*)-CMK was initially attempted using the synthetic strategy of the Boc-protected (*S*)-CMK.[6,7] This method involves the reaction of *N*-phthaloyl-L-phenylalanine with IBCF at 0°C to form a mixed anhydride intermediate. The mixed anhydride is reacted *in situ* at 0°C with diazomethane and quenched with hydrochloric acid to form the chloromethyl ketone product. Unfortunately, after several attempts, the desired product could not be isolated. Instead of going through the unstable mixed anhydride intermediate, the synthetic procedure was modified to use the acid chloride intermediate (Figure 6.3).[8] *N*-Phthaloyl-L-phenylalanine was reacted with oxalyl chloride to form the corresponding acid chloride, which was then reacted with trimethylsilyldiazomethane. After quenching with hydrochloric acid, the final product, *N*-phthaloyl-(3*S*)-3-amino-1-chloro-4-phenyl-2-butanone (Phth-CMK) was obtained. Phth-CMK was successfully isolated in 73% yield and characterized by ^{1}H and ^{13}C NMR, melting point, elemental analysis, and mass spectrometry.[2]

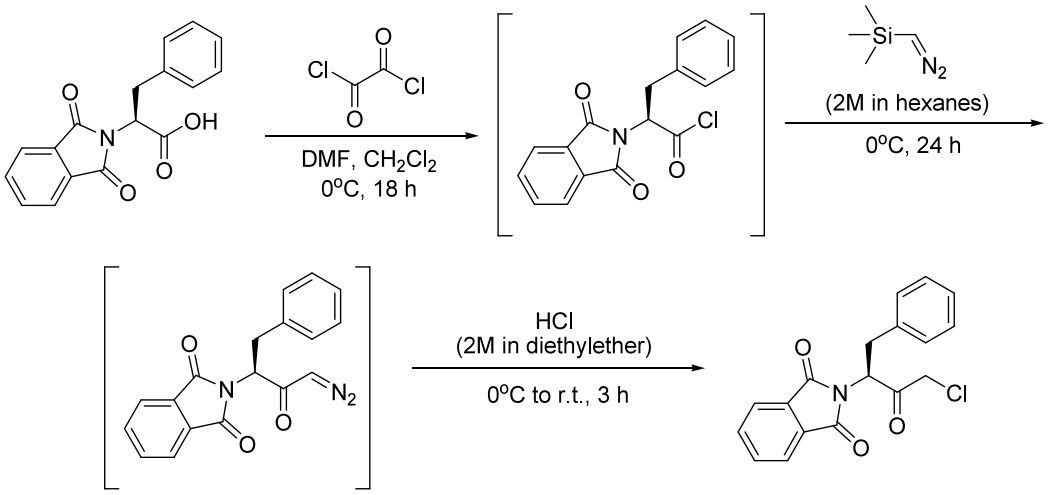

Figure 6.3: Synthesis of *N*-phthaloyl-(3*S*)-3-amino-1-chloro-4-phenyl-2-butanone (Phth-CMK).

Synthesis of Trifluoroacetamide-Protected (*S*)-CMK

Following the same synthetic scheme used to synthesize Phth-CMK, the desired trifluoroacetamide-protected product, *N*-trifluoroacetyl-(3*S*)-3-amino-1-chloro-4-phenyl-2-butanone (TFA-CMK), was isolated in 30% yield. An alternative synthetic route, in which the free amine derivative of (*S*)-CMK was directly reacted with trifluoroacetic anhydride to form TFA-CMK, was investigated (Figure 6.4). The previously isolated ammonium hydrochloride salt of (*S*)-CMK was first neutralized to form the free amine analog. Careful attention was paid to keep the free amine dilute and cold to prevent its decomposition. Trifluoroacetic acid was then added to successfully form TFA-CMK in 85% yield. The product was characterized by ^{1}H and ^{13}C NMR, melting point, elemental analysis, and mass spectrometry.

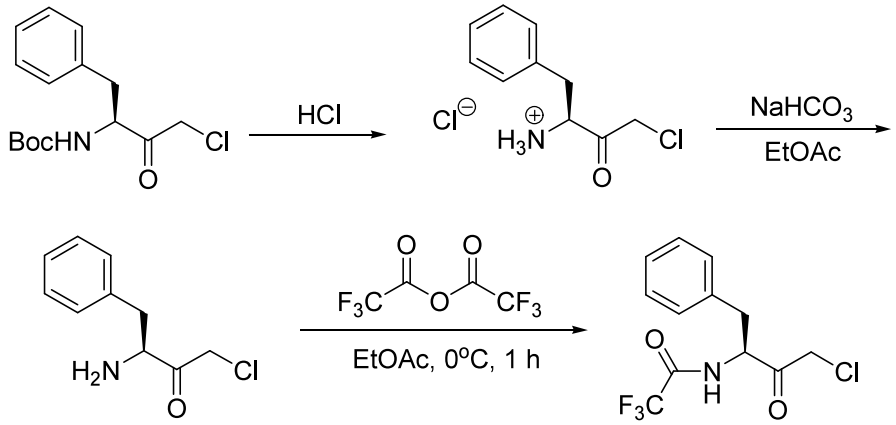

Figure 6.4: Synthesis of *N*-trifluoroacetyl-(3*S*)-3-amino-1-chloro-4-phenyl-2-butanone (TFA-CMK).

Reduction of (*S*)-CMK with Different Protecting Groups

Asymmetric Transfer Hydrogenation

The reduction of Phth-CMK via ATH was investigated (Figure 6.5). The ruthenium catalyst precursor {[Ru(*p*-cymene)Cl_2]$_2$} and TsEN ligand were stirred together

in methanol for one hour at room temperature followed by the addition of triethylamine and formic acid. The reaction started upon the addition of the Phth-CMK starting material. The Phth-CMK did not dissolve immediately but as the reaction progressed a homogeneous brown solution was formed. The reaction was run overnight then quenched with ammonium chloride and extracted in DCM. HPLC and ^{1}H NMR analysis showed complete conversion of the starting material with a DR of 2.1:1.

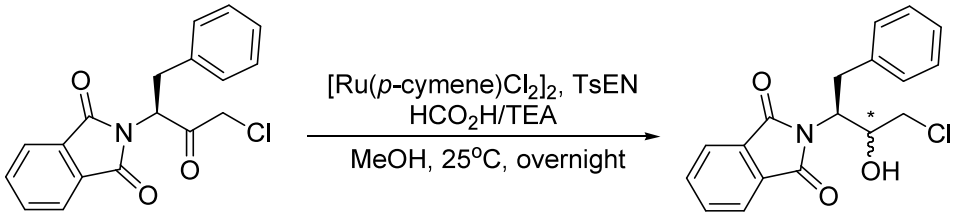

Figure 6.5: ATH reduction of Phth-CMK.

Reduction with Boron Reducing Agents

The reduction of an ammonium hydrochloride salt similar to the deprotected (*S*)-CMK with sodium borohydride was previously reported with a DR of 1.5:1 (Figure 6.6).[9] This approach was repeated in our laboratory. The reduction of the (*S*)-CMK hydrochloride salt was performed under the same conditions as in the literature with the exception of the solvent being pure methanol. Analysis of the post-reaction mixture by ^{1}H NMR showed that all of the ammonium hydrochloride salt had reacted and only the alcohol products were present. The DR was not determined as the HPLC method failed to separate the alcohol products. The alcohols were reacted with di-*tert*-butyl dicarbonate to reform the original (*S,S*)-CMA and (*R,S*)-CMA (Figure 6.7),[9] for which the HPLC method was well established. After the Boc protection, the DR was found to be 0.47:1. This DR is much lower than that reported in the literature (1.5:1). The protection

step of the salt with a Boc group should not have changed the original DR; however, a direct measurement of the DR on the salt would be unequivocal.

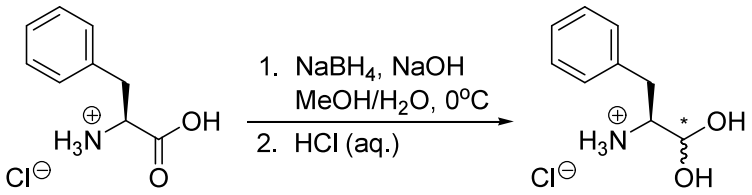

Figure 6.6: Reduction of ammonium salt.[9]

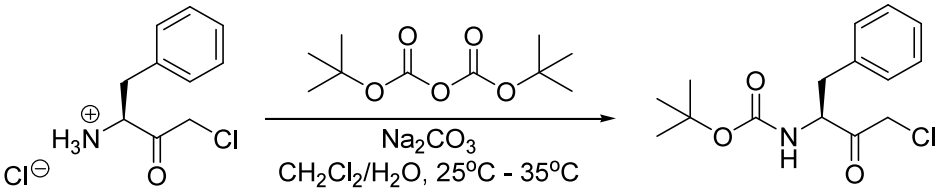

Figure 6.7: Boc protection of (*S*)-CMK ammonium hydrochloride salt.

Phth-CMK was also reduced with sodium borohydride using the same procedure as with the ammonium hydrochloride salt, except that the methanol was replaced with acetonitrile for homogeneity. The post-reaction analysis by HPLC indicated the formation of many unidentified compounds and some unreacted Phth-CMK. Sodium borohydride is prone to reducing the ketone but can also reduce the carbonyl groups of the protecting phthalimide group[10,11] and possibly cleave the phthalimide group altogether[12] (Figure 6.8). The lack of peaks corresponding to the products suggests that the side reactions are faster than the reduction of the ketone.

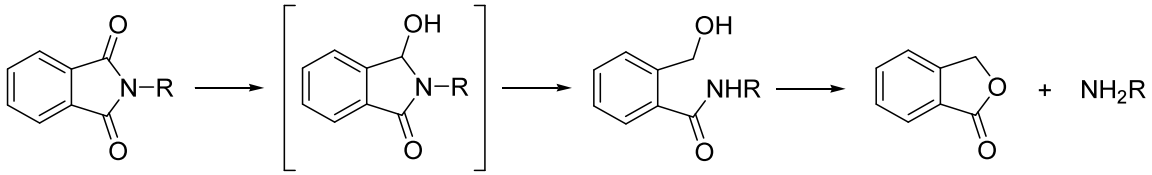

Figure 6.8: Reduction of phthalimide carbonyl and subsequent removal of phthalimide protecting group.

Meerwein-Ponndorf-Verley Reduction

The reduction of the (*S*)-CMK ammonium hydrochloride salt through the MPV reduction was attempted (Figure 6.9). The (*S*)-CMK salt was stirred in anhydrous isopropanol at 50°C and aluminum isopropoxide was added to start the reaction. Unfortunately, no reaction occurred with the MPV reduction of the ammonium hydrochloride salt. This is probably due to the low solubility of the salt in the organic solvent. Since the free amine of (*S*)-CMK was found to be unstable, I did not pursue reduction of this compound.

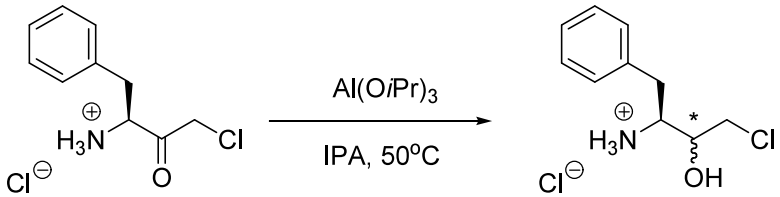

Figure 6.9: MPV reduction of (*S*)-CMK ammonium hydrochloride salt.

The previously synthesized Phth-CMK and TFA-CMK were next reduced using the MPV reduction. However, due to its low solubility in isopropanol, Phth-CMK did not react with aluminum isopropoxide in a pure isopropanol solution overnight at 50°C. Even when acetonitrile was added as a cosolvent, the starting material had a very low solubility in the 1:1 acetonitrile/isopropanol solvent mixture and reaction did not take

place. To circumvent this limitation, the reduction was attempted in refluxing isopropanol overnight. Even at this temperature, the solution was heterogeneous; however, the reaction did proceed. About 25% conversion of our starting material with a DR of about 1:1 was observed by HPLC analysis. Since the starting material readily dissolves in toluene, toluene was chosen as our reaction solvent with 10% isopropanol to speed up the reaction. Phth-CMK (Figure 6.10) and TFA-CMK (Figure 6.11) were both reduced in a 9:1 toluene/isopropanol solvent mixture. Each reduction was catalyzed by aluminum isopropoxide and the experiments were carried out in triplicate overnight at 50°C. These reactions were analyzed by HPLC and the results are summarized in Table 6.1. The products of the reductions of Phth-CMK and TFA-CMK were isolated and characterized by X-ray crystallography.

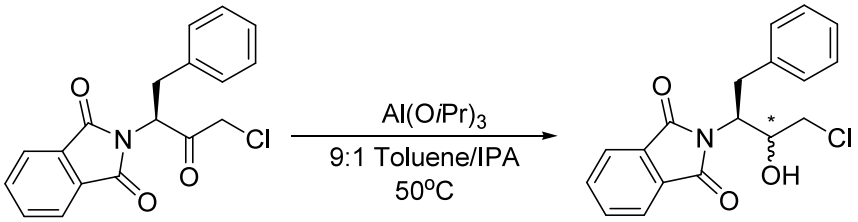

Figure 6.10: MPV reduction of Phth-CMK.

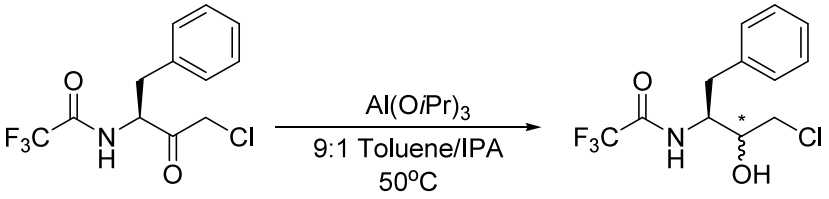

Figure 6.11: MPV reduction of TFA-CMK.

Table 6.1. MPV reduction of (*S*)-CMK, Phth-CMK, and TFA-CMK.

Reactant	DR	% Conversion	% Yield
(*S*)-CMK	0.05 ± 0.01	100 ± 0.0	90 ± 1.4
Phth-CMK	1.10 ± 0.00	99 ± 0.0	92 ± 0.1
TFA-CMK	0.03 ± 0.00	99 ± 0.0	99 ± 0.0

As Table 6.1 shows, the data supports the hypothesis that preventing hydrogen bonding will affect the diastereoselectivity of the reaction. By removing both hydrogens on the nitrogen in Phth-CMK, the diastereoselective preference for the (*S,S*) diastereomeric product was eliminated, giving an even product distribution. The reaction does not seem to be affected by the type of protecting group on the amine (Boc vs. trifluoroacetamide), only by the presence or absence of a hydrogen on the nitrogen that allows hydrogen bonding to occur.

CONCLUSIONS

In conclusion, the stereoselectivity of the reduction of (*S*)-CMK has been improved through the use of different protecting groups. The greatest improvement in selectivity was observed when the Boc protecting group of (*S*)-CMK was replaced with a phthalimide group. Specifically, preventing the hydrogen bonding between the amide proton of (*S*)-CMK and the alkoxy group of the aluminum isopropoxide in the MPV reduction reversed the diastereoselectivity in favor of (*R,S*)-CMA. In addition, the ATH reaction also showed an increase in DR from 0.45:1 with (*S*)-CMK to 2.1:1 with Phth-CMK.

EXPERIMENTAL METHODS

Materials and Equipment

All chemicals were ordered from Aldrich or VWR and used as received, unless otherwise noted. The (*S*)-CMK starting material was obtained from Ampac Fine Chemicals (Sacramento, CA). All solvents used in the MPV reduction were purchased as anhydrous from Aldrich and used as received.

^{1}H, ^{13}C, and ^{17}F NMR spectra were obtained from a Varian-Mercury VX400 MHz spectrometer using $CDCl_3$ as an internal reference, unless otherwise noted. Elemental analyses were performed by Atlantic Microlab (Norcross, GA). High resolution mass spectrometry (HRMS) experiments [either ESI or fast atom bombardment (FAB)] were performed by Georgia Institute of Technology Bioanalytical Mass Spectrometry Facility (Atlanta, GA). X-ray crystallography was performed by the X-ray Crystallography Lab at Emory University (Atlanta, GA). HPLC analysis was run on an Agilent 1100 series LC with a UV detector set to 210 nm.

Synthesis of (*S*)-CMK with Different Protecting Groups

Synthesis of (*S*)-4-Chloro-3-oxo-1-phenylbutan-2-aminiumchloride

(*S*)-CMK (5.00 g, 16.8 mmol) was dissolved in ethyl acetate (50 mL) and cooled to 0°C in an ice bath. Concentrated hydrochloric acid (15.3 mL, 503 mmol) was added dropwise to the solution. Upon complete addition of the acid, the ice bath was removed and the solution was stirred at room temperature for one hour. The white solid was filtered and washed with ethyl acetate and diethylether to give pure the pure ammonium hydrochloride salt (3.85 g, 16.4 mmol, 98%).

mp 170-172°C (literature mp 170°C[5]). ^{1}H NMR δ 3.17 (m, 2H), 4.51 (s, 1H), 4.62 (2H), 7.31 (m, 5H), 8.69 (s, 3H). ^{13}C NMR δ 35.0, 48.0, 57.2, 127.4, 128.9, 129.5, 134.5,

198.3. MS (ESI+) calculated for $C_{10}H_{13}NOCl_2$: 234.12. Found: 198.2 ($C_{10}H_{13}NOCl$). Elemental analysis calculated for $C_{10}H_{13}NOCl_2$: C, 51.30; H, 5.60; N, 5.98. Found: C, 54.41; H, 5.62; N, 6.01.

General Procedure for the Preparation of *N*-Protected α-Chloroketones (Phth-CMK and TFA-CMK)

N-Protected-L-phenylalanine (5.0 mmol) was placed under an argon atmosphere and anhydrous DCM (25 mL) and DMF (2 drops) were added to dissolve the solid. The solution was cooled to 0°C and oxalyl chloride (0.48 mL, 5.5 mmol) was slowly added to the solution over fifteen minutes. The solution was allowed to stir at 0°C overnight. Trimethylsilyldiazomethane (5.0 mL of a 2 M solution in hexanes, 10 mmol) was slowly added to the reaction mixture over one hour. The solution was allowed to stir at 0°C under argon for 24 hours. At this time hydrochloric acid (5.0 mL of a 2 M solution in diethylether, 10 mmol) was added at 0°C. After one hour, the solution was allowed to warm to room temperature and the reaction was opened to the atmosphere. After three hours, the organic layer was washed with saturated sodium bicarbonate and then with brine. The solvent was removed via rotary evaporation resulting in a yellow solid. The crude material was decolorized with charcoal in acetonitrile.

Synthesis of Phth-CMK

Phth-CMK was synthesized following the general procedure above. The decolorized material was recrystallized in a 9:1 mixture of hexanes/ethyl acetate. Phth-CMK was isolated as a white solid (1.2 g, 3.7 mmol, 73%).

mp 117–118°C (lit mp 119–120°C[2]). ^{1}H NMR δ 3.30 (br m, 2H), 4.80 (br q, 2H), 5.33 (q, 1H), 7.10 (m, 5H), 7.81 (s, 4H). ^{13}C NMR δ 32.9, 47.7, 57.9, 123.4, 126.7, 128.3, 128.8, 130.9, 134.8, 136.7, 167.1, 196.9. HRMS (FAB+) calculated for

$C_{18}H_{14}NO_3Cl$: 327.0662. Found: 328.0731 (M+H). Elemental analysis calculated for $C_{18}H_{14}NO_3Cl$: C, 65.96; H, 4.31; N, 4.27. Found: C, 65.90; H, 4.20; N, 4.21.

Synthesis of TFA-CMK

TFA-CMK was synthesized following the general procedure above. The ^{1}H NMR of the crude product showed the presence of TFA-CMK (~30% yield).

^{1}H NMR δ 2.84 (m, 1H), 3.24 (m, 1H), 4.74 (q, 2H), 4.85 (m, 1H), 7.23 (m, 5H), 9.83 (d, 1H).

Alternative Synthesis of TFA-CMK

The ammonium hydrochloride salt of (*S*)-CMK (20 mmol) was neutralized using saturated sodium bicarbonate in ethyl acetate. The organic layer was dried over magnesium sulfate and filtered over an ice bath. The dilute solution of the free amine was placed under an argon atmosphere and allowed to cool to 0°C. Trifluoroacetic anhydride (5.6 mL, 40 mmol) was added dropwise. The reaction mixture was poured into water (30 mL) after one hour and extracted with ethyl acetate (2 x 75 mL). The organic layer was washed with brine (2 x 30 mL), dried over magnesium sulfate, and concentrated under reduced pressure. Crystallization from toluene afforded the pure TFA-CMK, which was isolated as a white solid (5.1 g, 17 mmol, 85%).

mp 114–115°C (lit mp 112°C[13]). ^{1}H NMR δ 2.85 (m, 1H), 3.25 (m, 1H), 4.72 (q, 2H), 4.83 (m, 1H), 7.25 (m, 5H), 9.81 (d, 1H). ^{13}C NMR δ 34.4, 47.7, 58.3, 114.2, 117.1, 126.7, 128.3, 129.1, 136.8, 156.2, 156.5, 198.8. ^{17}F NMR δ -75. HRMS (FAB+) calculated for $C_{12}H_{11}ClF_3NO_2$: 293.0430. Found: 294.0517 (M+H). Elemental analysis calculated for $C_{12}H_{11}ClF_3NO_2$: C, 49.08; H, 3.78; N, 4.77. Found: C, 48.83; H, 3.61; N, 4.74.

Asymmetric Transfer Hydrogenation

The ATH reaction on Phth-CMK was performed following the same reaction procedure used with (*S*)-CMK as in Chapter 4. $[Ru(p\text{-cymene})Cl_2]_2$ (15 mg, 0.025 mmol) and TsEN (21 mg, 0.085 mmol) were stirred in methanol (5 mL) at room temperature for one hour. Triethylamine (0.560 mL, 4.02 mmol) and formic acid (0.184 mL, 4.88 mmol) were added to the reaction mixture. Phth-CMK (0.67 g, 2.1 mmol) was added to start the reaction. The Phth-CMK initially did not dissolve and formed a slurry. As the reaction progressed, the reaction mixture became a brown solution. The reaction was run overnight at room temperature. The reaction was quenched with ammonium chloride. The organics were extracted into DCM and washed with brine. The solution was dried over magnesium sulfate and the solvent was removed under vacuum. The product residue was analyzed by ^{1}H NMR and HPLC.

Reduction with Boron Reducing Agents

Sodium Borohydride Reduction of (*S*)-CMK Ammonium Hydrochloride Salt

Sodium borohydride (0.34 g, 5.6 mmol) and sodium hydroxide (0.17 g, 4.3 mmol) were dissolved in methanol (15 mL) and cooled to 0°C in an ice bath. The previously synthesized (*S*)-CMK ammonium hydrochloride salt (1.0 g, 4.3 mmol) was dissolved in methanol (10 mL) and added to the reaction mixture. After the reaction ran for one hour at 0°C, the reaction was quenched with an excess of hydrochloric acid in methanol (10 mL of a 2 M solution, 20 mmol). The solvent was removed under vacuum. The product mixture was analyzed by ^{1}H NMR and HPLC.

Boc-Protection of (*S*)-CMK Ammonium Hydrochloride Salt Reduction Products

The (*S*)-CMK ammonium hydrochloride salt reduction products were protected following a known method.[9] Sodium carbonate (0.34 g, 3.2 mmol) was dissolved in distilled water (10 mL). Di-*tert*-butyl dicarbonate (0.51 g, 2.3 mmol) was dissolved in DCM (10 mL) and this solution was added to the sodium carbonate. The products from the above mentioned sodium borohydride reduction were slowly added to the reaction mixture at room temperature. The reaction was heated to 35°C and run for one hour. The organic phase was diluted with DCM (20 mL) and washed with water and brine. The solvent was removed under vacuum. The resulting solid was analyzed by HPLC.

Sodium Borohydride Reduction of Phth-CMK

A solution of sodium borohydride (0.085 g, 3.1 mmol) and sodium hydroxide (0.18 g, 3.8 mmol) in acetonitrile (25 mL) was cooled to 0°C in an ice bath. Phth-CMK (0.5 g, 1.5 mmol) was added and the reaction was run overnight. The reaction was slowly warmed to room temperature and the solvent was removed under vacuum. The resulting solid residue was dissolved in ethyl acetate and washed with dilute acid, water, and brine. The organic phase was dried over magnesium sulfate and the solvent was removed under vacuum. The product was analyzed by HPLC.

Meerwein-Ponndorf-Verley Reduction

The MPV reduction of Phth-CMK and TFA-CMK was performed on a smaller scale compared to the MPV reductions described in Chapter 3. Phth-CMK or TFA-CMK and aluminum isopropoxide was dissolved in 9:1 toluene/isopropanol (anhydrous). This solution was heated to 50°C and run overnight. The reactions were run in triplicate. The amounts of the reagents used in each reaction are listed in Table 6.2. The reactions were quenched in an ice bath. Methanol (10 mL) was added along with hydrochloric

acid (1 mL of a 2 M solution) to quench the reactions. Samples (0.300 mL) of each solution were taken and analyzed on the HPLC.

Table 6.2: Reagent loadings in MPV reduction of Phth-CMK and TFA-CMK.

	Phth-CMK	TFA-CMK
Mass CMK (g)	0.262	0.156
Amount CMK (mmol)	0.801	0.532
Mass $Al(OiPr)_3$ (g)	0.085	0.057
Amount $Al(OiPr)_3$ (mmol)	0.416	0.279
Volume Solvent (mL)	2.5	1.67

Analysis of Reduction Products

Purification of Phth-CMK Reduction Products

Starting from the crude product mixture from the MPV reduction of Phth-CMK described above, the product compounds were separated by column chromatography. The solvent was removed under vacuum from the MPV reduction solution and the residue loaded on a silica column. The products were separated using an 8:2 hexane/ethyl acetate mobile phase. One of the diastereomeric products was isolated and recrystallized in a 7:3 hexane/ethyl acetate solvent mixture. The product crystallized as fine white needles.

Analysis of (*R,S*)-Phth-CMA

^{1}H NMR δ 3.22 (ddd, 2H), 3.46 (dd, 1H). 3.63 (dd, 1H), 4.18 (bs, 1H), 4.22 (m, 1H), 4.95 (ddd, 1H), 7.20 (m, 5H), 7.69 (m, 2H), 7.82 (bs, 2H). ^{13}C NMR δ 35.1, 45.9, 55.0, 71.0, 123.5, 126.8, 128.6, 129.0, 131.3, 134.3, 136.6, 172.2. Elemental analysis calculated for $C_{10}H_{15}NO_3Cl$: C, 65.36; H, 5.14; N, 4.23; Cl, 10.74. Found: C, 65.47; H, 4.95; N, 4.23, Cl, 10.76.

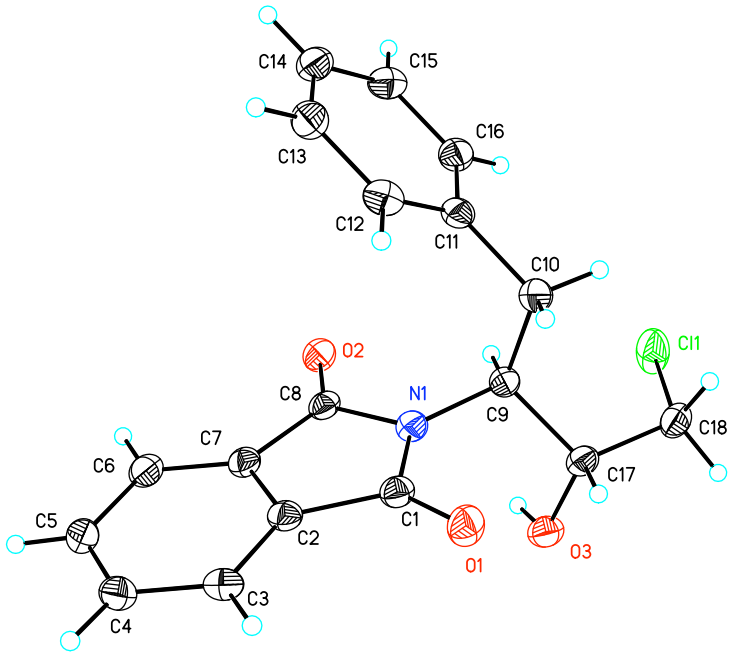

Figure 6.12: X-ray crystal structure of (*R,S*)-Phth-CMA.

Purification of TFA-CMK Reduction Products

Starting from the crude product mixture from the MPV reduction of TFA-CMK described above, the product compounds were separated by column chromatography. The solvent was removed under vacuum from the MPV reduction solution and the residue loaded on a silica column. The products were separated using a 9:1 hexane/ethyl acetate mobile phase. The main diastereomeric product was isolated and recrystallized in a 7:3 hexane/ethyl acetate solvent mixture to yield white needles.

Analysis of (*S,S*)-TFA-CMA

^{1}H NMR δ 2.75 (dd, 1H), 3.20 (dd, 1H), 3.53 (dd, 1H), 3.64 (dd, 1H), 3.82 (ddd, 1H), 4.20 (ddd, 1H), 7.20 (m, 5H). ^{13}C NMR δ 36.3, 47.6, 55.5, 73.6, 88.0, 127.5, 129.3, 130.3, 139.0, 159.2. Elemental analysis calculated for $C_{12}H_{13}NO_2ClF_3$: C, 48.73; H, 4.40; N, 4.74; Cl, 12.01; F, 19.29. Found: C, 48.95; H, 4.33; N, 4.81, Cl, 11.96; F, 19.01.

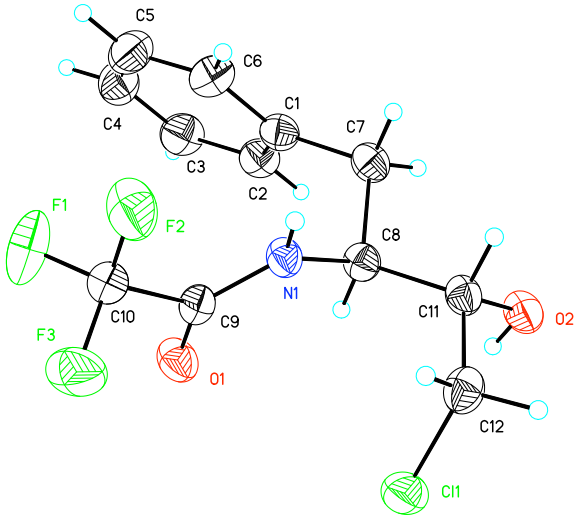

Figure 6.13: X-ray crystal structure of (*S*,*S*)-TFA-CMA.

REFERENCES

(1) Yin, J. J.; Huffman, M. A.; Conrad, K. M.; Armstrong, J. D. *Journal of Organic Chemistry* **2006**, *71*, 840-843.

(2) Bankowski, K.; Maslinski, W.; Pelka, J.; Drabarek, S. *Polish Journal of Chemistry* **1978**, *52*, 1289-1292.

(3) Fittkau, S.; Smalla, K.; Pauli, D. *Biomedica Bochimica Acta* **1984**, *43*, 887-899.

(4) Stahl, G.; Walter, R.; Smith, C. *Journal of Organic Chemistry* **1978**, *43*, 2285-2286.

(5) Rich, D.; Prasad, J.; Sung, C.; Green, J.; Mueller, R.; Houseman, K.; Mackenzie, D.; Malkovsky, M. *Journal of Medicinal Chemistry* **1992**, *35*, 3803-3812.

(6) Malik, A. A.; Clement, T. E.; Palandoken, H.; Robinson III, J.; Stringer, J. A. US Patent, 2003.

(7) Malik, A. A.; Clement, T. E.; Palandoken, H.; Robinson III, J.; Stringer, J. A. US Patent, 2005.

(8) Ye, T.; McKervey, M. A. *Tetrahedron* **1992**, *48*, 8007-8022.

(9) Onishi, T.; Nakano, T.; Hirose, N.; Nakazawa, M.; Izawa, K. *Tetrahedron Letters* **2001**, *42*, 5887-5890.

(10) Horii, Z.; Iwata, C.; Tamura, Y. *Journal of Organic Chemistry* **1961**, *26*, 2273.

(11) Uhle, F. *Journal of Organic Chemistry* **1961**, *26*, 2998.

(12) Osby, J.; Martin, M.; Ganem, B. *Tetrahedron Letters* **1984**, *25*, 2093-2096.

(13) Fittkau, S.; Smalla, K.; Pauli, D. *Biomed. Biochim. Acta* **1984**, *43*, 887-899.

CHAPTER 7 RECOMMENDATIONS

In summary, I have studied the stereoselective synthesis of (*R,S*)-CMA from its corresponding ketone, (*S*)-CMK, through three reduction methods: (1) MPV reduction, (2) ATH reaction, and (3) boron reducing agents. The highest DR (9.5:1) was achieved when a chiral catalyst was used either in the ATH reaction or with a borohydride reducing agent. I also discovered that switching the Boc protecting group of (*S*)-CMK with a phthalimide group, which replaces the acidic hydrogen on the amine, reverses the selectivity of the MPV reduction to give a DR as high as 1.1:1. While investigating the MPV reduction, I also observed a significant rate enhancement when the classic MPV catalyst, aluminum isopropoxide, was replaced with aluminum *tert*-butoxide.

The use of aluminum *tert*-butoxide to improve the rate of the MPV reduction is new intellectual property. Increasing the rate of the reaction can save both time and money since the reaction mixture does not need to be heated for a long period of time. Another way to reduce the cost of the MPV reduction is to decrease the amount of catalyst used. Not only does this lower the cost of the reagents and their subsequent disposal, but it would also improve the product purity by reducing the amount of catalyst that could leach into the final product. I recommend investigating the kinetics of the MPV reduction with smaller amounts of aluminum *tert*-butoxide catalyst. The current process, using about 0.5 molar equivalents of aluminum isopropoxide, requires two hours of reaction time at 50°C to go to completion. A smaller amount of aluminum *tert*-butoxide can be used to complete the MPV reduction in the same amount of time and the economics of either running the reaction for a shorter duration or using a smaller amount of catalyst can be compared.

Another aspect of the stereoselective MPV reduction that I recommend pursuing is the exploration of different protecting groups on (*S*)-CMK. I ran the MPV reduction on Phth-CMK and TFA-CMK, in addition to the original Boc-protected (*S*)-CMK. Although the Phth-CMK results were in agreement with the hypothesis that hydrogen bonding plays a key role in the diastereoselectivity of the classic MPV reduction, no other tertiary amine protecting groups were investigated. Steric bulkiness of the protecting groups may also play a big role in the selectivity and could be used to increase the DR further. I propose the use of multiple alkyl or aryl protecting groups on the amine to improve the stereoselectivity (Figure 7.1). Comparing the DR of the MPV reduction of (*S*)-CMK with different protecting groups would give more insight into the effect of the protecting group on the reduction.

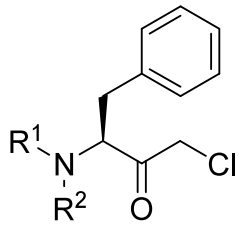

Figure 7.1: (*S*)-CMK with different protecting groups on the tertiary amine.

Although the ATH reaction has been shown to give good diastereoselectivity in the reduction of (*S*)-CMK, the chiral catalyst complex is expensive for industrial processes. Using the ruthenium catalyst precursor, I was able to achieve a DR as high as about 0.45:1. Other researchers have shown that modifications of (1*R*,2*R*)-TsDPEN have led to increases in the selectivity of the reaction.[1] I recommend pursuing similar ligands, as shown in Figure 7.2, which have a substituted amine group on TsEN. This achiral version of the modified ligand would be cheaper and could improve the diastereoselectivity.

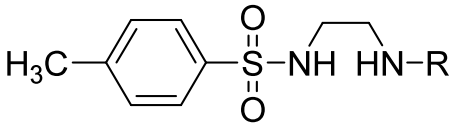

Figure 7.2: *N*-Alkyl-*N′*-tosyl-1,2-ethanediamine ligand.

The use of boron reagents is the most promising reduction method investigated. However, the research presented is only a preliminary screening of reducing agents. I recommend the optimization of the reduction of (*S*)-CMK using BH_3•THF in conjunction with the chiral oxazaborolidine (*R*)-(+)-CBS. Throughout the reactions explored, the reaction conditions changed, making it difficult to accurately compare the results. Further investigation of the effects of the reaction conditions, such as temperature, reaction time, and reagent concentrations, should be pursued to optimize the reaction.

Although the use of chiral oxazaborolidines results in high diastereoselectivity, these catalysts are expensive and are difficult to recycle after the reaction. Once the reaction has been optimized, I recommend attaching the chiral oxazaborolidines to a solid support for their use in a continuous flow process. A few methods for preparing supported oxazaborolidines have been reported in the literature.[2-6] Utilizing a solid support would increase the recyclability of the chiral catalysts, make the reduction process much more economical, and allow for a potential continuous flow process.

REFERENCES

(1) Martins, J. E. D.; Morris, D. J.; Wills, M. *Tetrahedron Letters* **2009**, *50*, 688-692.

(2) Price, M.; Sui, J.; Kurth, M.; Schore, N. *Journal of Organic Chemistry* **2002**, *67*, 8086-8089.

(3) Caze, C.; El Moualij, N.; Hodge, P.; Lock, C.; Ma, J. *Journal of the Chemical Society, Perkin Transactions 1* **1995**, 345-349.

(4) Caze, C.; El Moualij, N.; Hodge, P.; Lock, C. *Polymer* **1995**, *36*, 621-629.

(5) Farrall, M.; Freceht, J. *Journal of Organic Chemistry* **1976**, *41*, 3877-3882.

(6) Franot, C.; Stone, G.; Engeli, P.; Spondlin, C.; Waldvogel, E. *Tetrahedron - Asymmetry* **1995**, *6*, 2755-2766.

APPENDIX A MANGANESE(SALEN) CATALYST SYNTHESIS FOR APPLICATION IN ORGANIC AQUEOUS TUNABLE SOLVENT SYSTEMS

INTRODUCTION

Homogeneously catalyzed reactions generally run faster, give greater product selectivity, and result in higher yields than their heterogeneously catalyzed analogs. However, isolating the product and/or recovering the catalyst after the reaction is often difficult and can lead to product contamination. On the other hand, heterogeneous catalysts readily separate from the reaction mixture but the reaction is often slower than homogeneously catalyzed reactions due to mass transfer limitations.

To address these concerns, the OATS (Organic Aqueous Tunable Solvent) system was designed. OATS couples the benefits of efficient homogeneous catalysis with the ease of heterogeneous separation.[1] OATS consists of a mixed organic-aqueous solvent system (e.g., THF and water), which is fully miscible under ambient conditions. Upon addition of modest pressure (<30 bar) of carbon dioxide, a phase split occurs between the organic solvent and water. The hydrophobic products preferentially partition into the organic phase and easily separate from the hydrophilic catalyst, which remains in the aqueous phase. Furthermore, the water-soluble catalyst can be easily recycled. OATS has been proposed as a sustainable alternative to current pharmaceutical processes, reducing solvent waste and improving product quality by minimizing catalyst contamination.

This work explored the potential of OATS for the asymmetric oxidation of alkenes to chiral epoxides using a water-soluble salen catalyst. I intended to use hydrogen

peroxide as an environmentally benign oxidant. In this case, carbon dioxide acts as both a hydrogen peroxide activator[2] and a miscibility switch for product separation and catalyst recovery. In order for the catalyst and products to properly partition in the OATS system, the catalyst must remain in the aqueous phase while the product preferentially dissolves into the organic phase. Most salen catalysts used for asymmetric epoxidation of alkenes are hydrophobic, so a custom water-soluble catalyst was designed and synthesized. My work focused on the synthesis of this hydrophilic Mn(salen) catalyst. Although the Mn(salen) catalyst was successfully synthesized and characterized, I found that it was unstable in hydrogen peroxide. However, I propose many other future uses for this catalyst.

BACKGROUND

Gas-Expanded Liquids

Solvent choice can greatly influence chemical processing. Solvents can affect reaction rates, dictate separation processes, and impact human health and the surrounding environment, in addition to playing a major role in process economics.[3] Different processes, and often separate steps of the same process, may require different solvents. For instance, a solvent that enhances the solubility of reactants may be difficult to remove in subsequent purification steps. Unfortunately, no perfect solvents exist that work well in all processes.

One approach would be to use a solvent that can be changed as needed. For example, tunable solvents are solvents whose properties vary by changing an external stimulus (e.g., temperature or pressure). One of the most well-known categories of tunable solvents is supercritical fluids (SCFs).[4] These solvents exist at a pressure and temperature above their critical point (the thermodynamic point where the liquid and gas

densities merge and the liquid phase ceases to exist). The properties of SCFs, such as solvent strength and transportability, lie between those of gases and liquids and vary greatly by simply tuning the pressure. In addition to their tunability, SCFs like supercritical carbon dioxide are easily removed upon venting of the system. However, they require relatively high operating temperatures and pressures, which increases the operating costs. SCFs also have weaker solvent strength than organic solvents, which can limit their use in industrial applications.

Gas-expanded liquids (GXLs) make up the next generation of tunable solvents that combine the tunability of SCFs with the solvent power of traditional organic solvents.[5] GXLs are formed by the dissolution of a gas (usually carbon dioxide) into an organic solvent (e.g. methanol or acetonitrile) to create a volume-expanded solvent phase with pressure-tunable properties.[6] GXLs readily achieve a large range of solvent properties, from those of pure carbon dioxide to those of the pure organic solvent. Figure A.1 shows the relative transport properties and solvent power of GXLs compared to traditional organic solvents, SCFs, and gases. Some advantages of using GXLs as a solvent include improved chemical processing and reduced environmental impact. GXLs have enhanced gas solubility of gases such as hydrogen, oxygen, and carbon monoxide, which are important for hydrogenation, oxidation, and hydroformylation reactions. The use of GXLs also reduces the total volume of volatile organic solvents as compared to traditional processes and uses milder pressures than SCFs.

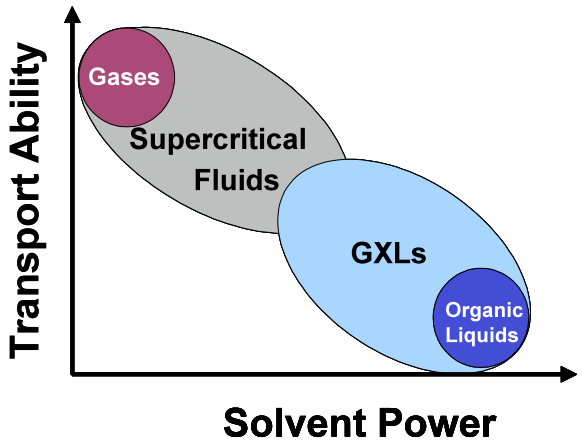

Figure A.1: Relative properties of GXLs compared to other solvent classes.

As a result of their advantageous properties, GXLs have been used in a variety of applications. The most common application of GXLs, gas-antisolvent crystallization, uses the poor solvent strength of the dissolved gas to precipitate solute molecules.[7] This technique has been applied to the synthesis of nanoparticles to produce particles with small size distributions.[8,9] The use of GXLs also improves catalytic hydroformylation, oxidation,[10,11] and hydrogenation reactions[12] by improving the gas solubility.[13] Carbon dioxide-expanded alcohols can also form reversible alkylcarbonic acids, which can catalyze reactions without the need for subsequent acid neutralization steps.[14] The versatility and tunability of GXLs allows for a multitude of additional applications, beyond the examples above.

OATS System

GXLs have been applied to the development of OATS, a reaction process that combines homogeneous catalysis with heterogeneous separations. The reaction runs homogeneously in a miscible mixed organic/aqueous solvent (e.g., THF and water). Upon completion of the reaction, carbon dioxide is added to the reaction mixture to induce a phase separation between the aqueous and gas-expanded organic phases.

The hydrophilic catalyst remains in the aqueous phase while the hydrophobic products partition into the organic phase, allowing for simple isolation of the products while recycling the catalyst for further use (Figure A.2).[1] The OATS process results in highly efficient reactions while reducing waste production and improving product quality by minimizing contamination.

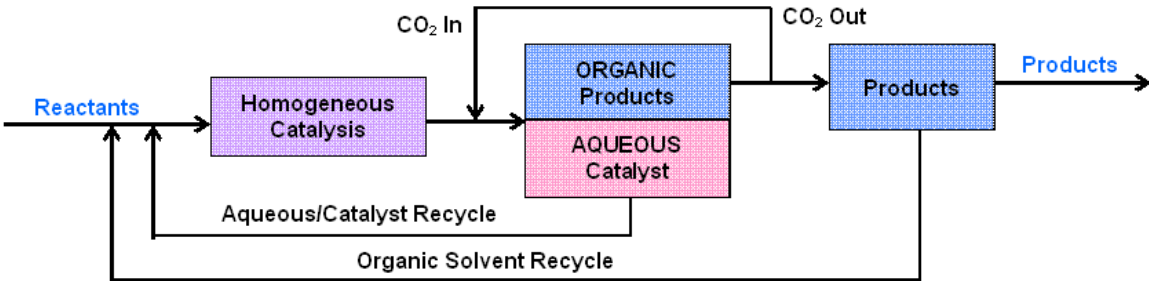

Figure A.2: OATS process schematic.

By utilizing carbon dioxide as a miscibility switch, OATS allows facile separation since the carbon dioxide-expanded organic phase becomes a poorer solvent for hydrophilic substances. As a proof of concept, a water-soluble dye was dissolved in a mixed water/acetonitrile solvent system. Upon the addition of 30 bar of carbon dioxide, a gas-expanded acetonitrile phase was formed, inducing a phase split. The water-soluble dye preferentially partitioned into the aqueous phase.[6] The benefits of the OATS system are summarized in Figure A.3, which shows OATS combining the properties of homogeneous catalysis (increased yields and product selectivity) with those of heterogeneous separations (facile catalyst removal and product purification).

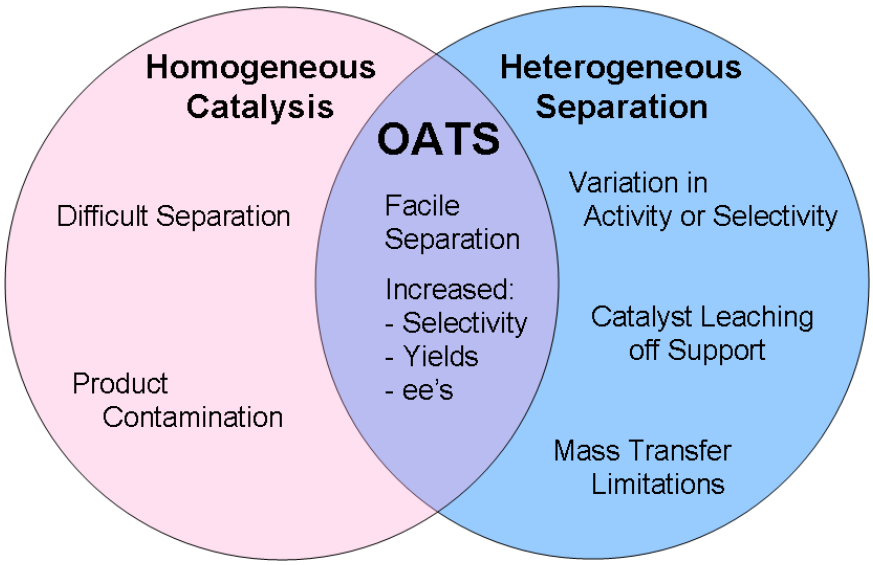

Figure A.3: Summary of OATS benefits.

The OATS system was applied to a number of pharmaceutically relevant reactions with promising results. OATS improved the substrate and catalyst solubility in the hydroformylation of hydrophobic olefins and allowed the catalyst to be recycled three times with no loss of activity.[15] The hydroformylation reaction was applied to long chain olefins that cannot be processed industrially in the commercial biphasic (water/organic) solvent, due to solubility issues. Although the system is biphasic, the reaction takes place in the aqueous phase, thereby relying on the olefin's solubility in water. By combining aqueous and organic solvents, OATS improved the reaction between the substrate and the catalyst by reducing mass transfer limitations. OATS has also been applied to biocatalysis, where the enzyme was successfully recycled in the aqueous phase after completion of the reaction.[16]

Salen Catalysts

In the past few decades, homogeneous chiral salen catalysts have emerged as a group of useful and important enantioselective catalysts.[17] Not only does the use of

chiral salen catalysts result in high enantiomeric excesses, but they also function well in a wide variety of reactions, including polymer formation,[18] kinetic resolution of epoxides,[19] sulfoxidation,[20] and alkene epoxidation.[21] The term "salen" refers to compounds with structures derived from *N,N'*-bis(salicylidine)ethylenediamine. These molecules arise from the simple condensation of a salicylaldehyde with a 1,2-diamine (Figure A.4). The salen ligand then complexes with a transition metal (e.g., Mn, Cr, Co, Cu, Ti, Ru) to form the salen catalyst. Researchers have obtained a large number of salen ligand variations through the addition of functional groups to either the aldehyde or diamine starting materials.[22] Most notably, the use of a chiral diamine results in chiral salen ligands for use in asymmetric reactions.

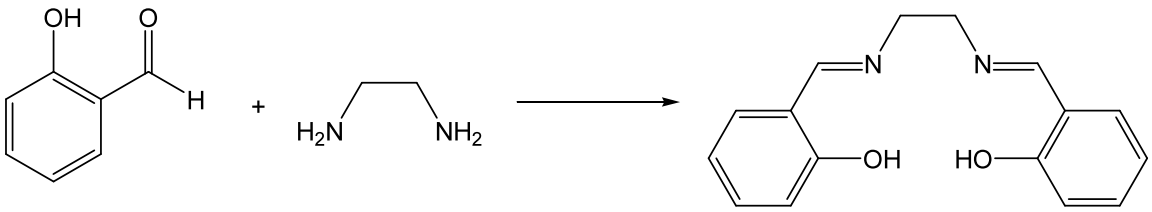

Figure A.4: Synthesis of generic salen ligand.

Epoxidation Reaction

One of the most common uses of chiral salen catalysts is the stereoselective epoxidation of alkenes. The production of pharmaceuticals often involves these chiral epoxide intermediates. As an example, Figure A.5 shows the epoxidation of indene to indene oxide, a crucial step in the synthesis of the AIDS treatment drug Crixivan®.[23] Epoxidations using salen catalysts traditionally run in an organic phase with an organic oxidant like peroxides, or a biphasic system with a hydrophilic oxidant such as sodium hypochlorite. The products subsequently get purified using column chromatography to remove the salen catalyst, which remains on the column, precluding recycling strategies.

OATS would allow for facile recovery and reuse of the expensive chiral catalyst while removing the need for additional product purification steps.

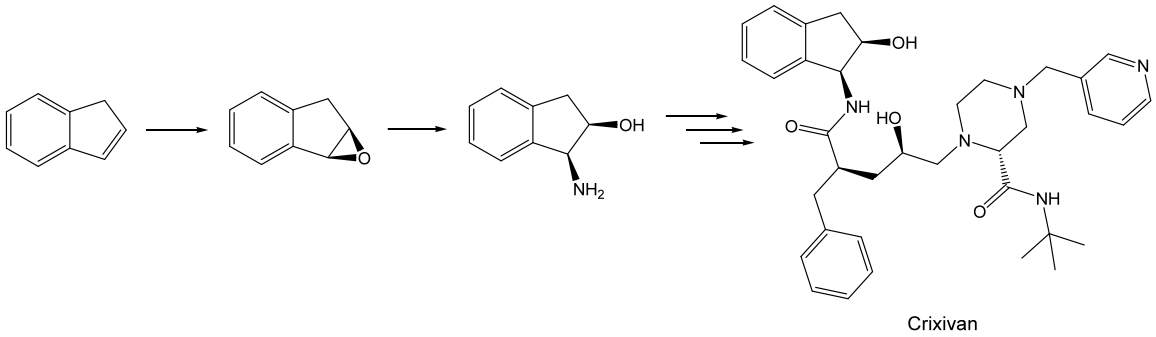

Figure A.5: Preparation of Crixivan® from indene.

In addition to catalyst recovery, the use of expensive organic oxidants or environmentally unfriendly halogenated oxidant systems represents a major challenge to epoxidation reactions. Hydrogen peroxide-based epoxidation provides an ideal alternative synthetic route. Besides its low cost, hydrogen peroxide is preferred because the only byproduct formed from its reaction is water. Researchers have successfully used hydrogen peroxide, in combination with chiral salen catalysts, to synthesize a variety of chiral epoxides.[24,25] Although hydrogen peroxide epoxidation slows the reaction compared to more active oxidants, it has previously been shown that supercritical carbon dioxide can enhance the rate of reaction by forming peroxycarbonic acid in situ.[2] I proposed to use carbon dioxide both to activate the hydrogen peroxide and to induce the phase separation for the OATS system.

RESULTS AND DISCUSSION

Synthesis of Mn(salen) Catalyst

First, a chiral salen catalyst that would preferentially partition into the aqueous phase of our OATS system was designed. Researchers previously investigated the application of the chiral phosphino catalyst shown in Figure A.6, whose synthesis exists in the literature.[26] However, preliminary investigations revealed that this catalyst only partitioned about 1:1 between water and acetonitrile in OATS, which would result in poor catalyst recovery and recycle. Instead of the phosphino groups, I proposed to use sulfonate groups to further increase the water solubility of the catalyst.

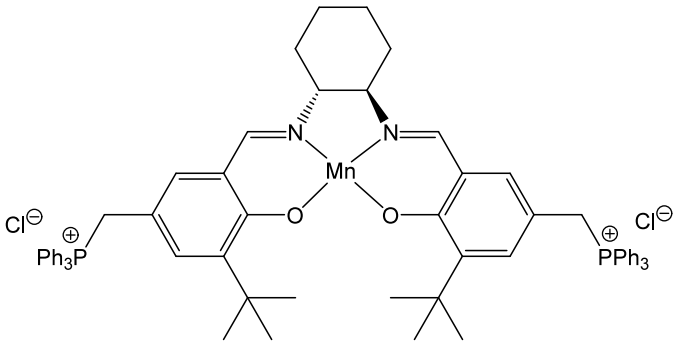

Figure A.6: Water-soluble Mn(salen) catalyst.

Figure A.7 shows the reaction scheme for the synthesis of the sulfonated Mn(salen) catalyst. I first sulfonated 3-(*tert*-butyl)-2-hydroxybenzaldehyde to improve the water solubility of the catalyst. Then this sulfonated intermediate was added to (1*R*,2*R*)-1,2-diaminocyclohexane in a condensation reaction. Finally, the Mn(salen) catalyst formed through the combination of the salen ligand with manganese acetate.

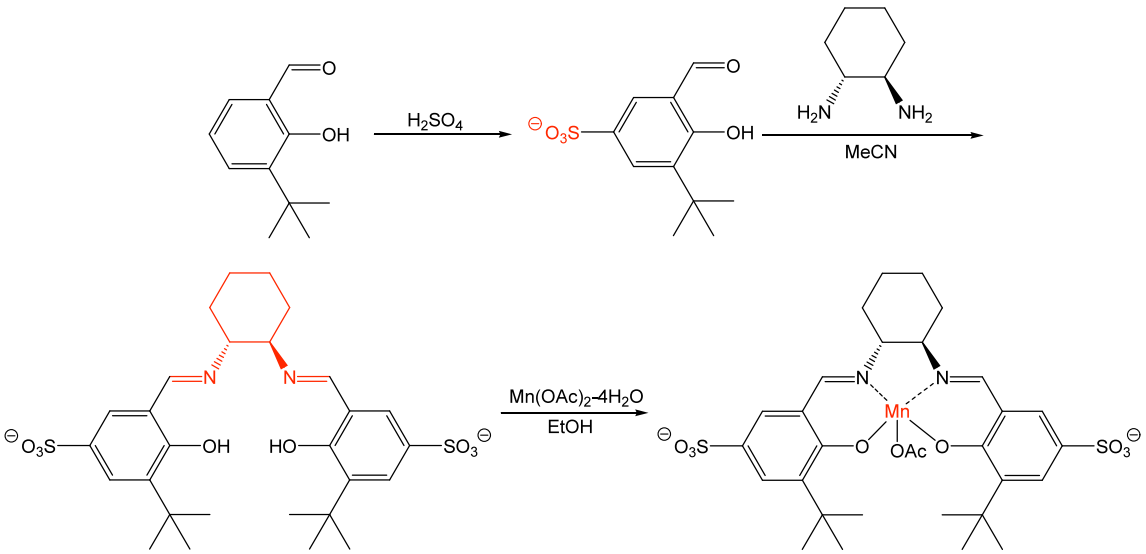

Figure A.7: Synthesis of Mn(salen) catalyst.

Synthesis of 3-*tert*-Butyl-5-formyl-4-hydroxybenzenesulfonate

Figure A.8 shows the first step towards synthesis of the desired Mn(salen) catalyst was sulfonation of 3-*tert*-butyl-2-hydroxybenzaldehyde. I followed a literature procedure using a similar starting compound (chlorobenzaldehyde).[27] The aldehyde was added dropwise to fuming sulfuric acid in an ice bath. After all of the aldehyde was added, the reaction mixture was heated to 85°C and reacted for an additional hour. The excess acid was neutralized with calcium carbonate and the resulting product was recrystallized in methanol. 3-*tert*-Butyl-5-formyl-4-hydroxybenzenesulfonate precipitated as an off-white powder, which was characterized by ^{1}H and ^{13}C NMR, IR, MS, and elemental analysis.

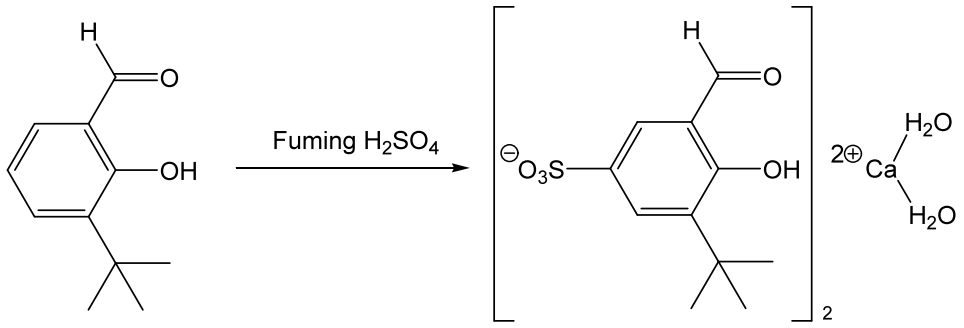

Figure A.8: Synthesis of 3-*tert*-butyl-5-formyl-4-hydroxybenzenesulfonate.

Synthesis of 5,5'-(1*E*,1'*E*)-(Cyclohexane-1,2-diylbis(azan-1-yl-1-ylidene))bis(methan-1-yl-1-ylidene)bis(3-*tert*-butyl-4-hydroxybenzenesulfonate)

Next, 3-*tert*-butyl-5-formyl-4-hydroxybenzenesulfonate was condensed with (1*R*,2*R*)-1,2-diaminocyclohexane (Figure A.9). In a literature procedure on a similar starting material [(3-*tert*-butyl-5-formyl-4-hydroxybenzyl)triphenylphosphonium chloride], the condensation reaction ran in ethanol.[28] However, the sulfonate salt did not dissolve well in ethanol, even at high temperatures, so acetonitrile was used as the reaction solvent instead. (1*R*,2*R*)-1,2-Diaminocyclohexane was added to 3-*tert*-butyl-5-formyl-4-hydroxybenzenesulfonate in acetonitrile and the reaction was run at 80°C. Filtering off the solid product and recrystallizing in methanol yielded yellow crystals of 5,5'-(1*E*,1'*E*)-(Cyclohexane-1,2-diylbis(azan-1-yl-1-ylidene))bis(methan-1-yl-1-ylidene)bis(3-*tert*-butyl-4-hydroxybenzenesulfonate), which was characterized by ^{1}H and ^{13}C NMR, IR, MS, and elemental analysis.

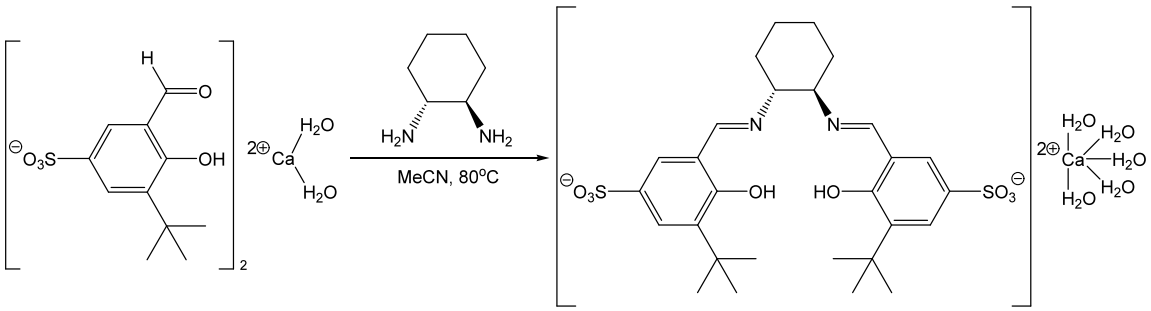

Figure A.9: Synthesis of 5,5'-(1*E*,1'*E*)-(cyclohexane-1,2-diylbis(azan-1-yl-1-ylidene))bis(methan-1-yl-1-ylidene)bis(3-*tert*-butyl-4-hydroxybenzenesulfonate).

Synthesis of Mn(salen) Catalyst Complex

The last step in the Mn(salen) catalyst synthesis involved mixing the salen ligand with the manganese metal center, as shown in Figure A.10. I stirred 5,5'-(1*E*,1'*E*)-(cyclohexane-1,2-diylbis(azan-1-yl-1-ylidene))bis(methan-1-yl-1-ylidene)bis(3-*tert*-butyl-4-hydroxybenzenesulfonate) together with manganese acetate tetrahydrate in ethanol. The reaction mixture refluxed at 80°C and ran for three hours. The product residue was recrystallized in methanol to give a dark brown powder. The Mn(salen) catalyst was characterized by MS, IR, and elemental analysis.

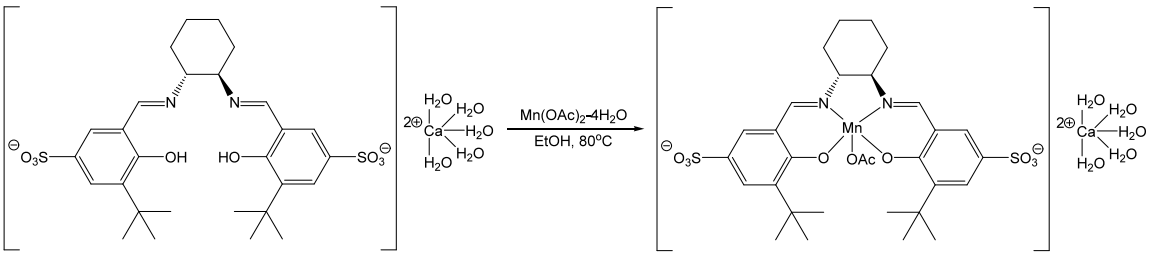

Figure A.10: Synthesis of Mn(salen) catalyst.

Mn(salen) Catalyst Stability

I first noticed the instability of the Mn(salen) catalyst in hydrogen peroxide when I set up a preliminary epoxidation experiment. After dissolving the catalyst in DMF, I

added a 30% hydrogen peroxide solution and the mixture immediately started to release gas and a large exotherm was observed. The catalyst decomposed during this reaction. To test the stability of my salen ligand and catalyst to hydrogen peroxide, the UV absorbance was measured over time. The salen ligand showed the same absorbance over the course of 24 hours in a 30% hydrogen peroxide solution. However, as Figure A.11 shows, the absorbance at a wavelength of 400 nm corresponding to the Mn(salen) catalyst in hydrogen peroxide decreased drastically in just a few minutes. Because of the catalyst's instability to the chosen oxidant, I stopped further work on this project.

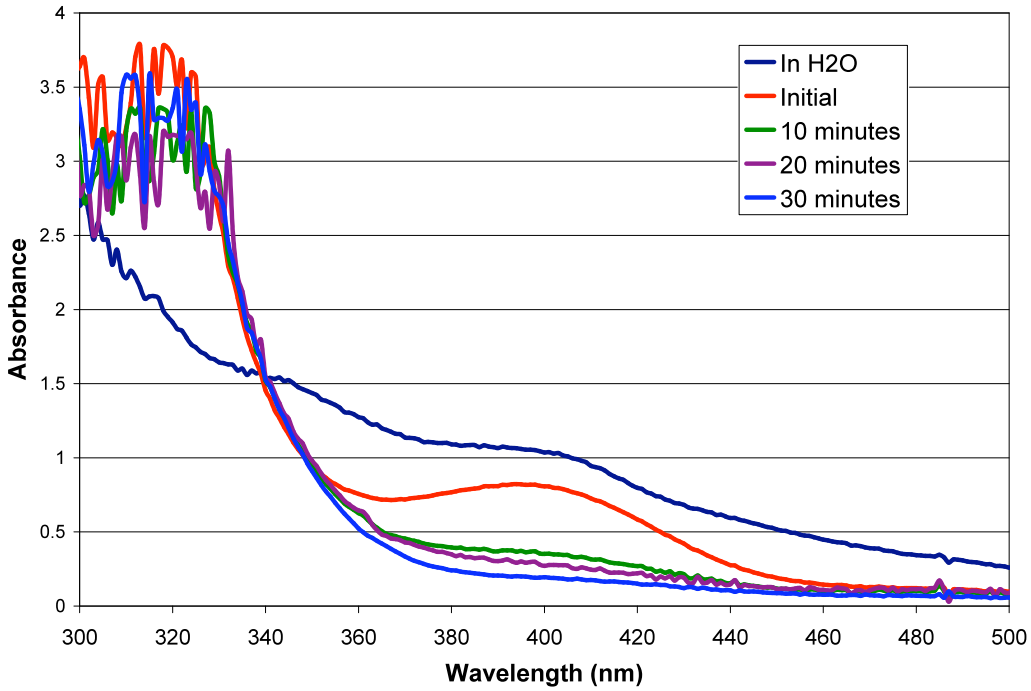

Figure A.11: UV-Vis spectra of Mn(salen) catalyst in water or H_2O_2.

CONCLUSIONS AND RECOMMENDATIONS

In conclusion, I successfully synthesized and characterized a water-soluble Mn(salen) catalyst. The synthetic approach to prepare the catalyst was not previously described in the literature. Unfortunately, the custom-made catalyst decomposed in the presence of the chosen oxidant, hydrogen peroxide. When the UV-vis absorbance of the catalyst in hydrogen peroxide was measured over time, it was found that the catalyst decomposed in less than ten minutes, much shorter than the reaction time for our proposed epoxidation reaction. I stopped any further research on this project at this point.

Although I did not quantify the partitioning coefficient of the catalyst between water and organic solvents, I observed good solubility of both the salen ligand and the Mn(salen) catalyst in water and minimal solubility of both in organic solvents used in OATS (acetonitrile, THF). Therefore, this catalyst has good potential for improved recovery in the OATS system, compared to the previously investigated phosphino Mn(salen) catalyst.

Chiral salen catalysts have found a wide range of applications in the chemical industry. The combination of my chiral salen catalyst and the OATS system could easily be applied to another reaction that does not utilize hydrogen peroxide, such as the kinetic resolution of epoxides. This system would still have the benefits of facile product purification and catalyst recycling, decreasing the operating costs of the process as well as the environmental impact.

I also propose a strategy to increase the stability of the Mn(salen) catalyst. Salen catalysts readily degrade through hydrolysis of the imine bond, yielding the diamine and aldehyde starting materials. Figure A.12 shows my proposed reduction and methylation of the previously synthesized salen ligand to increase its stability. The subsequent

Mn(salen) catalyst can then undergo stability testing for application to the proposed epoxidation reaction.

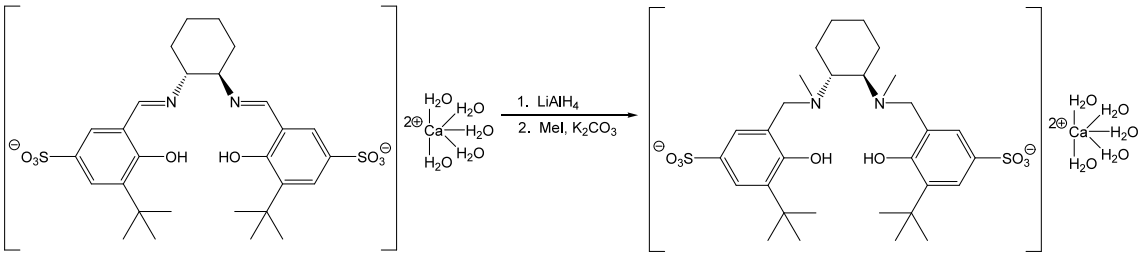

Figure A.12: Reduction and methylation of Mn(salen) catalyst.

EXPERIMENTAL METHODS

Materials and Equipment

All chemicals were ordered from Sigma-Aldrich or VWR and used as received, unless otherwise noted.

^{1}H and ^{13}C NMR spectra were obtained from a Varian-Mercury VX400 MHz spectrometer using d_6-DMSO or D_2O as an internal reference. Infrared spectra were recorded on a Bruker infrared spectrometer. Mass spectrum analysis was obtained from an ESI-MS by the Georgia Tech Bioanalytic Mass Spectrometry Facility (Atlanta, GA). Elemental analysis was performed by Atlantic Microlab, Inc. (Norcross, GA). UV-visible spectra were obtained on a Hewlett-Packard 8453 spectrometer.

Synthesis of Mn(salen) Catalyst

Synthesis of 3-*tert*-Butyl-5-formyl-4-hydroxybenzenesulfonate

Sulfonation of 3-*tert*-butyl-2-hydroxybenzaldehyde was done following a literature procedure used on a similar compound.[27] The glassware was dried in an oven overnight. A three-neck, round-bottom flask was set up with a thermocouple, a condenser with an argon gas line, and an addition funnel. The flask was placed in an ice bath, charged with fuming sulfuric acid (20 mL), and purged with argon for a few minutes. The addition funnel was loaded with 3-*tert*-butyl-2-hydroxybenzaldehyde (3.8 mL, 22 mmol). The aldehyde was added dropwise to the sulfuric acid over an hour, keeping the temperature in the flask below 10°C. The reaction was left to stir for an additional 15 minutes after all the aldehyde was added. The flask was removed from the ice and heated gradually to 85°C. The reaction was run at 85°C for one hour and then the flask was removed from the heat and cooled to room temperature. The reaction mixture was poured over ice (~200 mL). Calcium carbonate was added to the ice

mixture to neutralize the excess acid. Once the mixture stopped bubbling, the white solid (calcium sulfonate) was filtered off. The filtrate was dried under vacuum and the residue was recrystallized in methanol. The final product was an off-white powder.

^{1}H NMR (D_2O): 1.26 (s, 9H), 7.80 (s, 1H), 7.83 (s, 1H), 9.76 (s, 1H). ^{13}C NMR (D_2O): 28.44, 34.61, 119.78, 130.25, 131.17, 133.84, 139.48, 162.49, 199.00. Calculated for $Ca[C_{11}H_{13}SO_5]_2 \cdot 2H_2O$: C, 44.73; H, 5.12; S, 10.86. Found: C, 44.04; H, 5.04; S, 10.97. ν (cm^{-1}): 3400 (H_2O or OH), 1650 (C=O), 1440 and 1200 (S=O). ESI-MS *m/z* 257 $[C_{11}H_{13}SO_5]^-$.

Synthesis of 5,5'-(1*E*,1'*E*)-(Cyclohexane-1,2-diylbis(azan-1-yl-1-ylidene))bis(methan-1-yl-1-ylidene)bis(3-*tert*-butyl-4-hydroxybenzenesulfonate)

The condensation of 3-*tert*-butyl-5-formyl-4-hydroxybenzenesulfonate with (1*R*,2*R*)-1,2-diaminocyclohexane was done following a similar literature procedure.[28] The sulfonated aldehyde (0.50 g, 0.80 mmol) was stirred in acetonitrile (10 mL). The aldehyde was not completely soluble and formed a suspension. The mixture was heated to 80°C. (1*R*,2*R*)-1,2-diaminocyclohexane (0.092 g, 0.80 mmol) was added and the reaction was run at 80°C for four hours. The solid yellow product was filtered off and washed with DCM. The product was recrystallized in methanol to give yellow crystals.

^{1}H NMR (d_6-DMSO): 1.31 (s, 18H), 1.43 – 1.92 (br, 8H), 3.51 (m, 2H), 7.43 (s, 2H), 7.48 (s, 2H), 8.55 (s, 2H). ^{13}C NMR (d_6-DMSO): 24.38, 29.76, 33.12, 35.10, 70.88, 117.39, 127.48, 127.91, 136.41, 137.90, 161.53, 166.65. Calculated for $CaC_{28}H_{36}N_2S_2O_8 \cdot 5H_2O$: C, 46.54; H, 6.37; S, 8.86; N, 3.89. Found: C, 45.92; H, 6.25; S, 9.03; N, 4.17. ν (cm^{-1}): 3394 (H_2O or OH), 1628 (C=N), 1438 and 1184 (S=O). ESI- MS *m/z*593 $[C_{28}H_{26}S_2O_{10}]^{2-}$.

Synthesis of Mn(salen) Catalyst Complex

Using the previously synthesized 5,5'-(1*E*,1'*E*)-(cyclohexane-1,2-diylbis(azan-1-yl-1-ylidene))bis(methan-1-yl-1-ylidene)bis(3-*tert*-butyl-4-hydroxybenzenesulfonate), I made the Mn(salen) catalyst following a known procedure.[28] The salen ligand (0.15 g, 0.20 mmol) was stirred together with manganese acetate tetrahydrate (0.049 g, 0.20 mmol) in ethanol (4 mL). The mixture was refluxed at 80°C for three hours. The reaction mixture was removed from heat and cooled to room temperature. The solvent was removed under vacuum to give a brown solid residue. The residue was recrystallized in methanol to give dark brown crystals.

Calculated for $Ca[Mn(CO_2CH_3)C_{28}H_{34}N_2S_2O_8]\cdot 6H_2O$: C, 42.25; H, 5.75; S, 7.51; N, 3.29. Found: C, 42.26; H, 5.33; S, 7.63; N, 3.18. ν (cm^{-1}): 3425 (H_2O or OH), 1620 (C=N), 1433 and 1181 (S=O). ESI- MS *m/z* 645 $[MnC_{28}H_{34}N_2S_2O_8]^{2-}$.

Catalyst Stability

A solution of the salen ligand ($1x10^{-6}$ M) was made in 30% hydrogen peroxide. The UV-vis spectrum of this solution was taken periodically over the course of 24 hours. No change in absorbance was seen over this time period. The Mn(salen) catalyst was dissolved in both water and 30% hydrogen peroxide at concentrations of $2x10^{-6}$ M. The UV-vis spectrum of the catalyst in water was taken as a reference. An initial spectrum of the hydrogen peroxide solution was taken and subsequent spectra were recorded after 10, 20, and 30 minutes. The catalyst UV-vis spectra were normalized by subtracting the average absorbance between 800 and 850 nm for each spectrum.

REFERENCES

(1) Lu, J.; Lazzaroni, J.; Hallett, J. P.; Bommarius, A. S.; Liotta, C. L.; Eckert, C. A. *Industrial & Engineering Chemistry Research***2004**, *43*, 1586-1590.

(2) Nolen, S. A.; Lu, J.; Brown, J. S.; Pollet, P.; Eason, B. C.; Griffith, K. N.; Glaser, R.; Bush, D.; Lamb, D. R.; Liotta, C. L.; Eckert, C. A.; Thiele, G. F.; Bartels, K. A. *Industrial & Engineering Chemistry Research***2002**, *41*, 316-323.

(3) Constable, D. J. C.; Jimenez-Gonzalez, C.; Henderson, R. K. *Organic Process Research & Development***2007**, *11*, 133-137.

(4) Eckert, C. A.; Knutson, B. L.; Debenedetti, P. G. *Nature***1996**, *383*, 313-318.

(5) Jessop, P. G.; Subramaniam, B. *Chemical Reviews***2007**, *107*, 2666-2694.

(6) Eckert, C. A.; Liotta, C. L.; Bush, D.; Brown, J. S.; Hallett, J. P. *Journal of Physical Chemistry B***2004**, *108*, 18108-18118.

(7) Shishikura, A.; Kanamori, K.; Takahashi, H.; Kinbara, H. *Journal of Agricultural and Food Chemistry***1994**, *42*, 1993-1997.

(8) McLeod, M. C.; Kitchens, C. L.; Roberts, C. B. *Langmuir***2005**, *21*, 2414-2418.

(9) McLeod, M. C.; Anand, M.; Kitchens, C. L.; Roberts, C. B. *Nano Letters***2005**, *5*, 461-465.

(10) Musie, G.; Wei, M.; Subramaniam, B.; Busch, D. H. *Coordination Chemistry Reviews***2001**, *219*, 789-820.

(11) Xie, X. F.; Liotta, C. L.; Eckert, C. A. *Industrial & Engineering Chemistry Research***2004**, *43*, 7907-7911.

(12) Jessop, P. G.; Stanley, R. R.; Brown, R. A.; Eckert, C. A.; Liotta, C. L.; Ngo, T. T.; Pollet, P. *Green Chemistry***2003**, *5*, 123-128.

(13) Lopez-Castillo, Z. K.; Aki, S.; Stadtherr, M. A.; Brennecke, J. F. *Industrial & Engineering Chemistry Research***2006**, *45*, 5351-5360.

(14) Chamblee, T. S.; Weikel, R. R.; Nolen, S. A.; Liotta, C. L.; Eckert, C. A. *Green Chemistry***2004**, *6*, 382-386.

(15) Hallett, J. P.; Ford, J. W.; Jones, R. S.; Pollet, P.; Thomas, C. A.; Liotta, C. L.; Eckert, C. A. *Industrial & Engineering Chemistry Research***2008**, *47*, 2585-2589.

(16) Broering, J. M.; Hill, E. M.; Hallett, J. P.; Liotta, C. L.; Eckert, C. A.; Bommarius, A. S. *Angewandte Chemie-International Edition***2006**, *45*, 4670-4673.

(17) Baleizao, C.; Garcia, H. *Chemical Reviews***2006**, *106*, 3987-4043.

(18) Darensbourg, D. J.; Mackiewicz, R. M.; Phelps, A. L.; Billodeaux, D. R. *Accounts of Chemical Research***2004**, *37*, 836-844.

(19) Jacobsen, E. N. *Accounts of Chemical Research***2000**, *33*, 421-431.

(20) Katsuki, T. *Chemical Society Reviews***2004**, *33*, 437-444.

(21) Imanishi, H.; Katsuki, T. *Tetrahedron Letters***1997**, *38*, 251-254.

(22) Cozzi, P. G. *Chemical Society Reviews***2004**, *33*, 410-421.

(23) Vacca, J. P.; Dorsey, B. D.; Schleif, W. A.; Levin, R. B.; McDaniel, S. L.; Darke, P. L.; Zugay, J.; Quintero, J. C.; Blahy, O. M.; Roth, E.; Sardana, V. V.; Schlabach, A. J.; Graham, P. I.; Condra, J. H.; Gotlib, L.; Holloway, M. K.; Lin, J.; Chen, I. W.; Vastag, K.; Ostovic, D.; Anderson, P. S.; Emini, E. A.; Huff, J. R. *Proceedings of the National Academy of Sciences of the United States of America***1994**, *91*, 4096-4100.

(24) Shitama, H.; Katsuki, T. *Tetrahedron Letters***2006**, *47*, 3203-3207.

(25) Sawada, Y.; Matsumoto, K.; Katsuki, T. *Angewandte Chemie-International Edition***2007**, *46*, 4559-4561.

(26) Haikarainen, A.; Sipila, J.; Pietikainen, P.; Pajunen, A.; Mutikainen, I. *Bioorganic & Medicinal Chemistry***2001**, *9*, 1633-1638.

(27) Wallace, D.; Reglinski, J.; Taylor, M. K.; Kennedy, A. R. *Acta Crystallographica Section E-Structure Reports Online***2006**, *62*, M339-M341.

(28) Haikarainen, A.; Sipila, J.; Pietikainen, P.; Pajunen, A.; Mutikainen, I. *Journal of the Chemical Society-Dalton Transactions***2001**, 991-995.

APPENDIX B PACLITAXEL SIDE CHAIN SYNTHESIS

INTRODUCTION

Paclitaxel, commonly known by the trade name Taxol®, is a chemotherapy drug that is currently used to treat lung, breast, and ovarian cancers. The history of paclitaxel begins with a 1958 National Cancer Institute study that commissioned Department of Agriculture botanists to collect samples of over 30,000 plants to test for anticancer properties. In 1963, Wall discovered that the bark of the Pacific yew tree possessed antitumor qualities and the active ingredient was isolated and identified as paclitaxel four years later.[1] Prior to 1993, almost all paclitaxel produced was extracted from yew trees, a process which requires six 100-year old yew trees to be cut down for every patient treated. This led to a drive to produce paclitaxel synthetically, which was first published in 1994.[2-4] The total synthesis pathways published around this time all had very low yields (<1%), making them highly inefficient for manufacturing processes. Later, a shorter and more efficient synthetic route was developed from the natural product 10-deacetylbaccatin, isolated from the needles of Pacific yew trees. This shorter route involves the attachment of the paclitaxel side chain (Figure B.13) onto the 10-deacetylbaccatin structure.

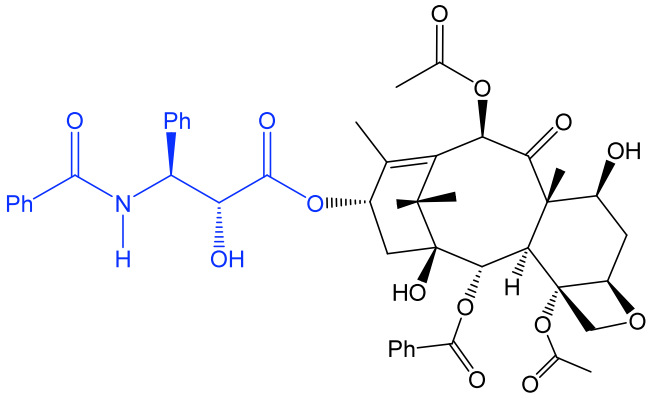

Figure B.13: Structure of paclitaxel with side chain highlighted.

Largely due to an enormous research and development effort, starting in government facilities and later in commercial labs, paclitaxel quickly became an all-time best-selling pharmaceutical. Paclitaxel was brought to the market by Bristol-Myers Squibb in 1993 as Taxol®. Annual sales peaked in 2000, reaching $1.6 billion. Unfortunately, the Pacific yew tree is one of the slowest growing trees in the world. Although other paclitaxel-like compounds may be extracted from various parts of yew trees, these are not as potent as paclitaxel itself.

Since the current synthetic method for the production of the paclitaxel side chain is complex and expensive, I investigated cheaper alternative routes to the paclitaxel side chain. Simplifying the synthetic pathway would make paclitaxel a cheaper and more readily available anti-cancer drug.

The aim of my research was to develop a proprietary synthetic pathway to the synthesis of the side chain. This appendix reports three approaches: (1) Jacobi synthesis, (2) acylsilane benzoin condensation, and (3) tungstophosphoric acid reaction.

RESULTS AND DISCUSSION

Jacobi Synthesis

A synthetic route for the paclitaxel side chain starting from *N*-benzoyl-2-phenylglycinaldehyde was investigated. Jacobi and Herradura reported the synthesis of (+)- and (-)-nephrosteranic acid from dodecyl aldehyde using potassium cyanide to form the cyanohydrin intermediate.[5] Upon ethanolysis, the cyanohydrin intermediate yielded the racemic mixture of the corresponding α-hydroxy ethyl ester products. The pure enantiomers were isolated upon resolution with quinine. The reaction scheme outlined in Figure B.14, using *N*-benzoyl-2-phenylglycinaldehyde as the starting material was investigated. The "Jacobi synthesis" would result in a simple and cheap method to produce the paclitaxel side chain molecule.

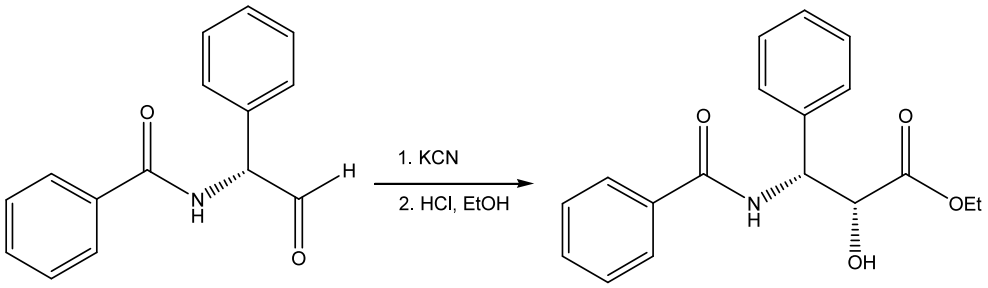

Figure B.14: Proposed synthetic pathway to paclitaxel side chain using Jacobi method.[5]

The starting material for the proposed synthesis of the paclitaxel side chain, *N*-benzoyl-2-phenylglycinaldehyde, is not commercially available. However, the unprotected carboxylic acid and alcohol derivatives are widely available. First, the 2-phenylglycinol was selected as the starting material. Upon oxidation, 2-phenylglycinol will yield the desired aldehyde, *N*-benzoyl-2-phenylglycinaldehyde. Several strategies are reported to carry out the oxidation of 2-phenylglycinol to its corresponding aldehyde.

Commonly, a protecting group was first introduced on the amine, followed by the controlled oxidation of the alcohol to the aldehyde (Figure B.15).

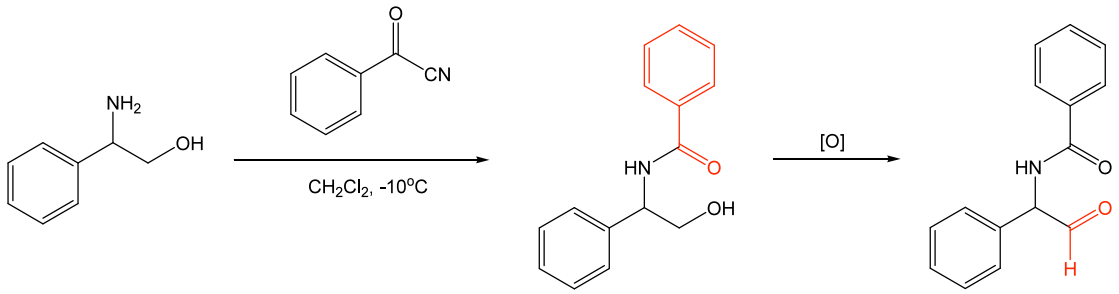

Figure B.15: Benzoyl protection and subsequent oxidation of 2-phenylglycinol.

Protection of 2-phenylglycinol

Following a literature procedure,[6] the amino group of 2-phenylglycinol was successfully and selectively protected with a benzoyl group (

Figure B.16). Equimolar amounts of 2-phenylglycinol and benzoyl cyanide were mixed together at -10°C and the product precipitated in less than twenty minutes. After completion of the reaction, the N-benzoyl-2-phenylglycinol was purified via trituration in DCM. *N*-benzoyl-2-phenylglycinol was isolated as a white powder in 66% yield and was characterized by ^{1}H and ^{13}C NMR. This *N*-benzoyl-2-phenylglycinol was used in subsequent reactions to make the aldehyde starting material.

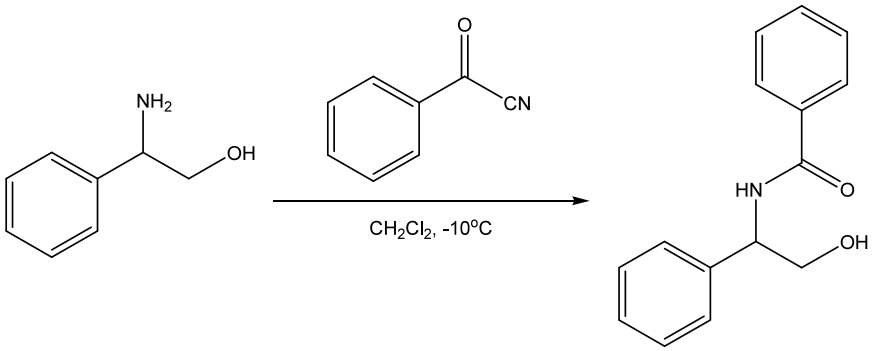

Figure B.16: Benzoyl protection of 2-phenylglycinol amino group.

Swern Oxidation

The Swern oxidation of *N*-benzoyl-2-phenylglycinol was originally chosen for its mild reaction conditions and high reported yields.[7] I first mixed cyanuric chloride and DMSO in THF at -30°C to form the activated sulfonium salt intermediate. Then *N*-benzoyl-2-phenylglycinol was added. After 30 minutes, the reaction was quenched with triethylamine (Figure B.17). The original workup procedure resulted in poor mass balance and impure product. The workup procedure was improved by changing the extraction solvent from diethylether to DCM. Thus, the mass balance was achieved. However, no aldehyde peaks were visible by ^{1}H NMR.

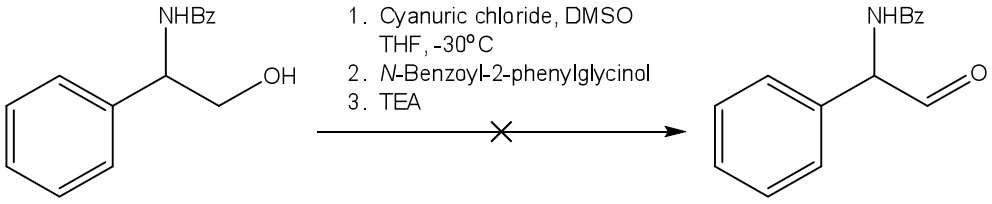

Figure B.17: Attempted Swern oxidation of *N*-benzoyl-2-phenylglycinol.

Dess-Martin Oxidation

The next strategy involved the Dess-Martin oxidation.[8] Dess-Martin periodinane was added to a solution of *N*-benzoyl-2-phenylglycinol in DCM at room temperature (Figure B.18). The starting material was completely consumed after two hours of reaction. Although peaks corresponding to the desired aldehyde product were visible by ^{1}H NMR, a large number of byproducts also present made isolation of the aldehyde very difficult. Column chromatography failed to yield the aldehyde in pure form. Because of the difficulty of product purification, this strategy was not pursued further.

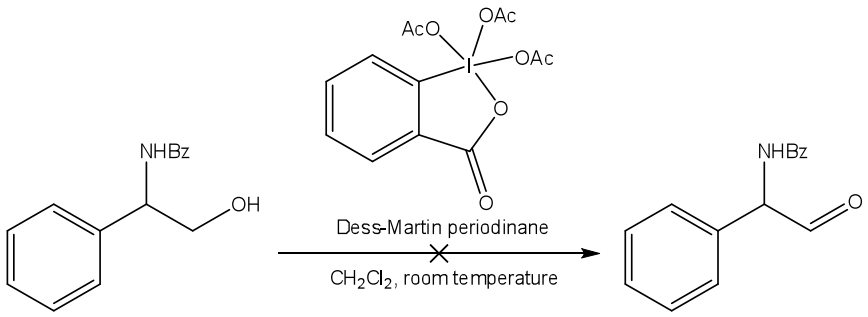

Figure B.18: Attempted Dess-Martin oxidation of *N*-benzoyl-2-phenylglycinol.

Pyridinium Dichromate Oxidation

The selective and mild oxidation of alcohols utilizing pyridinium dichromate as the oxidative agent was next investigated (Figure B.19). Pyridinium dichromate was added to a solution of *N*-Benzoyl-2-phenylglycinol in DCM and the reaction was run overnight at room temperature. As seen with the Dess-Martin oxidation, over-oxidation and partial reaction yielded a complex crude material (unreacted alcohol, desired aldehyde product, and carboxylic acid). The separation of *N*-benzoyl-2-phenylglycinaldehyde was unsuccessful.

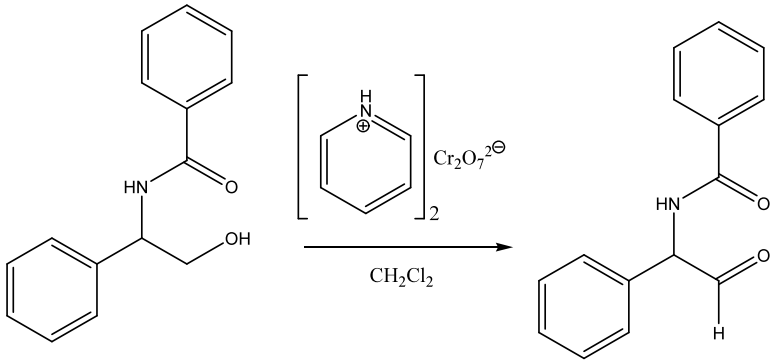

Figure B.19: Attempted pyridinium dichromate oxidation of *N*-benzoyl-2-phenylglycinol.

Manganese Dioxide Oxidation

Manganese dioxide was used to oxidize *N*-benzoyl-2-phenylglycinol (Figure B.20). Following a general oxidation procedure in the literature,[9] manganese dioxide was added to a solution of *N*-benzoyl-2-phenylglycinol in DCM at room temperature. The product mixture was analyzed by ^{1}H and ^{13}C NMR. For the first time, the desired aldehyde was the major product with about 50% of the overall products. The reaction time was optimized based on the maximum production of the aldehyde product with minimal oxidation to the carboxylic acid. Based on the ^{1}H NMR analysis, a reaction time of two days was deemed optimal.

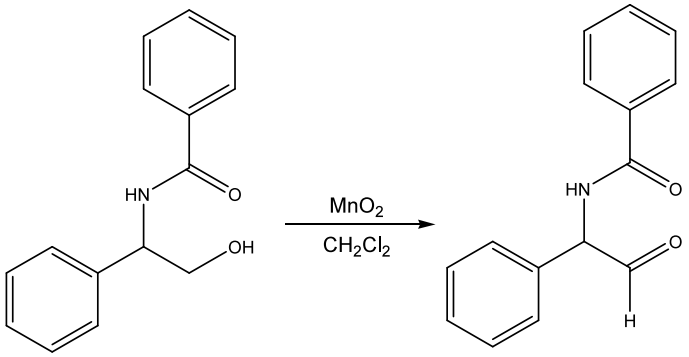

Figure B.20: Oxidation of *N*-benzoyl-2-phenylglycinol with manganese dioxide.

Due to the fine powdery nature of the manganese dioxide, the workup and isolation of the aldehyde product was strenuous and difficult. The product mixture was filtered on multiple Celite pads to remove all traces of the manganese dioxide. After purification on a silica column, only about 1% of the aldehyde product was isolated. I also tried centrifuging the crude product mixture before filtration on Celite but the manganese dioxide was not successfully centrifuged out of the solution. In addition, I ran a continuous extraction from the manganese dioxide remaining on the Celite to recover all of the aldehyde product, but I was still unable to close the mass balance. Although this method gave the best yield of the aldehyde in the crude product mixture and a small amount of the aldehyde was isolated for the first time, the overall yield was not viable.

Acylsilane Benzoin Condensation

Since the starting material for the Jacobi synthesis (*N*-benzoyl-2-phenylglycinaldehyde) was difficult to isolate, I investigated alternative methods to synthesize the paclitaxel side chain. One method was acylsilane benzoin condensation (Figure B.21). When a silyl intermediate is used, the benzoin condensation directs the ketone placement to be adjacent to the phenyl ring, which is desired for the paclitaxel side chain. So I first investigated two methods to synthesize the trimethylsilyl ketone: 1) Capperucci's (trimethylsilyl)cuprate method, and 2) Katritzky's benzotriazole synthesis.

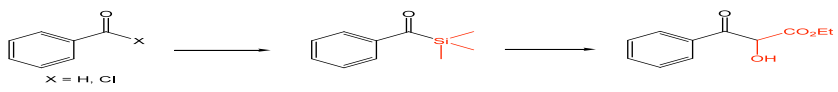

Figure B.21: Acylsilane benzoin condensation general reaction scheme.

Capperucci (Trimethylsilyl)cuprate Synthesis

The method used by Capperucci to synthesize the trimethylsilyl phenyl ketone is a relatively simple one-pot synthesis with a published yield of 87% (Figure B.22).[10] A solution of hexamethylphosphoramide (HMPA) and hexamethyldisilane was mixed with methyl lithium in anhydrous THF at -78°C. The solution was warmed to 0°C and reacted for fifteen minutes. The solution was cooled to -23°C and copper cyanide and benzoyl chloride were added to the reaction mixture. The reaction was quenched with ammonium chloride and the organics were extracted into diethylether. However, although my experimental observations were identical to the literature procedure, I was unable to reproduce their product yields. The ^{1}H and ^{13}C NMR showed many overlapping peaks and the GC-MS showed only starting material.

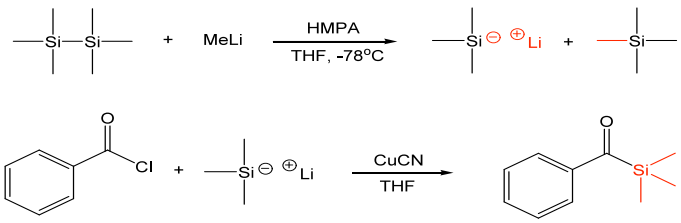

Figure B.22: Capperucci (trimethylsilyl)cuprate reaction scheme.

Katritzky Benzotriazole Synthesis

Katritzky and coworkers established an alternative procedure for synthesizing trimethylsilyl ketones using a benzotriazole intermediate (Figure B.23).[11,12] This reaction method reportedly provided 80% yield of the desired product. The first step is to synthesize the benzotriazole ether from benzaldehyde, benzotriazole, and triethylorthoformate. After the reaction was run at room temperature for three hours, the

products were extracted into diethylether, dried, and analyzed by ^{1}H and ^{13}C NMR. The NMR spectra were very complex, showing many overlapping peaks, which prevent the identification of the product peaks. The product mixture was analyzed by GC-MS, which did not show a peak for the desired product (based on the mass). Purification was unsuccessful. This pathway was stopped.

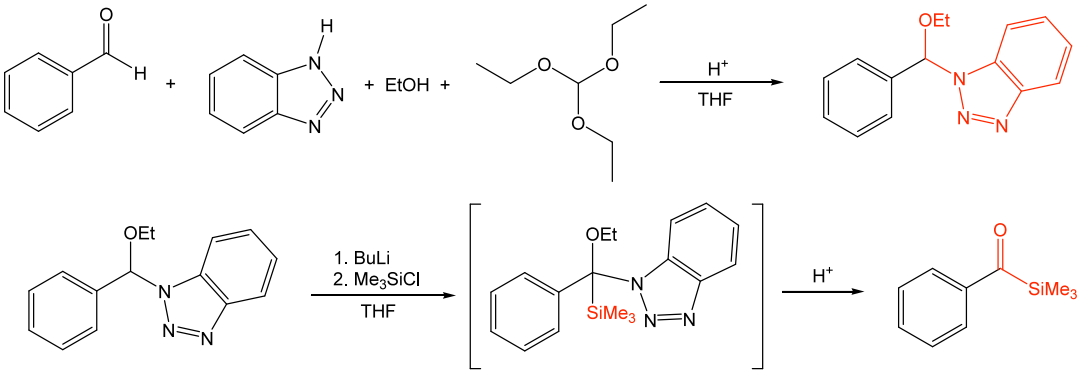

Figure B.23: Katritzky benzotriazole reaction scheme.

Tungstophosphoric Acid Reaction

Another method I investigated was the tungstophosphoric acid catalyzed oxidation of aromatic alkenes to α-hydroxyketones. Zhang and coworkers used this technique successfully on styrene.[13] They showed that the reaction proceeds regioselectively with the ketone group adjacent to the aromatic ring. Starting from *trans*-cinnamic acid, I proposed to synthesize the desired α-hydroxyketone shown in Figure B.24. I chose to pursue this reaction because it follows a relatively simple one step procedure with mild reaction conditions and reagents that are not sensitive to air or water. In addition, the tungstophosphoric acid catalyst is much cheaper than most transition metal catalysts. As an initial investigation, I repeated the literature reaction with styrene as the starting material. Styrene was added to a solution of 12-

tungstophosphoric acid, cetylpyridinium chloride, and hydrogen peroxide in chloroform. The reaction was run overnight at reflux. Analysis of the crude reaction mixture by ^{1}H NMR and GC-MS showed the disappearance of the starting material. However, it was difficult to isolate the desired product from the crude mixture, even after the workup procedure was optimized.

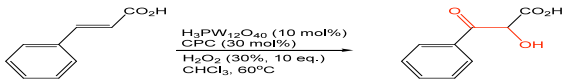

Figure B.24: Tungstophosphoric acid catalyzed oxidation of *trans*-cinnamic acid.

CONCLUSIONS AND RECOMMENDATIONS

In conclusion, I investigated multiple means to synthesize the paclitaxel side chain through cost-effective and simple reaction procedures. The methodologies investigated include the Jacobi synthesis from *N*-benzoyl-2-phenylglycinaldehyde, acylsilane benzoin condensation, and the tungstophosphoric acid catalyzed oxidation of *trans*-cinnamic acid. In all the cases investigated, product purification was a significant road block to achieving our goal of identifying a potential industrial process.

The Jacobi reaction reacting an aldehyde with potassium cyanide in the presence of sodium metabisulfite allows for the formation of the corresponding cyanohydrins. This later can undergo ethanolysis in acidic conditions to yield the α-hydroxyethyl ester. The starting alcohol, *N*-benzoyl-2-phenylglycinol, was prepared and its synthesis was optimized and scaled up. Unfortunately, after trying many methods to oxidize the alcohol to the aldehyde (Swern oxidation, Dess-Martin oxidation, pyridinium

dichromate oxidation, and manganese dioxide oxidation), the aldehyde was not successfully isolated on a usable scale.

The Capperucci synthetic method used water sensitive and highly reactive reagents that led to synthesis of many side products that made isolation of our desired product difficult. The Katritzky benzotriazole method seemed more promising but still led to many side products.

The most promising reaction was the simple synthesis of the side chain via oxidation of *trans*-cinnamic acid. Although the 12-tungstophosphoric acid catalyzed oxidation was reported successfully in the literature, I was unable to reproduce their results on styrene. However, this method would be a relatively cheap and simple means to obtain the paclitaxel side chain.

Although I attempted a few different methods to synthesize the paclitaxel side chain, the lack of chemoselectivity was a major roadblock for industrial applications. In the future, I would recommend focusing on the tungstophosphoric acid reaction, as it seems the most promising.

EXPERIMENTAL METHODS

Materials and Equipment

All chemicals were ordered from Sigma-Aldrich or VWR and used as received, unless otherwise noted. ^{1}H and ^{13}C NMR spectra were obtained from a Varian-Mercury VX400 MHz spectrometer using $CDCl_3$ or d_6-DMSO as an internal reference.

Jacobi Synthesis

Synthesis of N-Benzoyl-2-phenylglycinol

The amino protection of 2-phenylglycinol was done following a literature procedure using benzoyl cyanide to selectively protect the amino group.[6] 2-phenylglycinol (0.69 g, 5.0 mmol) was dissolved in DCM (15 mL) in a sodium chloride/ice/water bath. Benzoyl cyanide (0.66 g, 5.0 mmol) was dissolved in DCM (4 mL) and this solution was added dropwise to the starting material. The hydrogen cyanide generated in this reaction was subsequently treated with a sodium hydroxide solution for further disposal. A white precipitate formed almost immediately but the reaction was allowed to run for an additional 20 minutes. The solvent was removed under vacuum to give the crude product. Trituration in DCM was used to remove any remaining starting material and the product was filtered off and dried. This reaction was also successfully scaled up by a factor of ten. This procedure resulted in a white powdery product in a yield of 66%.

^{1}H NMR (d_6-DMSO): 3.64 (m, 2H), 4.93 (t, 1H), 5.06 (q, 1H), 7.23 – 7.89 (m, 10H), 8.68 (d, 1H). ^{13}C NMR (d_6-DMSO): 40.60, 49.10, 111.18, 111.35, 111.77, 112.46, 112.53, 115.49, 118.97, 125.68, 150.54.

Swern Oxidation

The reaction procedure for the Swern oxidation was adapted from literature with changes to the workup procedure.[7] Cyanuric chloride (0.66 g, 3.6 mmol) was dissolved in THF (20 mL) in a calcium chloride/ice/water bath. DMSO (1.25 mL, 17.6 mmol) was added and left to react for 30 minutes. Then *N*-benzoyl-2-phenylglycinol (0.72 g, 3.0 mmol) in THF (10 mL) was added slowly. After an additional 30 minutes, triethylamine (2.0 mL, 14 mmol) was added. The reaction mixture was removed from the ice bath and warmed to room temperature 15 minutes after addition of the triethylamine. The solvent was removed under vacuum and the residue was dissolved in DCM and the organic phase was washed with 1 N HCl, saturated sodium bicarbonate, then brine. The combined organic phase was dried over magnesium sulfate and the solvent removed under vacuum. This afforded an off-white product which did not have the desired product by ^{1}H NMR and was not further analyzed.

Dess-Martin Oxidation

The Dess-Martin oxidation of *N*-benzoyl-2-phenylglycinol was done according to a literature procedure.[8] Dess-Martin periodinane (1.0 g, 2.4 mmol) was added to a solution of *N*-benzoyl-2-phenylglycinol (0.49 g, 2.0 mmol) in DCM (7.5 mL) at room temperature. DCM (2 x 3 mL) was added to the solution every 15 minutes. The reaction was monitored by thin layer chromatography, which showed the disappearance of the starting material after two hours. Diethylether (7 mL) was added to the reaction and the solution was washed with a solution of sodium thiosulfate (5.65 g) in an 80% saturated sodium bicarbonate solution. The aqueous layer was extracted with diethylether then the combined organics were washed with saturated sodium bicarbonate, water, and brine. The organic solution was dried over magnesium sulfate and the solvent was removed under vacuum. Trituration of the residue in hexane was done to remove some

impurities and left at -15°C for one hour. The solvent was removed under vacuum. The product was washed with a 4:1 hexane/ether solution and dried to give a light yellow powder in 69% yield.

Pyridinium Dichromate Oxidation

N-Benzoyl-2-phenylglycinol (0.50 g, 2.0 mmol) and pyridinium dichromate (0.78 g, 2.0 mmol) were stirred in DCM (10 mL), forming a dark brown suspension. The reaction was run overnight at room temperature. The reaction mixture was diluted with diethylether and filtered. The organic solution was run through a silica plug before the solvent was removed under vacuum.

Manganese Dioxide Oxidation

N-Benzoyl-2-phenylglycinol (1.5 g, 6.0 mmol) and manganese dioxide (20 g, 0.23 mol) were stirred in DCM (50 mL) for 48 hours at room temperature. The reaction slurry was filtered on Celite until the filtrate was colorless. The solvent was removed under vacuum to give an off-white solid (0.43 g, 44% yield of crude product).

Acylsilane Benzoin Condensation

Capperucci (Trimethylsilyl)cuprate Synthesis

The method published by Capperucci and coworkers was followed to synthesize phenyl(trimethylsilyl)methanone.[10] HMPA (1 mL, 5.7 mmol) and hexamethyldisilane (0.5 mL, 2.4 mmol) were cooled in a dry ice/acetone bath (the mixture froze). Methyl lithium (1.25 mL of a 1.6 M solution in hexane, 2 mmol) and anhydrous THF (3 mL) were added. The dry ice/acetone bath was replaced with an ice bath (0°C). The reaction mixture was a homogeneous solution. After about 15 minutes, the solution turned bright red. At this point, the solution was cooled in an ice/calcium chloride bath (-23°C). Copper cyanide

(90 mg, 1 mmol) was added and this solution was stirred for 30 minutes. Benzoyl chloride (0.23 mL, 2 mmol) was dissolved in THF (1.5 mL) and added to the reaction mixture dropwise. The reaction was stirred on the ice/calcium chloride bath for five minutes and then warmed to room temperature over one hour. The reaction was quenched with a saturated aqueous ammonium chloride solution. The organics were extracted into diethylether and washed with water. The solvent was removed under vacuum to give a dark yellow oil.

Katritzky Benzotriazole Synthesis

Following Katritzky's published procedure, benzaldehyde (2.0 mL, 20 mmol), ethanol (2.3 mL, 40 mmol), benzotriazole (3.0 g, 25 mmol), triethyl orthoformate (10 mL, 60 mmol), and sulfuric acid (6 drops) were stirred in THF (30 mL) at room temperature for three hours. The mixture was then heated to reflux for an additional three hours. The organics were extracted into diethylether (200 mL), washed with saturated sodium carbonate (2 x 100 mL) and water (100 mL). The solvent was removed under vacuum and purified on a silica column with 1:3 ethyl acetate/hexane.

Tungstophosphoric Acid Reaction

The oxidation of styrene to an α-hydroxyketone was run according to a literature procedure.[13] 12-tungstophosphoric acid (0.59 g, 0.21 mmol), cetylpyridinium chloride (0.22 g, 0.62 mmol), and hydrogen peroxide (2.0 mL of a 35% solution, 20 mmol) were mixed together in chloroform (15 mL). Styrene (0.23 mL, 2 mmol) was added to start the reaction. The reaction was run at reflux (60°C) overnight. The reaction was removed from heat and quenched with 10% sodium bisulfite and 10% sodium hydroxide. The organics were extracted in chloroform, washed with brine, and dried over magnesium sulfate. The solvent was removed under vacuum to give a brown oil.

REFERENCES

(1) Wani, M.; Taylor, H.; Wall, M.; Coggon, P.; McPhail, A. *Journal of the American Chemical Society* **1971**, *93*, 2325-&.

(2) Holton, R. A.; Somoza, C.; Kim, H. B.; Liang, F.; Biediger, R. J.; Boatman, P. D.; Shindo, M.; Smith, C. C.; Kim, S. C.; Nadizadeh, H.; Suzuki, Y.; Tao, C. L.; Vu, P.; Tang, S. H.; Zhang, P. S.; Murthi, K. K.; Gentile, L. N.; Liu, J. H. *Journal of the American Chemical Society* **1994**, *116*, 1597-1598.

(3) Holton, R. A.; Kim, H. B.; Somoza, C.; Liang, F.; Biediger, R. J.; Boatman, P. D.; Shindo, M.; Smith, C. C.; Kim, S. C.; Nadizadeh, H.; Suzuki, Y.; Tao, C. L.; Vu, P.; Tang, S. H.; Zhang, P. S.; Murthi, K. K.; Gentile, L. N.; Liu, J. H. *Journal of the American Chemical Society* **1994**, *116*, 1599-1600.

(4) Nicolaou, K. C.; Yang, Z.; Liu, J. J.; Ueno, H.; Nantermet, P. G.; Guy, R. K.; Claiborne, C. F.; Renaud, J.; Couladouros, E. A.; Paulvannan, K.; Sorensen, E. J. *Nature* **1994**, *367*, 630-634.

(5) Jacobi, P. A.; Herradura, P. *Canadian Journal of Chemistry-Revue Canadienne De Chimie* **2001**, *79*, 1727-1735.

(6) Murahashi, S. I.; Naota, T.; Nakajima, N. *Tetrahedron Letters* **1985**, *26*, 925-928.

(7) De Luca, L.; Giacomelli, G.; Porcheddu, A. *Journal of Organic Chemistry* **2001**, *66*, 7907-7909.

(8) Wroblewski, A. E.; Piotrowska, D. G. *Tetrahedron-Asymmetry* **2002**, *13*, 2509-2512.

(9) Ohloff, G.; Giersch, W. *Angewandte Chemie-International Edition in English* **1973**, *12*, 401-402.

(10) Capperucci, A.; Deglinnocenti, A.; Faggi, C.; Ricci, A.; Dembech, P.; Seconi, G. *Journal of Organic Chemistry* **1988**, *53*, 3612-3614.

(11) Katritzky, A. R.; Lang, H. Y.; Wang, Z. Q.; Zhang, Z. X.; Song, H. M. *Journal of Organic Chemistry* **1995**, *60*, 7619-7624.

(12) Katritzky, A. R.; Wang, Z. Q.; Lang, H. Y. *Organometallics* **1996**, *15*, 486-490.

(13) Zhang, Y. F.; Shen, Z. X.; Tang, J. T.; Zhang, Y.; Kong, L. C.; Zhang, Y. W. *Organic & Biomolecular Chemistry* **2006**, *4*, 1478-1482.